PhD degree in Systems Medicine (curriculum in Human Genetics)

European School of Molecular Medicine (SEMM),

University of Milan and University of Naples "Federico II"

XXXI Cycle

Unraveling the molecular pathogenesis of ineffective erythropoiesis in Congenital Dyserythropoietic Anemia Type II: *in vitro* evaluation of RAP-011 treatment

Gianluca De Rosa

CEINGE, Naples

Matricola n. R11483

Supervisor: Prof. Achille Iolascon

CEINGE, Naples

Added Supervisor: Dr. Roberta Russo

CEINGE, Naples

Anno accademico 2018-2019

Table of contents

List of Abbreviations

ActR, activin receptor
BFU-E, burst-forming unit-erythroid
BM, bone marrow
BMP, bone morphogenetic protein
CBC, complete blood count
CDA, congenital dyserythropoietic anemia
CFU-E, colony-forming unit-erythroid
CLSD, cranio-lenticulo-sutural dysplasia
CMP, common myeloid progenitor
COP, coat protein
DBA, Diamond-Blackfan anemia
DEB, diepoxybutane test
EM, electron microscopy
EPO, erythropoietin
ER, endoplasmic reticulum
EryP, erythroid progenitor
ESA, erythropoiesis-stimulating agents
FA, Fanconi anemia
GDF, growth differentiation factor
Hb, hemoglobin
HbF, fetal hemoglobin
HC, healthy control
HHA, hereditary hemolytic anemia
HS, hereditary spherocytosis
HSC, hematopoietic stem cell
HSP-70, heat-shock protein-70
Ht, hematocrit
IBMFS, inherited bone marrow failure syndrome
LDH, lactate dehydrogenase
MCH, mean corpuscolar hemoglobin
MCHC, mean corpuscolar hemoglobin concentration
MCV, mean cell volume
MEP, megakaryocytic-erythroid progenitor
MkP, megakaryocyte progenitor
MPP, multipotential progenitor
NGS, next-generation sequencing
PBL, peripheral blood lymphocyte
PBMC, peripheral blood mononuclear cell
PK, pyruvate kinase
PLT, platelets
ProEB, proerythroblast
RBC, red blood cell
RDW, red blood cell distribution width
TD, transfusion dependency
TGF, transforming growth factor
XLTDA, X-linked thrombocytopenia with or without dyserythropoietic anemia

Figures Index

ABSTRACT

Congenital Dyserythropoietic Anemias (CDAs) are subtypes of bone marrow failure syndromes, hallmarked by ineffective erythropoiesis. The most common form is CDA type II (CDAII), showing moderate/severe anemia, relative reticulocytopenia, jaundice, splenomegaly, and iron overload. It is inherited as an autosomal recessive disorder due to loss-of-function mutations in the *SEC23B* gene. Molecular pathogenesis of CDA II still has to be investigated because the described animal models did not recapitulate the clinical features observed in humans. To date, treatments for CDAII patients consist of supportive therapy, such as erythrocyte transfusions, or bone marrow transplantation or splenectomy in transfusion-dependent cases. Recently, members of TGF-β superfamily have been studied as potential regulators of erythropoiesis, especially the growth differentiation factor 11 (GDF11). Through the binding of specific receptors, GDF11 leads to an inhibited late-stage erythropoiesis. Indeed, two GDF11 inhibitors, ACE-011 and ACE-536, have been associated with an improvement of hematologic parameters. Studies with the mouse counterpart of ACE-011, RAP-011, on a mouse model of β-thalassemia showed increased differentiation of erythroid cells, improvement of the anemic condition and reduced iron overload in treated mice.

The first aim of our study was the establishment of a cellular model of CDA II, that could reproduce the main defects of the disease, such as the lack of the erythroid differentiation due to the low or absent expression of *SEC23B* gene. For this aim, we selected the K562 cell line and, through short-hairpin RNA-based strategy, we obtained two different clones

of K562 showing a stable silencing of *SEC23B*. Then, we decided to assess the effects of RAP-011 on this CDA II model, by investigating the pathway involved in the GDF11 signaling. This treatment simulated the ligand trap function played by RAP-011 towards GDF11. The administration of RAP-011 resulted in a reduction of SMAD2 phosphorylation induced by GDF11 and, moreover, in an increase of different erythroid differentiation markers.

I. INTRODUCTION

1. Background

Red blood cells are produced in the bone marrow and released in circulation to deliver the oxygen from the lungs to the other organs of the body, even though they are responsible for the transport of other gases, such as carbon dioxide and nitric oxide, involved in cellular respiration and tissue oxygen supply.

This function is made possible by the presence of the hemoglobin in the erythrocytes. Indeed, this protein, due to the presence of the heme, binds inhaled oxygen in the lungs and delivers it to the other organs. The oxygen delivery to the body organs depends on the hemoglobin level of the blood, and the hemoglobin value is normally correlated with the number of erythrocytes in the circulation. The number of erythrocytes in a healthy individual remains remarkably constant for long periods of time, they have a finite life span of approximately 110–120 days, and about 1% are recognized as senescent and removed daily from the circulation (Koury et al. Blood Rev, 2014).

Erythropoiesis begins with hematopoietic stem cells (HSCs) in the bone marrow where they interact with specific mesenchymal stem cells and colonize specialized HSCs niches (Mendez-Ferrer S et al. Nature, 2010). Following this interaction, their asymmetric cellular divisions result in other HSCs or in multipotential progenitor (MPPs) cells (Figure I.1A). The MPPs cells can differentiate in all the blood cell lineages, including the erythroid cells, in a process regulated by a series of decisions linked to the microenvironment (Smith JN et

al. Stem Cells, 2013). Following stages towards the erythroid lineage from MMPs include the common myeloid progenitor (CMP), the megakaryocytic-erythroid progenitor (MEP) and finally the burst-forming unit-erythroid (BFU-E) which is the first stage solely committed towards the erythroid lineage (Gregory CJ et al. Blood, 1977)

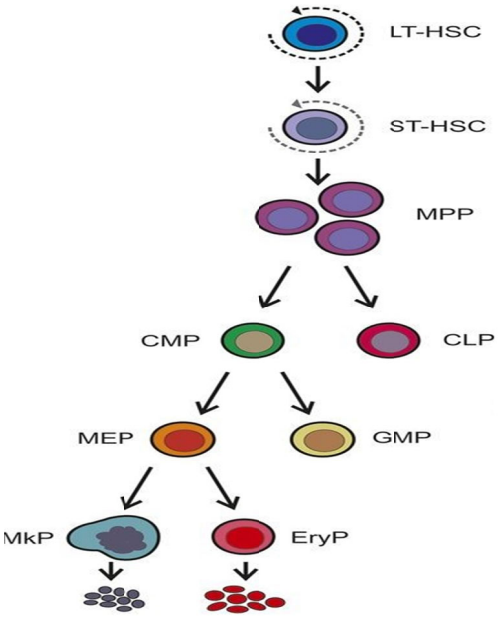

Figure I.1A. Erythroid lineage. The hematopoietic stem cells (HSC) divide and give rise to the multipotential progenitor, that is responsible for all the hematopoietic lineage. Concerning the erythroid lineage, it differentiates into a common myeloid progenitor first (CMP) and then in a megakaryocytic-erythroid progenitor (MEP). This precursor could generate megakaryocyte progenitors (MkP) or the erythroid progenitors (EryP) (Adapted from Carolien M. Woolthuis and Christopher Y. Park, Blood 2016).

Then, following BFU-E, next stages of erythroid differentiation take place in a morphological structure known as "erythroblastic island", consisting of a central macrophage surrounded by all the different stages of erythroid cells (An X et al. Int J Hematol, 2011).

Differentiation stages in the erythroblastic island can be divided into two different phases: 1) EPO-dependent stages and 2) terminally differentiating erythroblasts (Figure I.1B). Erythropoietin (EPO) is the key component of the feedback mechanism that regulates erythropoiesis based on oxygen delivery by the mature erythrocytes to the peripheral

tissues (Koury MJ. Blood, 2014). During the first phase, there is an expansion of colony-forming-unit erythroid (CFU-E) cells and proerythroblasts (ProEB), and this process needs a high concentration of EPO to prevent programmed cell death by apoptosis (Koury MJ et al. Science, 1990). The second phase consists of erythroblasts which do not need EPO for survival, but the presence of two major transcription factors, GATA1 and KLF1 (Merika M et al. Mol Cell Biol, 1995; Gregory RC. Blood, 1996), capable of addressing these immature erythroblasts towards the enucleated red cell through the increased transcription of some specific erythrocytes products (globins, membrane skeleton proteins, enzymes) (Hattangadi SM et al. Blood, 2011). The last event of erythroid development is characterized by the loss of the nucleus from the reticulocyte, the last red cells precursor, resulting in the formation of reticulocytes that contain most of the cytoplasm and hemoglobin, as well as the proteins needed to form a unique cytoskeletal network. Then, from this area of the bone marrow, reticulocytes and mature red blood cells are released in circulation (Geiduschek and Singer. Cell, 1979; Koury ST et al. J Cell Biol, 1989; Lee JC et al. Blood, 2004). Steady-state levels of RBCs are maintained by the continuous production and release of reticulocytes into the bloodstream to balance the removal of senescent RBCs by macrophage cells, which are localized primarily in the spleen (Bennett and Kay. Exp Hematol, 1981).

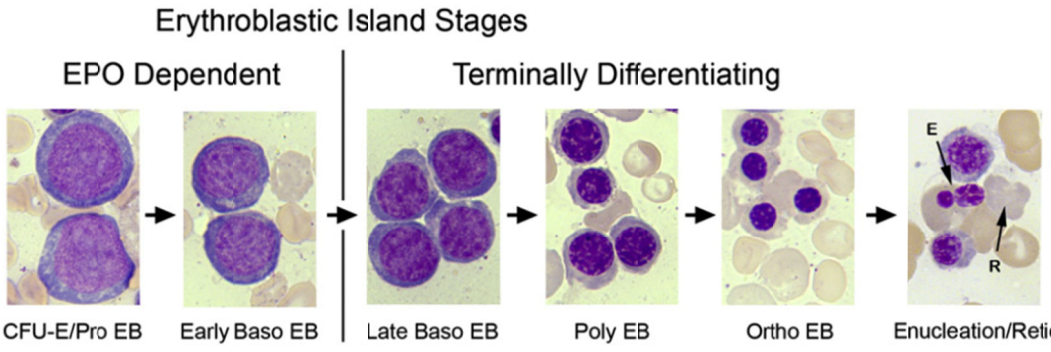

Figure I.1B. This figure resumes the two distinct phases of erythroid differentiation. 1) During the EPO-dependent stages, CFU-E, proerythroblasts, and early basophilic erythroblasts are dependent on EPO for their

survival and their expansion. 2) During the second phase, there is an increase of some erythroid-specific components and a decrease in cell size from late basophilic erythroblasts to polychromatic erythroblasts, orthochromatic erythroblasts and finally, the enucleation from the reticulocytes represents the crucial event of the erythroid development, preceding the mature erythrocytes formation (Koury et al. Blood 2014).

Erythroid lineage impairment leads to the establishment of the anemia, a condition characterized by a lack of red cells or hemoglobin. A few or abnormal red cells and low or abnormal hemoglobin are responsible for a reduced delivery of oxygen from the lungs to the various organs, with the fatigue as the main symptom arising. Anemias can be classified as acquired, occurring for example as a result of a blood loss or a deficient-iron diet, or inherited, due to genetic defects in genes involved in erythropoiesis.

Concerning the inherited anemias, the hereditary hemolytic anemias (HHA) embrace a highly heterogeneous group of disorders characterized by hemolytic anemia of variable degree and by complex and often unexplained genotype-phenotype correlations. HHA are genetic disorders caused by mutations in more than 80 genes controlling red blood cell (RBC) production, structure, and function. Mutations in these genes can lead to alterations in hemoglobin (Hb) levels, RBC differentiation and proliferation, cell membrane structure, and activity of erythrocyte enzymes. This large group of pathologies comprises:

1. Hemoglobinopathies: disorders due to the presence of abnormal structure of the globin chains of the hemoglobin molecule;

2. Thalassemias: these pathologies are the consequence of a quantitative defect in the globin chains of the hemoglobin molecule (α-thalassemia, β-thalassemia);

3. Hyporegenerative anemias: reduced or impaired production of red blood cells in the bone marrow (congenital dyserythropoietic anemias, myelodysplastic syndrome, aplastic anemia, Fanconi anemia)

4. Hemolytic anemias due to red cell membrane defects: anemic condition occurring for defects in red cell membrane proteins, such as hereditary spherocytosis (HS), and hereditary stomatocytosis.

I will deal with the characterization of congenital dyserythropoietic anemias.

2. Congenital dyserythropoietic anemias: classification and diagnostic criteria

Dyserythropoiesis is defined as a condition of abnormal erythropoiesis affecting the differentiation and proliferation pathways of the erythroid lineage with consequent defective production of RBCs (Iolascon et al. Curr Opin Hematol, 2011). This condition, common to different red blood cell disorders, is typical of dyserythropoietic anemias in which there are both morphological and functional disorders, with the predominant phenomena being erythroblast abnormalities and ineffective erythropoiesis, respectively (Wickramasinghe and Wood. Br J Haematol, 2005). Ineffective erythropoiesis is a term used to describe the destruction of developing erythroid cells in the marrow. Normally, a few die within the bone marrow (BM) (Odartchenko et al. Cell Tissue Kinet, 1971), but ineffective erythropoiesis is prominent in disorders of nucleic acid, heme, or globin synthesis.

Dyserythropoietic anemias can be divided into primary and secondary forms, and both inherited and acquired forms can occur. Particularly, congenital dyserythropoietic anemias (CDAs) are hereditary diseases that embrace a heterogeneous group of rare anemias resulting from different types of abnormalities that occur during the late stages of erythropoiesis. CDAs can be considered subtypes of inherited bone marrow failure syndromes (IBMFS) being hallmarked by morphological abnormalities of erythroblasts in the BM and ineffective erythropoiesis as the predominant mechanism of anemia, accompanied by a hemolytic component (Iolascon et al. Blood, 2013). Common clinical features of patients with CDAs are anemia, jaundice, splenomegaly, normal or reduced

reticulocyte count, ineffective erythropoiesis, and morphological abnormalities at BM examination (Gambale et al. Expert Rev Hematol, 2016).

Despite these common clinical findings, CDAs can be classified in different types on the basis of different morphological and molecular features. The most common classification, proposed by Heimpel and Wendt, is still used and shows three main forms (CDA I, CDA II and CDA III) while other forms not fully represented by these criteria are known as CDA variants (Iolascon et al. Haematologica, 2012) (Table I.1, Figure I2.A).

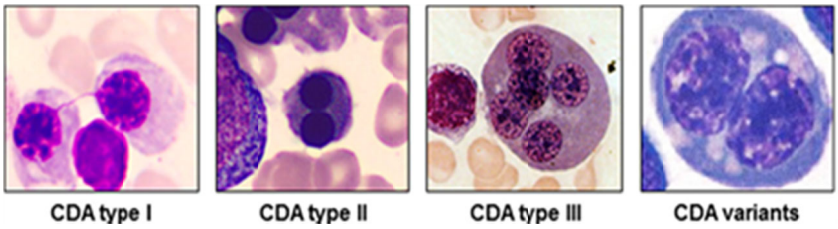

Figure I.2A. Pathognomonic marrow erythroblasts. The BM erythroblasts morphology of different types of CDAs is shown. In CDAI it is possible to observe polychromatic erythroblasts with the typical bridges between the nuclei pairs. CDAII image shows a binucleated erythroblast, while CDAIII bone marrow image has a multinucleated erythroblast. CDA variants image presents basophilic stippling and internuclear bridging (Adapted from Iolascon et al, Blood 2013).

Disease symbol	Phenotype	Bone marrow biopsy	
		Optical microscopy	*Electron microscopy*
CDA I	Congenital dyserythropoietic anemia type I	Binucleated erythroblasts (3-7%); thin chromatin bridges between nuclei of erythroblasts	"Swiss cheese appearance" of the erythroblasts heterochromatin
CDA II	Congenital dyserythropoietic anemia type II	Binucleated (10-30%); rare multinucleate erythroblasts	Double plasma membrane of the erythroblasts
CDA III	Congenital dyserythropoietic anemia type III	Giant multinucleate (up to 12 nuclei) erythroblasts	Clefts within heterochromatin, autophagic vacuoles, iron-laden mitochondria, myelin figures in the cytoplasm
CDA IV	Congenital dyserythropoietic anemia type IV	Tri- and multi-nucleate erythroblasts	Invagination of nuclear membrane, intra-nuclear precipitated and nuclear blebbing
XLTDA	Thrombocytopenia X-linked with or without dyserythropoietic anemia	Erythroblasts: megaloblastic features, nuclear irregularities, bi- and multi-nucleation Megakaryocytes: Small, dysplastic with signs of incomplete maturation	Reduced numbers of platelet alpha granules and dysplastic features in megakaryocytes and platelets

Table I.1. A classification of different CDAs is shown. Criteria of this classification are based on morphological features (Gambale et al. Expert Rev Hematol, 2016).

In the last two decades, many advances have been made in the knowledge of CDAs, particularly with the identification of the causative genes that helped to investigate the molecular pathogenesis of this class of disorders and to unravel novel aspects of the molecular biology of erythropoiesis. Nowadays, according to the Online Mendelian Inheritance in Man (OMIM) compendium of human genes and genetic phenotypes, six different types of CDAs can occur (Table I.2). Indeed, this list can continuously be updated with new causative genes thanks to the development of high-throughput technologies, such as next-generation sequencing (NGS). This kind of approach, through the identification of new genetic variants underlying hereditary disorders, results in many advantages for the genetic and clinical research but also for the achievement of a correct diagnosis and careful patient management (Gambale et al. Expert Rev Hematol, 2016).

Disease symbol	**Phenotype**	**Phenotype MIM number**	**Gene** *location*	**Inheritance**	**N cases**[§]
CDA Ia	Congenital dyserythropoietic anemia type Ia	224120	CDAN1 *15q15.2*	AR	< 100
CDA Ib	Congenital dyserythropoietic anemia type Ib	615631	C15orf41 *15q14*	AR	< 10
CDA II	Congenital dyserythropoietic anemia type II	224100	SEC23B *20p11.23*	AR	> 200
CDA III	Congenital dyserythropoietic anemia type III	105500	KIF23 *15q21*	AD	< 20
CDA IV	Congenital dyserythropoietic anemia type IV	613673	KLF1 *19p13.2*	AD	< 10
XLTDA	Thrombocytopenia X-linked with or without dyserythropoietic anemia	300367	GATA1 *Xp11.23*	XLR	< 10

[§] Number of cases with positive molecular analysis
AD, Autosomal dominant; AR, Autosomal recessive; XLR, X-linked recessive

Table I.2. This table summarizes the OMIM classification that considers all the different types and subtypes of CDAs and their causative genes, with all the genetic information, including chromosomal position, inheritance, and a number of described cases (Gambale et al. Expert Rev Hematol, 2016).

CDA type I

Typical clinical features of CDA I are macrocytic anemia with a mean corpuscular volume (MCV) ranging between 100 and 120 fl, relative reticulocytopenia accompanied with variable values of Hb and splenomegaly, whose development is observed in adolescence or adulthood. Moreover, about 20% of cases show congenital anomalies, particularly syndactyly in hands or feet, absence of nails or supernumerary toes, pigeon chest deformity and short stature (Iolascon et al. Haematologica, 2012; Gambale et al. Expert Rev Hematol, 2016). Morphological exams at BM level reveal hypercellularity and erythroid hyperplasia (E:G of 4 and 8 times the normal), with 30-60% of polychromatic erythroblasts showing abnormalities of nuclear and chromatin structure such as thin chromatin bridges between the nuclei pairs of erythroblasts. A minority of erythroblasts shows bi- or multinuclearity, and the nuclei of binucleated cells are of different size and shape. At electron microscopy (EM), heterochromatin is denser than normal and forms demarcated clumps with small translucent vacuoles, giving rise to the metaphor of "Swiss cheese appearance" (Heimpel et al. Eur J Haematol, 2010).

CDA I is inherited in an autosomal recessive manner, and two different subtypes have been described following the identification of two causative genes. The first causative gene in which pathogenic variants were identified has been *CDAN1* (chr15q15.2) (Dgany et al. Am J Hum Genet , 2002) that encodes a ubiquitously expressed protein, codanin-1 (Table 1-2). Codanin-1 is part of the cytosolic Asf1-H3-H4-importin-4 complex, which is implicated in

nucleosome assembly and disassembly (Ask K et al. EMBO J, 2012). More than 300 patients with CDA I and approximately 60 unique disease-causing mutations have been described so far (Iolascon et al. Blood, 2013; Roy and Babbs. Br J Haematol, 2019). Cdan1 knockout mice die in utero before the onset of erythropoiesis, suggesting a critical role of codanin-1 in other developmental processes beyond erythroid cell lineage (Renella et al. Blood, 2011). Homozygous or compound heterozygous in *CDAN1* gene cover approximately 50% of CDA I patients, while in 30% of cases only a single mutant allele can be identified (Babbs et al. Haematologica, 2013; Ahmed MR et al. Blood, 2006). Recently, the second causative gene of CDA I has been identified. In particular, two different mutations in *C15orf41* gene (Chr 15q14) were found in three unrelated Pakistani families, classified as affected by CDA Ib (Table 1-2) C15orf41 is predicted to encode a divalent metal ion-dependent restriction endonuclease, with a yet unknown function. In cultured erythroblasts, C15orf41 produces a spliced transcript encoding a protein with homology to the Holliday junction resolvases (Babbs et al. Haematologica, 2013). However, it has been demonstrated that C15orf41, as well as CDAN1, interacts with Asf1b, supporting the hypothesis of an interplay between these two proteins during DNA replication and chromatin assembly (Gambale et al. Expert Rev Hematol, 2016; Roy and Babbs. Br J Haematol, 2019). Only seven C15orf41 variants have been described so far (Russo R et al. Front Physiol, 2019).

CDA type II

A correct CDA II diagnosis is based on some clinical findings such as the presence of normocytic anemia of variable degree, with normal or only slightly increased reticulocyte count, but not adequate to the degree of anemia; the hemolytic component, due to the ineffective erythropoiesis, explains the onset of jaundice and splenomegaly. Although CDA II generally presents mild anemia (mean Hb 9.6 ± 0.2 g/dL), a wide spectrum of

clinical presentations can occur, from asymptomatic to severe (Hb range 3.6-16.4 g/dL). Indeed, approximately 10% of cases result symptomless, whereas 20% of patients undergo a regimen of transfusion dependency. Main complications for CDAII patients (also CDAI patients) arise from the alteration of iron balance, that is mainly due to the increased but ineffective erythropoiesis, as well as it is observed in other bone marrow failure syndromes, but also to the hemolytic component and the transfusion-dependency many patients undergo (Gambale et al. Expert Rev Hematol, 2016). The increased iron absorption and systemic iron overload follow the downregulation of hepatic hormone hepcidin (Kautz et al. Blood, 2014). Different regulators of hepcidin have been studied, like the growth differentiation factor 15 (GDF15) and the soluble hemojuvelin (HJV), being both increased in CDA I and CDA II patients (Casanovas G et al. J Mol Med, 2011; Tamary et al. Blood, 2008; Shalev et al. Eur J Haematol, 2013). Recently, the erythroblast-derived hormone erythroferrone (ERFE) has been identified as a regulator of iron metabolism (Kautz et al. Nat Genet, 2014), and it was proposed as a marker of CDA II, given its increased levels in patients affected by this condition (Russo R et al. Blood, 2016).

Mean age of onset symptoms of CDA II is approximately 3-4 years but very often a correct diagnosis is reached only in the adulthood (22.2 ± 1.7 years) because of the occurrence of mild symptoms or the misdiagnosis of CDA II with HS. Similarly to CDA I, the BM exams show erythroid hyperplasia with subsequent increased E:G and the presence of more than 10% mature binucleated erythroblasts with equal size of two nuclei; this represents one of the most common features of CDA II (Russo et al. Am J Hematol, 2014). The analysis of RBC membrane proteins by sodium dodecyl sulfate-polyacrylamide gel electrophoresis (SDS- PAGE) reveals a narrower band size and faster migration of band 3 in most of the CDA II patients (95%) (Figure I.2B). This is a consequence of the hemolytic component that is responsible for an increased clusterization of this protein on the RBC

surface, leading to IgG binding and phagocytosis of RBCs (De Franceschi et al. Exp Hematol, 1998). This biochemical feature represented the most reliable hallmark to diagnose CDA II until *SEC23B* (20p11.23) was identified as the causative gene of this disorder (Schwarz et al. Nat Genet, 2009).

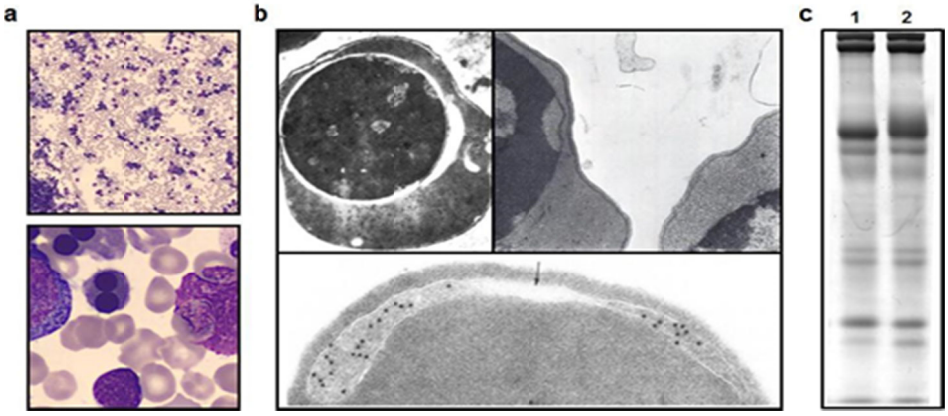

Figure I.2B. Morphological and biochemical features of CDA II erythroblasts. (a) CDA II bone marrow at light microscopy highlights erythroid hyperplasia with bi- or multinucleated late erythroid precursors. (b) CDA II bone marrow at EM highlights morphological abnormalities of CDA II erythroblasts. (c) Biochemical analysis of RBC membrane proteins from CDA II patient (lane 1) shows the typical hypoglycosylation of Band 3, with increased anodic mobility on SDS-PAGE compared to healthy control (lane 2).

SEC23B gene encodes the homonymous member of the COPII complex, which is involved in the secretory pathway of eukaryotic cells. This multi-subunit complex mediates anterograde transport of correctly folded cargo from the ER toward the Golgi apparatus (Schwarz et al. Nat Genet, 2009). Given its autosomal recessive inheritance pattern, CDA II onset is due to loss-of-function mutations of the *SEC23B* gene. Most of the cases (86%) show biallelic mutations in the *SEC23B* gene (homozygosis or compound heterozygosis occurs), although a subset of patients with an incomplete

pattern of inheritance (14.0%) has been identified. Nowadays, more than 400 CDA II patients were diagnosed, and approximately 100 different mutations in *SEC23B* have been described so far (Russo R et al. Am J Hematol, 2014; Bianchi P et al. Br J Haematol, 2016).

CDA type III

CDA III is the rarest form among classical CDAs. Clinically, patients present with absent to moderate anemia, normal or slightly elevated MCV, the normal or faintly low relative number of reticulocytes and, in some cases (about 20% of described patients), RBC transfusion-dependency. Common symptoms are weakness, fatigue, and headache; jaundice and biliary symptoms are also reported while, unlike from other CDAs, none of the described patients show an enlarged liver or spleen. Hemolysis is also present as attested by low or absent haptoglobin and increased LDH. Morphological exams show erythroid hyperplasia with giant multinucleated erythroblasts at bone marrow level (Iolascon et al. Blood, 2013). In 2013, the causative gene of this condition was identified by target sequencing: *KIF23* gene (Chr.15q21) encodes a kinesin-superfamily protein MKLP1 that is a component of centralspindlin, a subcellular structure required for proper formation of the central spindle and the midbody and thus essential for cytokinesis (Liljeholm et al. Blood, 2013). MKLP1 mutant affects the function of this protein during cytokinesis, leading to the formation of the large multinucleated erythroblasts found in BM of the patients.

Transcription factor-related CDAs

CDA IV and X-linked thrombocytopenia with or without dyserythropoietic anemia (XLTDA) belong to this subgroup of CDAs (Table I.2). To date, four patients with

CDA IV have been reported, and all of them are characterized by the occurrence of normocytic anemia, generally severe, with Hb 5-9.5 g/dL but they presented with a normal or slightly increased reticulocyte count with respect to the degree of anemia; moreover, elevated values of HbF (>30%) are also observed (Arnaud et al. Am J Hum Genet, 2010; Jaffray et al. Blood Cells Mol Dis, 2013). Bone marrow images show erythroid hyperplasia and dyserythropoiesis signs, such as basophilic stippling of polychromatic erythroblasts and erythrocyte, and internuclear bridging is observed. All four patients exhibit the same autosomal-dominant mutation (p.Glu325Lys), in the heterozygous state, in *KLF1* gene (19p13.2) (Table I.2). *KLF1* encodes the homonymous protein, which is an essential erythroid-specific transcription factor, member of the Krüppel-like factor family. KLF1 is a well-known transcriptional activator in erythropoiesis, but it also exerts transcriptional repression in megakaryopoiesis. It plays a critical role in regulating the switch between fetal and adult Hb expression and is required in terminal erythroid differentiation for the cell-cycle progression (Siatecka et al. Mol Cell Biol, 2007).

XLTDA is a CDA variant characterized by anemia of variable degree since it can show hydrops fetalis and transfusion-dependency or dyserythropoiesis without anemia, macro-thrombocytopenia with hypo-granulated platelets (PLT) and bleeding tendency. BM features are dyserythropoiesis, reduced megakaryocytes with cytoplasmic vacuoles and absence of platelet membrane demarcation (Gambale et al. Expert Rev Hematol, 2016). This is an X-linked recessive disease (Table I.2), due to mutations in the X chromosomal gene *GATA1* (Xp11.23), encoding for the zinc finger DNA binding protein GATA1. This latter belongs to the GATA family of transcription factors, involved in the regulation of hematopoiesis. In particular, GATA1 plays an essential role in the development and maintenance of both erythroid and megakaryocytic lineages. GATA1 has two zinc finger domains: the C-terminal is necessary for DNA

binding, while the N-terminal mediates interaction with FOG1 (friend of GATA1), a cofactor of GATA1. Of note, the most likely pathogenic mechanism in these disorders involves GATA1-FOG1 interaction (Gao J et al. Exp Hematol Oncol, 2015).

The role of the transcriptional regulator of different genes and pathways may explain how different mutations in the same gene can result in disparate phenotypes. Indeed, beyond CDA IV, *KLF1* mutations have been associated with in(Lu)blood type and hereditary persistence of fetal hemoglobin. Similarly, there are different syndromic conditions related to *GATA1* mutations, in which thrombocytopenia can be associated with thalassemia, congenital erythropoietic porphyria, or Diamond–Blackfan anemia (DBA)-like disease. Moreover, the co-inheritance of GATA1 and other CDA-gene mutations could explain the occurrence of more severe phenotypes (Ciovacco et al. Gene, 2008; Di Pierro et al. Eur J Haematol, 2015). Given some common clinical features between the CDAs or between CDAs and other forms of inherited bone marrow failure syndromes, differential diagnosis, classification, and patient stratification are often very difficult. Indeed, the variety of unspecific and overlapping phenotypes often hampers the correct clinical management of the patients.

In particular, the differential diagnosis with thalassemia is important in suspected cases of either CDA IV or CDA variants GATA1-related. Among IBMFS, DBA and FA are disorders that most frequently undergo differential diagnosis with CDAs. Unlike the CDAs, FA generally presents reduction to absent trilinear hematopoiesis, acute myelogenous leukemia or solid tumors; moreover, it can also present developmental abnormalities more frequently compared to CDAs, particularly CDA I. The positivity to the diepoxybutane (DEB) test is a very sensitive and specific tool for guiding FA diagnosis (Chirnomas and Kupfer. Pediatr Clin North Am, 2013). Similarly to CDAs, DBA presents an isolated inherited red cell production failure. However, unlike CDAs, DBA BM exhibits reduced proliferation and survival of erythroid progenitors. Moreover, growth retardation,

congenital malformations, and increased HbF levels are more frequent features of DBA compared to CDAs. Increased activity of erythrocyte adenosine deaminase is a good II level test for establishing the diagnosis of DBA (sensitivity 84%, specificity 95%, positive and negative predictive values 91%) (Fargo et al. Br J Haematol, 2013).

CDAs can be also misdiagnosed with hereditary hemolytic anemias. For example, CDA II shares several clinical findings with hemolytic anemias due to red cell membrane defects, such as HS (King MJ et al. Int J Lab Hematol, 2015). Of note, CDA II patients are often erroneously diagnosed as HS, and consequently, they undergo unnecessary splenectomy. The lack of substantial improvement after intervention leads to a re-examination of the case, allowing the correct diagnosis of CDA II. The most useful pointer to correctly establish the diagnosis of CDA II is the inadequate reticulocyte count for the degree of anemia. Indeed, the marrow stress is higher in CDA II compared to HS for the same Hb level as attested by the increased sTfR levels observed in CDA II patients (Russo et al. Am J Hematol, 2014). Moreover, another relevant issue was about the differential diagnosis between CDA and PK (pyruvate kinase) deficiency. Pyruvate kinase deficiency is hemolytic anemia hallmarked by the deficiency of pyruvate kinase enzyme, with consequences on the red cells metabolism. However, due to some shared clinical manifestations between CDAs and PK deficiency, a relevant number of PK deficient patients (about 36%) were misdiagnosed with CDA. In this case, only a multigene panel-based approach helped to solve the issue, through the identification of mutations in PKLR gene in patients who were wrongly diagnosed with CDA (Russo R et al. Am J Hematol, 2018).

Following this classification, now I will discuss CDA II, describing the molecular pathogenesis, the role of the causative gene, the epidemiology, and the patient's management.

3. SEC23B: molecular and functional characterization

In 2009 a study performed by different research groups highlighted the role of *SEC23B* as the causative gene of CDA II. Notably, 33 individuals, who were diagnosed with CDA II on the basis of clinical, morphological, and biochemical criteria were enrolled for a genome-wide SNP analysis. First results of this study led to the identification of a single common homozygous region on chromosome 20p11.23–20p12.1 so that it was possible to hypothesize which of the genes of this region could be involved in CDAII onset. Given the impaired cis, medial, and trans-N-glycan Golgi processing of erythroblast glycoproteins in CDA II, the role of the proteins involved in the secretory pathways was considered. Therefore, sequencing of the *SEC23B* gene unraveled different mutations in the patients that could justify their phenotype, so they concluded that this was CDAII causative gene (Schwarz et al. Nat Genet, 2009). This finding represented a turning point for the story of this disorder because, from this moment on, a lot of studies investigated the role of this gene and the mechanisms involved in the molecular pathogenesis.

SEC23B encodes the homonymous protein that is one of the components of COPII complex, whose function is to transport vesicles of newly-synthesized proteins from endoplasmic reticulum towards the Golgi apparatus (anterograde transport), and this process represents the counterpart of the retrograde transport (from Golgi apparatus towards endoplasmic reticulum) played in the opposite direction by COPI complex (Figure I.3A). This process, occurring at the ER exit sites, is particularly accurate and, indeed, requires a quality control system to operate in order to transport only properly folded proteins (Russo R. et al. Am J Hematol, 2013).

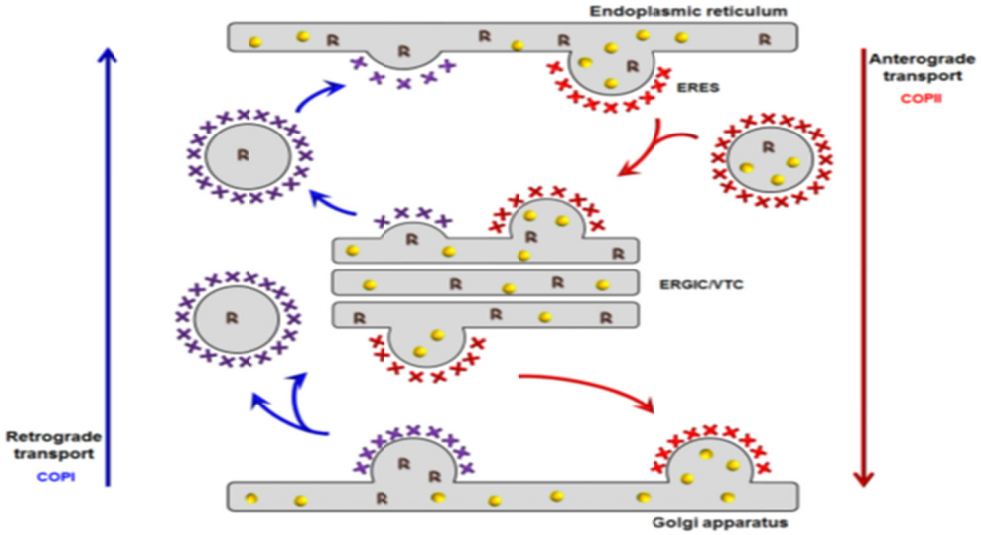

Figure I.3A. Vesicle trafficking played by COPI and COPII complexes, for retrograde and anterograde transport, respectively, is shown (Russo R. et al. Am J Hematol, 2013).

The multimeric COPII coat is comprised of five key subunits: SAR1 (a small GTPase), the SEC23-SEC24 inner coat complex, and the SEC13-SEC31 outer coat complex (Figure I.3B). The complex assembly begins at the ER sites, and it is triggered by GTP-bound active SAR1 that recruits the complex SEC23-SEC24 through its binding with SEC23, while SEC24 interacts with the cargo proteins. Finally, SAR1-SEC23-SEC24, with the cargo proteins loaded, binds the heterotetramer SEC13-SEC31 in order to assemble a protein coat (Satchwell et al. Haematologica, 2013).

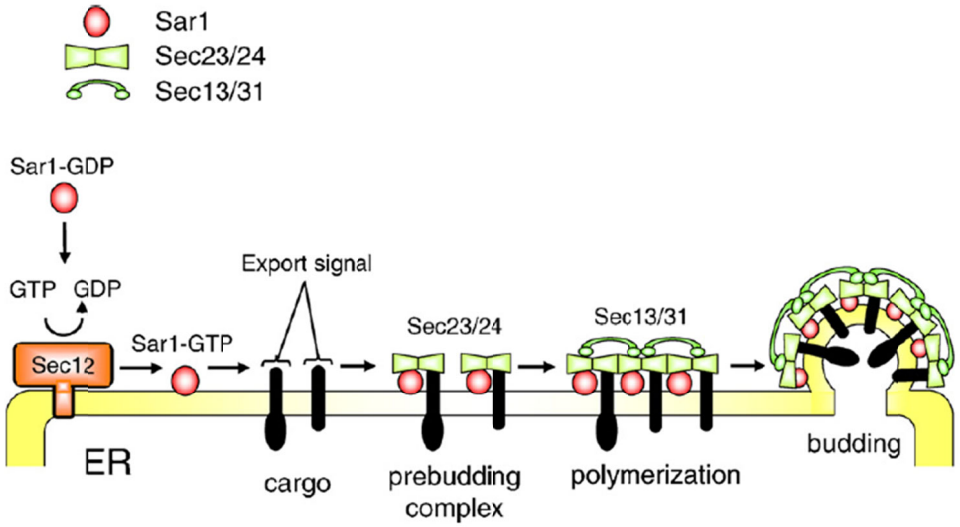

Figure I.3B. Different steps of vesicle formation, from the selection of the cargo to the prebudding complex formation, the polymerization of different players and the budding of the vesicle are shown. Moreover, it is shown how different components have a specific role in each phase of this process (Adapted from Sato et al. FEBS Lett, 2007).

Different isoforms exist for these proteins, each encoded by a different gene: two isoforms of Sar1, Sec23 and Sec31, and four isoforms of Sec24, have been reported, while only one isoform of Sec13 has been characterized (Russo R et al. Am J Hematol, 2013). Particularly, SEC23 isoforms, SEC23A and SEC23B, share 85% amino acid sequence identity, even if they are encoded by different genes, and are ubiquitously expressed. Despite this high percentage of identity, these two isoforms are responsible for two different disorders charged two different tissues: while SEC23B mutations are causative of CDA II, involving erythroid cells development, SEC23A has been found out to be the causative gene of Cranio-lenticulo-sutural dysplasia (CLSD), an autosomal recessive disorder characterized by late-closing fontanels, sutural cataracts, facial dysmorphisms, and skeletal defects. The reason why mutations of SEC23B are confined to the erythroid lineage development (as well as SEC23A downregulation leads to a bone development disease), can be found in a peculiar role of this protein for the red blood cells development, more than other systems. A hypothesis comes from one of the biochemical hallmarks of CDAII, the hypoglycosylation of the protein Band 3 on red blood cells membranes. Indeed, since complex COPII is involved in the transport of proteins properly folded and modified, SEC23B deficiency may have a role in this defect of transport that leads to a reduced membrane exposure of a working form of Band 3. As a result of this dysfunction, red blood cells show higher amounts of aggregated Band 3 on the membranes. Moreover, aggregated proteins can bind naturally occurring antibodies, mediating the phagocytosis and the removal of the erythrocytes from the circulation; this may be the explanation for the hemolysis typical in CDAII. However, mutations in the SEC23B gene can explain the

aberrant glycosylation of erythroblasts, but it is still unclear how the reduced function of this gene can affect the cell division along the erythroid differentiation generating bi- or multinucleated erythroblasts. However, in vitro studies showed that during erythroid differentiation there was an increased expression of SEC23B 5-7 fold over SEC23A expression, underlining the specific role of this gene for the erythroid lineage (Schwarz et al. Nat Genet, 2009).

4. CDA II animal models

The pathophysiology study of CDA II is difficult mainly due to the absence of a reliable animal model. Zebrafish model was obtained through the antisense morpholino technology aimed at inhibiting SEC23B expression. In this case, a reduction of the lower jaw was observed 3 days post fertilization as well as the presence of binucleated erythroblasts typical of CDAII. However, other characteristics of the disorder, such as the hypoglycosylation of band 3 or the duplication of rough ER, were not observed. Moreover, this model could not allow recapitulating the human phenotype because of the lethality of *sec23b* morphants at day 6 post-fertilization (Schwarz et al. Nat Genet, 2009). Different models of SEC23B-deficient mice have been generated without reproducing CDA II phenotype. Indeed, SEC23B deficiency results in different phenotypes in humans and mice (Tao et al. Proc Natl Acad Sci, 2012; Khoriaty et al. Mol Cell Biol, 2014). In particular, the absence of phenotype in SEC23B-deficient mice seems to be related to the different SEC23B/SEC23A expression ratio in murine and human tissues. Indeed, this ratio is higher in mouse pancreas compared to BM, whereas it is higher in human BM relative to the pancreas. Of note, SEC23A and SEC23B are paralogous components of the COPII complex. This observation is in agreement with the compensatory expression of SEC23A that seems to ameliorate the effect of low SEC23B expression alleles in CDA II patients. Interestingly, concerning CDAII patients, a compensatory mechanism SEC23A-mediated

that could balance the deficiency of SEC23B expression, was observed (Russo R et al. Blood Cells Mol Dis, 2013). Therefore, recent studies underlined the interchangeable functions of *SEC23A* and *SEC23B in vivo*; indeed, the SEC23A-upregulation was demonstrated to ameliorate the phenotype of SEC23B-deficient mice (induced by lentiviral infection), increasing primary erythroid human cell numbers, correcting the defective hypoglycosylation of membrane proteins (Pellegrin et al. Br J Haematol, 2019) and reverting the lethal pancreatic phenotype observed in mice (Khoriaty et al. Proc Natl Acad Sci U S A, 2018).

5. Epidemiology and mutations knowledge

The prevalence of CDAs varies widely among European regions, with minimal values of 0.04 cases/million in North Europe and the highest in Mediterranean countries, particularly in Italy (2.49/million). This is mainly true for CDA II, which is more frequent than CDA I with an overall ratio of approximately 3.0 (Heimpel et al. Eur J Haematol, 2010). The studies on molecular epidemiology of CDA I and II highlighted the elevated allelic heterogeneity of both conditions as most of the causative variations are inherited as private mutations (Iolascon A et al. Haematologica, 2012).

To date, according to the International Registry of CDAII, > 400 cases and approximately 100 different variants have been described (HGMD professional database, 2019). The allelic heterogeneity is another feature of this disorder but, even though most mutations result from independent events, there are 4 SEC23B mutations (R14W, E109K, R497C, I318T) accounting for more than 50% of the mutant alleles (Iolascon et al. Haematologica, 2010; Russo R et al. Am J Hematol, 2011) (Figure I.5A).

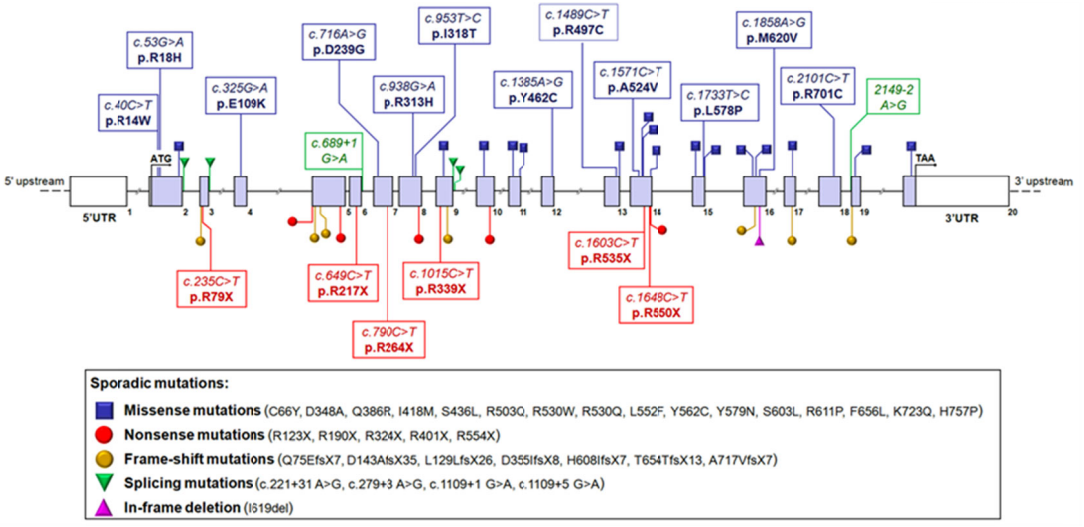

Figure I.5A. This image shows the distribution of some of the SEC23B variants described. It is possible to observe how there is a heterogeneous distribution in terms of localization and type of variants (missense, nonsense, frameshift, splicing mutations, and in-frame deletion) (Adapted from Russo R. et al. Am J Hematol, 2011).

Two variants are very common in Italy, but the frequency of the amino acidic substitution Arg14Trp (R14W) results particularly higher in Italian patients compared to the Non-Italian patients (26.3% vs. 10.7%), whereas the distribution of Glu109Lys (E109K) shows a similar trend between Italian and Non-Italian patients (28% vs. 25%). The elevated frequency of these mutational events in a geographic area has been studied, and it goes under the name of "founder effect", that is the loss of the genetic variation occurring when a new population is established by a very small number of individuals from a larger population. Therefore, both these mutations have a precise geographic derivation: aminoacidic substitution Glu109Lys may have originated in the Middle East (it is still prevalent in the Moroccan Jews), while Arg14Trp may have originated in Southern Italy, and this would explain the increased frequency of CDAII in Italy (Figure I.5B). However, despite this high frequency, Arg14Trp aminoacidic substitution is most commonly found in

heterozygous patients, while only one case of homozygous has been described (Russo R et al. Am J Hematol, 2011; Russo R et al. Am J Hematol, 2014).

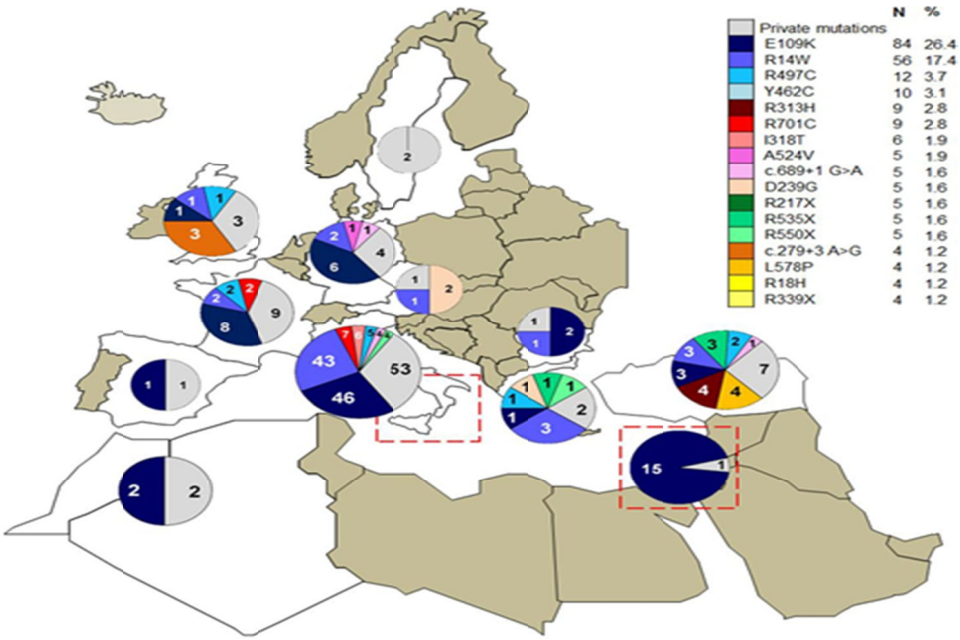

Figure I.5B. Molecular geocode of *SEC23B* alleles in Europe. In white are represented the countries in which have been reported CDA II cases so far. Mutations found in more than three independent pedigrees were shown with different colors. For each variant, the total number of alleles and the relative frequency were indicated. Private mutations (i.e., the mutations present in less than 3 unrelated patients) were colored in gray. Pie charts show the number of alleles for each mutation. The dotted red line highlights the region in which a founder effect has been demonstrated. (Adapted from Russo R et al. Am J Hematol, 2014).

6. Management and therapeutic approaches

First symptoms for CDA II patients can already be observed at birth since affected children show jaundice and anemia more frequently than the normal population. Moreover, the bone marrow failure presents during the early childhood (2/3 years), then from this point forward, it is recommended to achieve a complete blood count (CBC) at least every three months in order to follow the development of the disorder. From adolescence and during the adulthood, for patients undergoing transfusion regimen (transfusion-dependent, TD) it

is necessary to evaluate the CBC and the iron balance very frequently, while for non-TD patients timing for the CBC depends on the degree of anemia. A parameter to monitor the degree of the anemia in these patients is the amount of Hb: patients with moderate/severe anemia show less than 9 g/dL of Hb compared to those with mild anemia. Finally, iron overload has to be examined annually by evaluation of ferritin and transferrin saturation, while MRI-T2 can be performed every five years in order to exclude or evaluate the degree of hepatic or heart iron overload.

Management of CDA II patients is also based on the choice of correct therapeutic approach to adopt, depending on the clinical situation. For example, patients presenting with severe anemia (Hb < 7 g/dL) may undergo a transfusion regimen and the frequency of the transfusions is usually related to the degree of anemia. Another option is represented by bone marrow transplantation, that has been performed in some cases successfully (Russo R et al. Am J Hematol, 2014; Unal S et al. Pediatr. Transplant, 2014; Modi G et al. Case Rep Hematol, 2015). Moreover, splenectomy also leads to benefits, especially when performed on TD-patients whose number of transfusions is reduced or abolished following the surgical treatment. Instead, for non-TD CDA II patients, the surgical removal of the spleen only shows a slight increase of Hb values (King MJ et al. Int J Lab Hematol, 2015). While for hereditary spherocytosis the effectiveness of splenectomy was demonstrated, the role of this surgical procedure in other anemias has been controversial for long. Recently, ultimate guidelines on the outcome of the splenectomy in hemolytic anemias were collected and the differences in the usefulness of this practice depending on the type of disorder were highlighted. According to these guidelines, splenectomy is recommended only for CDAII patients showing a severe degree of anemia and/or symptomatic splenomegaly (Iolascon et al. Haematologica, 2017).

Finally, the iron overload typical of this condition is treated with the administration of iron chelators and this strategy is based on the guidelines for the treatment of thalassemic

patients, given the lack of guidelines for chelation treatment of CDA II patients (Angelucci E et al. Haematologica, 2008). Nevertheless, all of these described treatments only represent some supportive cares to alleviate the main symptoms of this condition, but no therapeutic strategy aimed to overcome the maturation arrest typical of CDA II was proposed.

However, in the last decade, there was a lot of interest in the effects on hematologic parameters of a drug, ACE-011, developed by Acceleron Pharma and Celgene Corporation and proposed for the treatment of bone loss. In the context of phase I clinical trial, the administration of Sotatercept (commercial name of ACE-011) to postmenopausal women, seemed to contribute to an improvement in the osteolytic lesions, as expected, but also an increase of red blood cells, hemoglobin values, and hematocrit levels (Raje N et al. Curr Opin Mol Ther, 2010). These findings suggested the possibility that this drug could restore the erythroid development impaired by genetic defects, such as the hemolytic anemias. Sotatercept is a chimeric protein composed of the extracellular domain of the Activin Receptor IIA (ACVR2A) and the Fc of the human IgG1 (Ruckle J et al. J Bone Miner Res, 2009) (Figure I.6A).

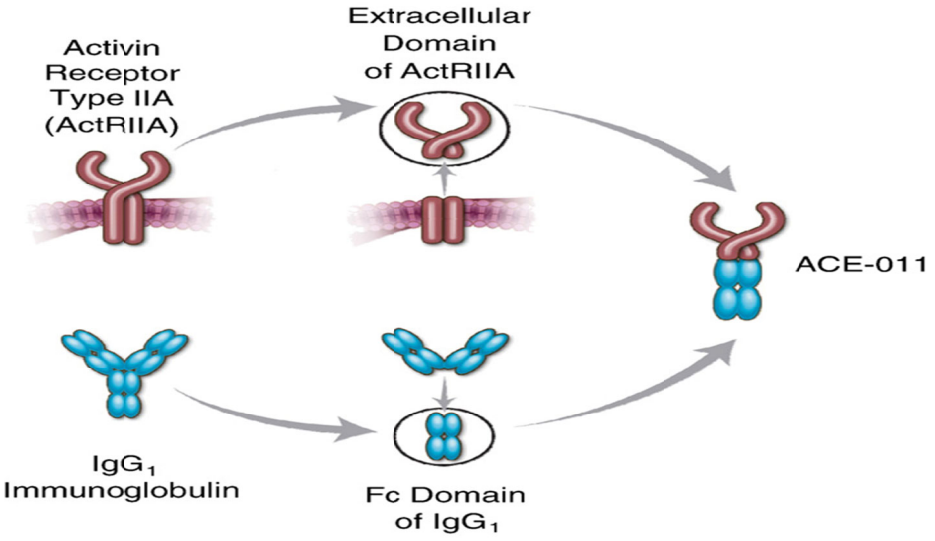

Figure I.6A. Sotatercept is the result of the extracellular domain of the Activin Receptor IIA, aimed at recognizing the specific ligand, and the Fc domain of the IgG1 immunoglobulin. This structure makes this drug a "ligand trap" capable of competing with the natural Activin Receptor IIA in the binding of TGF-β superfamily member (Adapted from Lotinun S et al. Bone, 2010).

Activins, as well as Growth Differentiation Factors (GDFs) and Bone Morphogenetic Factors (BMPs), are cytokines belonging to the Transforming Growth Factor-β family (TGF-β) whose signaling is mediated by twelve different serine/threonine kinase receptors (7 type I and 5 type II receptors) (Harrison CA et al. Growth Factors, 2011; Akhurst RJ et al. Nat Rev Drug Discov. 2012; Breda L et al. Hematol Oncol Clin North Am, 2014). Activin receptors II are shared by different GDFs and BMPs (Tsuchida K et al. Cell Commun Signal, 2009), but the downstream pathway activated by these molecules requires the formation of a ternary complex between Activin receptors type I (ACVR1A and ACVR1B) and Activin Receptors type II (ACVR2A and ACVR2B) (Worthington JJ et al. Trends Biochem Sci. 2011). Sotatercept recognizes and binds the ligand of the Activin Receptor IIA, inhibiting the interaction between ligand and receptor and, accordingly, the ligand downstream pathway. For this reason, different studies focused on its effects in order to establish if it could be proposed as a therapeutic agent for bone marrow failure syndromes hallmarked by dyserythropoiesis. These studies underline how these effects were possible due to the neutralization of a possible negative regulator of erythropoiesis that is produced by BM stromal cells, that have a relevant role in creating the microenvironment of developing erythroid cells (Iancu-Rubin C et al. Exp Hematol, 2013). Encouraging results were obtained by treating wild-type mice with RAP-011 (murine ortholog of ACE-011). Red blood cells parameters showed increases in red blood cell count, hemoglobin and hematocrit values, and reticulocyte count. The activity of RAP-011 requires the presence of BM accessory cells because of the production of a TGF-β molecule recognized by the ligand trap (Carrancio S et al. Br J Haematol, 2014). The levels

of some members of TGF-β superfamily were assessed, but only one of this resulted upregulated in thalassemia: Growth Differentiation Factor 11 (GDF11). Indeed, the assessment of GDF11 levels in β-thalassemic mice sera showed an upregulation of the molecule in comparison with the levels detected in wild-type mice, respectively. The same trend was observed in the assessment between the sera of thalassemic patients and healthy controls (Dussiot M et al. Nat Med, 2014). Given these encouraging results, Sotatercept has been proposed as a possible therapeutic agent capable of overcoming the ineffective erythropoiesis condition typical of β-thalassemia, but also of Diamond-Blackfan Anemia (Ear J et al. Blood, 2015) and Myelodysplastic Syndrome (Mies A et al. Curr Hematol Malig Rep, 2016).

Finally, following these *in vitro* studies and their interesting results, the effects of Sotatercept and Luspatercept on the erythropoiesis were assessed in different clinical trials. Particularly, clinical trials on β-thalassemic patients (Motta I et al. Expert Opin Investig Drugs, 2017; Cappellini MD et al. Haematologica, 2019; Piga A et al. Blood, 2019) and Myelodysplastic patients (Mies A et al. Semin Hematol, 2017; Platzbecker U et al. Lancet Oncol. 2017; Komrokji R et al. Lancet Haematol, 2018; Bewersdorf et al. Leukemia, 2019) obtained encouraging results in terms of increased hemoglobin levels and tolerability.

7. Aims

Congenital Dyserythropoietic Anemia type II is the most common form among the CDAs, although it is still considered a rare disorder. Probably, it is possible to assume that its frequency is still underestimated because of the availability of diagnostic methods and the differential diagnosis with the other hereditary anemias with overlapping features (Russo R et al. Am J Hematol, 2014; Russo et al. Am J Hematol, 2018). In the last years a major knowledge on CDA II causative gene and the advent of next-generation sequencing technologies allowed to simplify the diagnostic procedures and to identify novel *SEC23B*

variants (Russo R et al. Am J Hematol, 2018). However, still little is known about the molecular pathogenesis of this disease, also because of the lack of a reliable animal model reproducing the features of CDA II. Moreover, the management of patients is still based on supportive cares for the different symptoms arising from the disorder.

The first aim of my study was the establishment of a cellular model of CDA II capable of recapitulating the defect at the basis of this disorder. For this purpose, we selected K562 cells that can be considered the most suitable for studies on red cell disorders, among the secondary cell lines. Since CDA II is a loss-of-function disorder, we reached our purpose by stably silencing *SEC23B* expression in K562 cells by means of short hairpins RNA. Following the shRNA-based knockdown of K562 cells, we assessed the effects of SEC23B silencing on some typical erythroid characteristics in order to determine if this could be a reliable model for CDA II.

In the second part, we decided to evaluate the effects of RAP-011 (murine ortholog of ACE-011) on *SEC23B*-silenced K562 cells. Indeed, given the common features between β -thalassemia and CDA II, we decided to test the effectiveness of the ligand trap on our model in a preclinical study. Before assessing if RAP-011 could restore erythroid differentiation, we also focused on the effects of GDF11 on cells in order to understand if it could have a role in CDA II molecular pathogenesis.

II. MATERIALS AND METHODS

1. Cell cultures

K562 cell line (ATCC, Manassas, VA) is a model of chronic myelogenous leukemia (CML), so it is representative of cells of the myeloid lineage (Lozzio CB et al. Blood, 1975). K562 cells were maintained in RPMI medium (Sigma Aldrich, Milan, Italy) supplemented with 10% FBS (Sigma Aldrich), 2% Pen/Strep (Sigma Aldrich) and 1% L-Glutamine (Sigma Aldrich). Cells were grown in humidified 5% CO2 at 37°C.

2. Production of Lentiviral particles and infection of K562 cell line

To obtain a SEC23B loss-of-function model of CDAII on K562 cells we applied the short-hairpin RNA-based strategy. Short-hairpin RNAs are artificial RNA molecules capable to silence target gene expression via RNA interference. The expression of these shRNAs in mammalian can be obtained through the delivery of plasmids or viral vectors (Paddison PJ et al. Gene Dev. 2002). In this study, a pGIPZ Lentiviral shRNAmir vector was used to knockdown SEC23B gene expression (Thermo Fisher Scientific, Inc.). We used two different shRNAs for SEC23B (sh-70 and sh-74). A non-silencing pGIPZ Lentiviral shRNAmir was used as control (RHS4346, sh-CTR). HEK-293T were transfected by 10µg of sh-RNA plasmid DNA and 30µl of Trans-Lentiviral packaging Mix (Open Biosystems) and 25µl of TransFectin (Bio-Rad) in 10mm plate. The supernatants (10 ml for points) were harvested after 24 hours, centrifuged at low speed to remove cell debris and filtered through a 0.45 µm filter. HEK293T cells were seeded at the concentration of $5x10^5$ cells and, after reaching a confluence of 70%, they were transduced with different dilutions of viral vector stocks. For each transduction, 8 µg/ml of Polybrene (Sigma Aldrich) was used (Zhang B et al. Genet Vaccines Ther. 2004). After 48 hours of incubation, the transduced

cells were examined microscopically for the presence of TurboGFP expression (90-95%). The reported data are representative of the experiments performed and confirmed by using both lentiviral vectors for each gene. The lentiviral particles of sh-CTR, sh-70 and sh-74 (50 MOI) were used to infect the K562 cell line. After 48h of infection, the cells were maintained in puromycin (0.5 mg/mL) for 2 weeks and then analyzed for GFP+ expression and sorted by cell sorting flow cytometry assay. The sorted GFP+ cells were then assayed for SEC23B expression to verify the stability of the produced clones. The strategy used for the production of these K562 sh-SEC23B cells was already described (Russo R et al. Blood, 2016). The efficiency of SEC23B silencing of these clones was assessed by gene and protein expression analyses, through quantitative-real time PCR and Western Blot, respectively, where the expression levels of the sh-*SEC23B* clones were compared to the ones observed in the Sh-CTR.

3. Erythroid differentiation

Erythroid differentiation of K562 *SEC23B*-silenced cells was performed through the administration of hemin. Hemin is an iron-containing porphyrin with chlorine that can be formed from a haemgroup, such as haem b found in the hemoglobin of human blood. Particularly, it contains ferric iron (Fe3+) ion with a coordinating chloride ligand. Hemin was demonstrated to induce the development of erythroid phenotypic features when administered to K562 cells, such as the increased synthesis of fetal hemoglobin (HbF) (Benz EJ Jr et al. Proc Natl Acad Sci U S A, 1980).

In our study, 50 μM hemin (Sigma) was added to the culture medium of the K562 sh-CTR, sh-*SEC23B*-70 and sh-S*EC23B*-74 (4×10^5/mL). Cell samples were collected at specific time points: before hemin addition, day 0, and at days 1, 2 and 3 after hemin addition. Cell samples were used for the assessment of differentiation obtained through this process. In our study, differentiation was assessed by FACS detection of transferrin receptor 1 (CD71)

and glycophorin A (CD235), being both surface markers of differentiation of erythroid precursors (Andolfo I et al. Haematologica, 2010). Similarly, 600 μM sodium butyrate (Sigma) was administered to K562 sh-CTR, sh-*SEC23B*-70 and sh-*SEC23B*-74 and the same time points were considered to assess its effects: day 0, before sodium butyrate, and days 1, 2 and 3.

4. Patients

Twenty-two CDA II patients and 17 age and gender-matched healthy controls (HCs) were enrolled in the study. Peripheral blood leukocytes (PBLs) and plasma were isolated from both CDA II patients and HCs. Samples were obtained after informed consent, according to the Declaration of Helsinki. CDA II diagnosis was based on clinical findings, biochemical and molecular analyses.

Plasma was separated from blood following centrifugation of 10 minutes at 3000 rpm. Plasma was collected from the top of the tubes and transferred to 2 ml tubes, stored at -80 °C. Mononuclear cells were isolated using Ficoll-Hypaque (1.077-0.001 kg/L; Sigma-Aldrich, Milan, Italy). These pellets were collected for the isolation of RNA and stored at -80 °C.

5. RAP-011 treatment

K562 sh-CTR and sh-SEC23B-74 cells were selected for RAP-011 treatment. Recombinant human GDF11 protein (R&D Systems, 1958-GD) was used at 50 ng/ml, while RAP-011 (a murine version of Sotatercept, ACE-011), provided by Celgene Corporation, was used at 0.05 μg/μl.

The first treatment was aimed at evaluating the right concentrations of the main components of this experiment (GDF11 and RAP-011) and the effects of this strategy, based on GDF11-administration versus a combined GDF11+RAP-011 administration. In

the second case, the addition of the ligand trap should inhibit the binding of GDF11 and so, the activation of its downstream pathway. K562 sh-CTR cells were counted, led to a concentration of 400.000 cells/ml and induced in erythroid differentiation by the administration of hemin, as previously described. After 3 and 6 days, cells were divided for three different groups: non-treated cells, GDF11-treated cells, and GDF11+RAP-011-treated cells. The first group represents our negative control, while GDF11 addition should reproduce the pathologic context and the third group simulates the ligand trap activity exerted by the RAP-011 towards the GDF11. Cells were collected after 3 hours, centrifugated and the resulting pellets were used for protein extraction.

The second treatment was repeated on both sh-CTR and sh-SEC23B-74 cells. A time-course treatment with three different points was performed: 0.5 hours, 1 hour and 2 hours. At each of this interval, the same amount of cells was collected through centrifugation and the resulting pellets were used for different applications (RNA isolation, extraction of total proteins and nuclear proteins, immunofluorescence, cell cycle analysis).

6. Cell viability assay

K562 sh-CTR and K562 sh-SEC23B-74 cells were counted and seeded as six replicates into 96-well plates at a density of $1x10^4$ cells per well. Cells were treated with two different concentrations of RAP-011 (50 and 100 μM) and cells treated with the vehicle were used as control. Cell viability was assessed after 24h, 48h and 72h from the start point by using the 3-(4,5-dimethylthiazol-2-yl)-2,5-diphenyltetrazolium bromide assay according to the manufacture protocol (Promega, Milan, Italy). In the case, 10 μl was of this solution was added to each well and cells were incubated for 3 hours at 37. Then, cells were centrifugated, the medium was aspirated as much and replaced for 1 hour with 100 ul DMSO that dissolves formazan crystals. Following this step, we read the absorbance of the

plate at 570 nm by a spectrophotometer. These values are proportional to the viability and the metabolism of cells.

7. Gene expression analysis

RNA isolation

Total RNA was extracted from PBLs and K562 cells using Trizol reagent (Life Technologies). This reagent is mainly composed of phenol capable of lysing cell or tissue samples and isolating RNA from all the other components. Following the addition of Trizol on cell pellets, we lysed the cells pipetting different times, then samples were incubated for 5 minutes at room temperature to help the dissociation of the nucleoproteins complex. Then, chloroform was added (per 1 ml of Trizol, we used 300 µl of chloroform), samples were mixed and centrifugated for 20 minutes at 13000 rpm at +4 C. Following this step, we had a lower red phenol-chloroform, an interphase, and an aqueous phase. The upper phase, containing the RNA, was transferred to another clean tube and mixed with isopropanol (volume ratio 1:1) to precipitate the RNA. For this purpose, the tubes were shaken and centrifugated for 15 minutes at 13000 rpm at 4 °C. After removing the supernatant, we had a white pellet corresponding to the RNA. We resuspended the pellet in Ethanol 75% (prepared in DEPC water) to wash the RNA and centrifugated for 10 minutes at 13000 rpm at 4 °Cs. At this point, we removed the supernatant and we let the pellet air-dry. Then, the RNA was resuspended in DEPC water, the tubes were transferred in a heat block for 10 minutes at 65 °C, in order to let the RNA solubilize. Finally, RNA samples were stored at -80 °C.

Retrotranscription

Quantization of RNA samples was obtained through the spectrophotometer that is designed to measure the absorbance and calculate the concentration of nucleic acids (260 nm) Synthesis of cDNA from total RNA (1 µg) was performed using a cDNA synthesis kit

(Applied Biosystems, Milan, Italy). This kit consists of the Reverse Transcriptase that performs the synthesis of cDNA from RNA, the dNTPs used for the synthesis, the Random Primers and a Buffer containing components necessary for the RT activity.

- ✓ RT Buffer (10x): 2 μL
- ✓ dNTPs (25x): 0.8 μL
- ✓ RT primers (10x): 2 μL
- ✓ RT: 1 μL
- ✓ H_2O: To final volume
- ✓ RNA: 1 μg

We used the thermocycler since this reaction requires different temperatures in order to obtain the synthesis.

Quantitative real-time PCR analysis

Gene expression analysis on cDNA samples was based on Quantitative Real-Time PCR (qRT-PCR) using Power SYBR Green PCR Master Mix (Applied Biosystems). This method represents a variant of PCR, allowing to obtain a measurement of the amplified samples. For each sample, we used 60 ng of cDNA as template, the Mix containing the polymerase and all the components necessary for the reaction, and the forward and reverse primers to recognize the selected genes. In the case, qRT-PCR was performed to evaluate the gene expression of *GDF11*, *SEC23B, SEC23A, GATA1, KLF1, ABCB6, ALAS2, HBB, HBG, BCL-2, BAX, BAD, CCNA2, ACVR1A, ACVR1B, ACVR2A, ACVR2B, FAM132B* genes. Samples were amplified on Applied Biosystems 7900HT Sequence Detection System using standard cycling conditions. The primers were designed by the Primer Express 2.1 program (Applied Biosystems). β-actin and GAPDH were used as internal controls. Relative gene expression was calculated by using the $2^{-\Delta Ct}$ method, while the mean fold change = $2^{-(\text{average } \Delta\Delta Ct)}$ was assessed using the mean difference in the ΔCt between the gene and the internal control[11].

8. Protein expression analysis

Protein extraction

Proteins were extracted from cell lines pellets using RIPA lysis buffer (TRIS-HCl pH 7.5 50 mM, NaCl 150 mM, Triton 1%, Glycerol 10%, SDS 0.1%) in presence of a protease inhibitor cocktail (Roche) and a phosphatase inhibitor cocktail (Roche). Samples in the tubes were vortexed to lyse the cells for 15 minutes at 4 °C and then centrifugated to isolate the protein content. Protein extract concentrations were determined by the Bradford assay (BioRad, Milan, Italy) that is based on the binding of protein molecules to Coomassie dye that results in a change of color of the solution from brown to blue, depending on the concentration of the samples. Each sample was quantified with Bradford solution through the measurement of the absorbance at 595 nm. The concentration values were obtained through the comparison with a standard curve, showing increasing amounts of bovine serum albumin (BSA). Every measurement was performed in duplicate and a mean of the values was used.

Western Blot

Total protein extracts (30 or 50 μg) were mixed with Sample Buffer Laemli 2X (SBL) and heated at 100 °Cfor 5 minutes. Both the 2-mercaptoethanol contained in the SBL and the heating were used to help protein denaturation. Indeed, these samples were analyzed by sodium-dodecyl sulfate polyacrylamide gel electrophoresis (SDS-PAGE), a method based on electrophoresis that separates charged molecules by mass. Proteins are negatively charged by SDS contained in the SBL and in the matrix of the gel, so the separation of the proteins is due to the migration from a negative to a positive pole. Gels were prepared with different concentrations of polyacrylamide depending on the size of the protein to investigate. The proteins, separated on the gel depending on their mass, were then

transferred to PVDF (polyvinylidene difluoride) membranes (Biorad, Milan, Italy), that are useful for all the applications of the Western Blot. This membrane is activated with Ethanol, so it is positively charged during the transfer and naturally attracts the proteins negatively charged from the polyacrylamide gel. In order to check if the proteins were transferred properly from the gel, the membrane was stained with Ponceau S Solution. This red solution allows a reversible detection of the protein bands on the membrane. Then, the membrane was incubated with Nonfat-Dried Milk (NFDM) or BSA to saturate all the non-specific sites in order to have cleaner and more specific signals. Following this step, membranes were incubated with following primary antibodies: rabbit anti-SEC23B antibody (1:500; SAB2102104, Sigma Aldrich, Milan, Italy), rabbit anti-pSMAD2 (1:500; 43108,Cell Signaling), rabbit anti-SMAD 2/3 (1:1000;5678, Cell Signaling). Mouse anti-β-actin antibody (1:12000; A5441, Sigma Aldrich, Milan, Italy) and rabbit anti-GAPDH (1:1000; 2118, Cell Signaling) were used as the controls for equal loading. Following the incubation of these primary antibodies, goat anti-mouse IgG (1:4000; GtxMu-003, ImmunoReagents, Inc.) and goat anti-rabbit IgG (1:4000; GtxRb-003, ImmunoReagents, Inc.) were used. Signal was obtained through Chemiluminescence detection with photographic films or CCD cameras. Semi-quantitative analysis of protein expression was performed as previously described (Russo R et al. Blood Cells Mol Dis, 2013). The bands were quantified by Quantity One software (Biorad) to obtain an integrated optical density (OD) value, which then was normalized with respect to the β-actin or GAPDH.

Secreted proteins

Expression of secreted proteins was assessed by loading plasma samples (from patients and healthy controls) to SDS-PAGE, followed by transfer to PVDF membrane and incubation with the anti-GDF11 antibody (1:500; ab124721, Abcam, Cambridge, UK) and the goat anti-rabbit IgG (1:4000; GtxRb-003, ImmunoReagents, Inc.), as previously described. Normalization of results was obtained through the Ponceau red staining of the blots.

Subcellular fractionation

Subcellular fractionation in nuclear and cytosolic proteins was performed according to the Schreiber method (Schreiber et al 1990). Harvested cells were washed twice with ice-cold PBS and homogenized with ice-cold buffer [10 mM HEPES, pH 7.9; 1.5 mM $MgCl_2$, 1 mM EDTA, 0.5 mM DTT, 10% (v/v) glycerol, 1mM PMSF, and protease inhibitor cocktail (Roche)]. After resuspension, we syringed suspension and then centrifuged in order to separate cytosolic suspension from the nuclear pellet. Then, the nuclear pellet was resuspended in the same lysis buffer in the presence of KCl 3M. Nuclear extract was stored in ice for 1h, then centrifuged for 30 minutes at 16.000 g.

For protein expression analysis, 15 μg of nuclear proteins extracts were loaded to SDS-PAGE, transferred to PVDF membrane and saturated with NFDM, as previously described. Membranes were incubated with mouse anti-GATA1 antibody (1:500; H00002623-M06, Abnova), mouse anti-HSP-70 (1:5000; SAB4200714, Sigma Aldrich, Milan, Italy) and rabbit anti-SMAD4 (1:1000; ab215968, Abcam). Rabbit anti-LAMIN-B (1:50; sc-6216, Santa Cruz) and mouse anti-TBP (1:1000; ab51841, Abcam) were used as the control for equal loading of nuclear proteins. Semi-quantitative analysis of protein expression was performed as previously described.

9. Immunofluorescence

K562 sh-CTR and K562 sh-SEC23B-74 GDF11-treated and GDF11+RAP-011 treated cells were counted and $1x10^6$ of them were centrifugated. Then, cells were fixed, by resuspending the pellet with the Paraformaldehyde solution (PFA) and incubating for 10 minutes at room temperature. After centrifugation to remove PFA, the cell pellet was washed with Ammonium Chloride dissolved in PBS (two incubations of 10 minutes separated by centrifugations of 5 minutes) at room temperature. Then, cells were resuspended in PBS at a concentration of $1x10^6$/ml. Cells were plated on microscopic

slides ($3x10^5$ cells) that had been previously treated with polylysine. Polylysine shows positive charges, so it can bind easily negatively charged proteins on the cell surfaces. Polylysine was dissolved in solution and added to the slides in order to allow the adhesion of the cells. Then, plated cells underwent permeabilization by adding Triton 0.1%, in order to allow the binding of the antibodies to intracellular proteins. As previously described for Western Blot, cells were incubated with BSA/PBS to saturate the non-specific sites. Afterward, cells were incubated with primary antibody (rabbit anti-GATA1, 1:50) and secondary antibody (Alexa Fluor 546 goat anti-rabbit; Life Technologies) at 1:200 dilution. Nuclei were stained with 1 μg/ml DAPI in PBS for 15 min at room temperature. The coverslips were mounted in 50% glycerol (v/v) in PBS and imaged by Zeiss LSM 510 Meta confocal microscope equipped with an oil immersion plan Apochromat 63× objective 1.4 NA. Red channel excitation of Alexa546 by the Helium/Neon laser 543 nm line was detected with the 560-700 nm emission bandpass filter (using the Meta monochromator). Blue channel excitation of DAPI by the blue diode laser 405 nm line was detected with the 420-480 nm and emission bandpass filter.

10. Cell cycle analysis

K562 sh-CTR and K562 sh-SEC23B-74 cells were collected following both the GDF11 and GDF11 + RAP-011 treatment to perform flow cytometry analysis. Cells were washed twice in PBS 1X and after they were resuspended in 1 ml of a solution consisting of 29 μg/μl propidium iodide (SIGMA), 25 μg/μl RNAse (SIGMA), and 0.004% NP40 in PBS 1X. Cells were incubated for 3 hours at 37°C. The flow cytometry analysis was performed by the flow cytometry facility at CEINGE Institute.

11. Statistical analysis

Quantitative data were compared using Student's t-test or Mann Whitney test, as appropriate. Qualitative data by chi-square test, correlation analysis by Spearman's rho (ρ) correlation coefficient. A two-sided $p<0.05$ was considered statistically significant.

III. RESULTS

1. K562 as a cell line model for erythroid cell development

In order to find a cell line capable to reproduce red blood cells development features, we chose the K562 cell line. K562 cells are a human myelogenous leukemia cell line and can be used to reproduce the erythroid or megakaryocytic development, depending on the administered drugs used for the differentiation. We tested these cells ability to undergo erythroid differentiation by using hemin (50 µM). After 3 days the differentiation was evaluated by calculating the percentage of K562 cells positive for the transferrin receptor (CD71+ cells). This analysis exhibited an increase in the percentage of positive cells for this surface receptor that is about 5-fold on day 1, about 11-fold on day 2 and about 14-fold on day 3 (Figure III.1A).

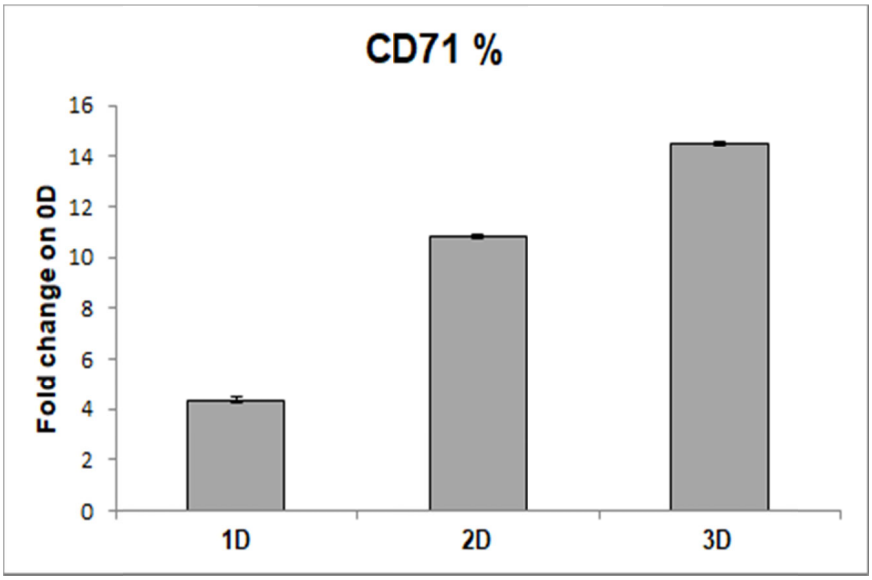

Figure III.1A. Percentages of K562 cells showing CD71 surface receptor following hemin addition at days 1, 2 and 3. A constant increase of this percentage was shown as a result of a fold change on the percentage of CD71+ K562 cells at day 0. These results were produced by FACS analysis.

This method of stimulation to the erythroid differentiation was compared with another one, based on the administration of another drug, the sodium butyrate (2 mM). In this case, an increase in the number of CD71+ K562 cells was also observed, but the percentages of differentiation, folded on day 0, were lower than the ones observed with hemin addition (Figure III.1B).

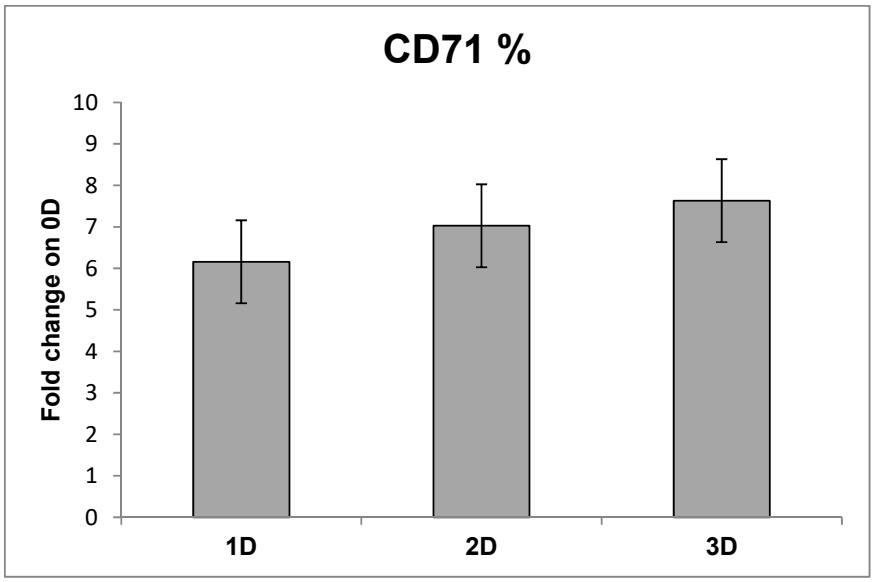

Figure III.1B. Percentages of K562 cells showing CD71 surface receptor following sodium butyrate addition at days 1, 2 and 3. The increases in percentages of CD71 positive cells were 6-fold, 7-fold and 7.6-fold for 1, 2 and 3 days, respectively. These values were shown as a result of a fold change on the percentage of K562 cells showing CD71 on their surface at day 0. These results were produced by the FACS analysis.

2. ***Silencing of SEC23B expression in K562 cells***

K562 cell line was chosen as a model for our studies on CDAII given its ability to reproduce some erythroid features, such as the presence of the transferrin receptor on their

surface. Indeed, K562 cells were infected with short hairpin RNAs lentivirus targeting *SEC23B* (CDAII causative gene) expression. Following the sorting of GFP+ cells, the silencing of the targeted gene, SEC23B, was assayed in the two selected clones of K562 sh-*SEC23B*-70 and K562 sh-*SEC23B*-74 cells in comparison with the expression showed by K562 sh-CTR cells. Gene expression analysis was performed in order to assess the levels of interference of *SEC23B* expression. By gene expression analysis, K562 sh-SEC23B-74 cells showed lower levels of *SEC23B* compared to K562 sh-CTR cells, while sh-SEC23B-70 cells exhibited an even more marked downregulation (2.3- and 3.7-fold decrease, respectively, compared to the sh-CTR) (Figure III.2A).

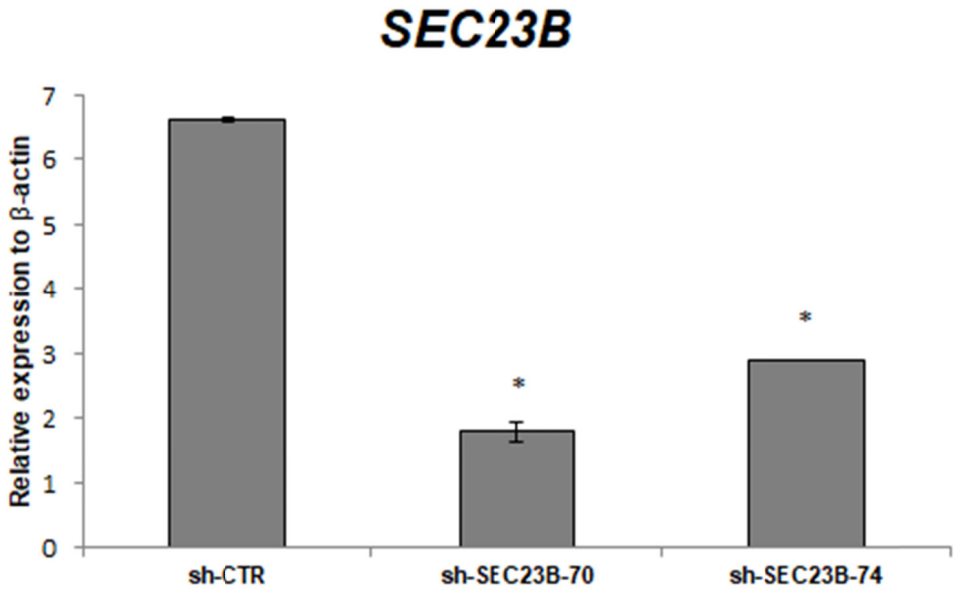

Figure III.2A. mRNA levels of SEC23B in K562 cells stably silenced for *SEC23B* after infection with short hairpins targeting *SEC23B* lentivirus. These gene expression results of K562 sh-SEC23B-70 and K562 sh-SEC23B-74 are compared with the gene levels of K562 sh-CTR, through quantitative real-time PCR. β-actin is the reference gene. Data are presented as mean ± SD. P-value by Student t-test; ** $p < 0.01$; * $p < 0.05$.

The effects of SEC23B silencing, mediated by the short hairpin RNAs on K562 cells, were also assessed through the detection of SEC23B protein levels in both the clones of K562 sh-SEC23B-70 and sh-SEC23B-74 stable clones compared with the amount of the same

protein produced by sh-CTR cells. The downregulation of SEC23B expression following the shRNAs silencing was confirmed at protein level too, in K562 sh-SEC23B-70 and K562 sh-SEC23B-74 (Figure III.1B). Moreover, a quantification of the protein values of both the sh-SEC23B clones and sh-CTR was performed through optical density. The graph of these values is shown below the Western blot panel (Figure III.2B).

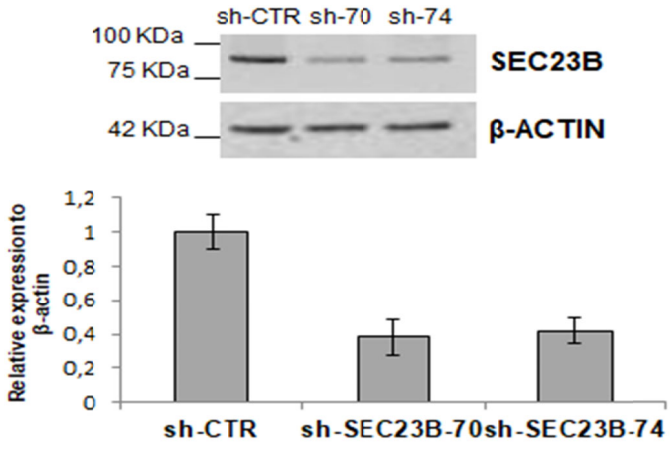

Figure III.2B. Protein expression assessment of SEC23B in K562 sh-CTR and sh-SEC23B stable clones. SEC23B protein expression in sh-CTR, sh-SEC23B-70 and sh-SEC23B-74 cells by western blot is shown. β-actin is the protein used as the loading control. In the below panel, a graph shows the quantification of SEC23B protein levels detected by the western blot, using β-actin as a reference protein.

Moreover, gene expression of *SEC23A*, paralog gene of *SEC23B*, was evaluated in K562 sh-CTR, sh-SEC23B-70 and sh-SEC23B-74 cells. An upregulation of *SEC23A* gene expression was observed in K562 sh-SEC23B-74 compared to the K562 sh-CTR (1.4 fold), as expected for a cell line model reproducing CDAII features. Instead, in K562 sh-SEC23B-70 a strong decrease of *SEC23A* compared to the K562 sh-CTR (3.1 fold) was shown, maybe due to a less specific activity of short hairpin 70 (Figure III.2C).

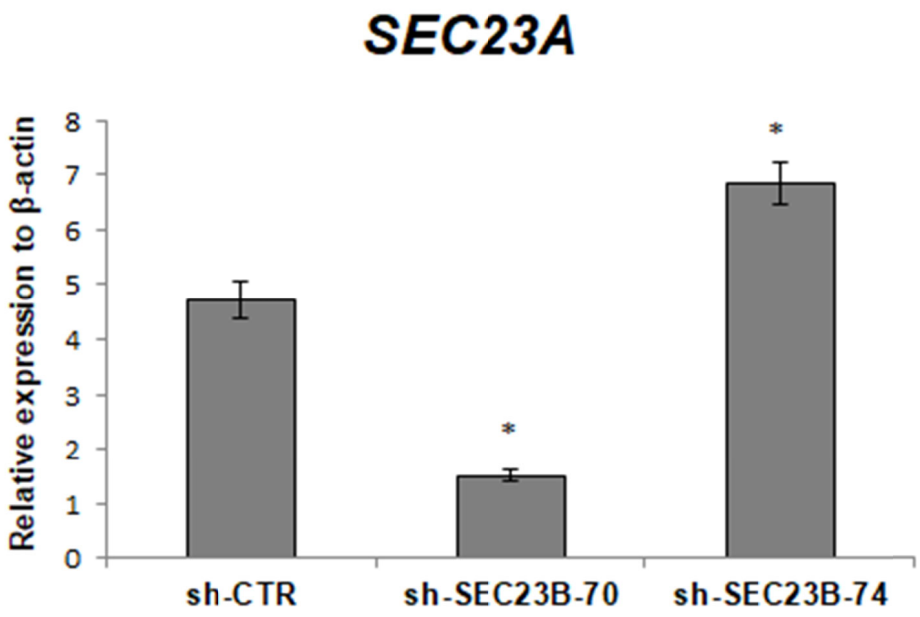

Figure III.2C. mRNA levels of SEC23A in K562 sh-CTR and both the K562 sh-SEC23B cells. These gene expression results of K562 sh-SEC23B-70 and K562 sh-SEC23B-74 are compared with the gene levels of K562 sh-CTR by qRT-PCR. While K562 sh-SEC23B-74 cells exhibit upregulation of *SEC23A* compared to the sh-CTR, sh-SEC23B-70 clone had a decreased *SEC23A* expression. β-actin is the reference gene. Data are presented as mean ± SD. P-value by Student t-test; ** $p < 0.01$; * $p < 0.05$.

3. Erythroid differentiation of K562 sh-CTR and sh-SEC23B cells

In order to assess the potential to display erythroid features of the K562 sh-SEC23B cells compared to the K562 sh-CTR cells, a treatment based on hemin administration was performed. This experiment was evaluated by the detection of erythroid differentiation marker CD71 in K562 sh-CTR, sh-SEC23B-70 and sh-SEC23B-74 cells after 2 and 5 days from the addition of hemin. The percentages of cells showing this surface marker at all these time points were calculated and, while an increase of K562 sh-CTR cells expressing CD71 was shown, K562 sh-SEC23B-70 and sh-SEC23B-74 CD71+ cells displayed a strong decrease at day 2 and 5 (Figure III.3A). Particularly, at day 2 and day 5, there was an increase of CD71+ sh-CTR cells (close to 1.7 fold and 1.6 fold, respectively). Otherwise, sh-SEC23B-70 and sh-SEC23B-74 showed a reduced amount of cells

expressing CD71 marker at day 2 (1.9 and 1.5 fold, respectively) and at day 5 (5.6 and 3.4 fold, respectively), demonstrating impairment of erythroid differentiation.

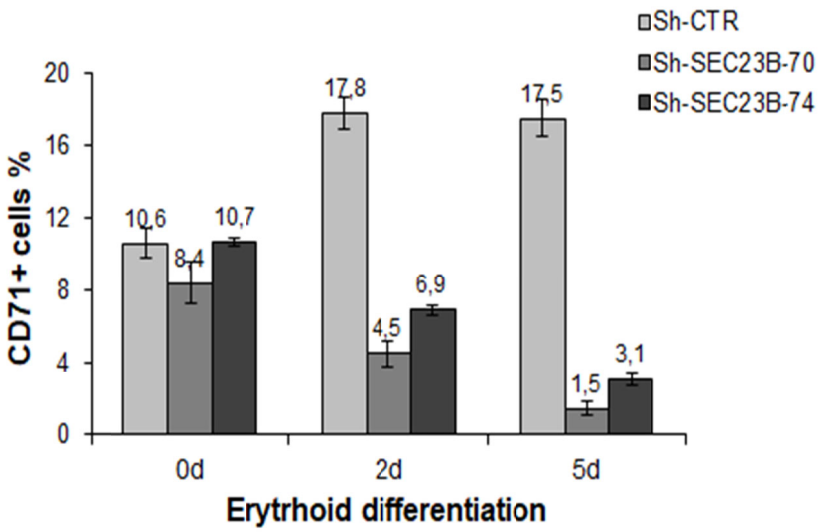

Figure III.3A. Percentages of K562 sh-CTR, sh-SEC23B-70 and sh-SEC23B-74 CD71+ cells following hemin administration were shown. The outcome of the erythroid differentiation was assessed at day 2 and day 5 from the day of hemin addition. These values result from FACS analysis.

Moreover, *SEC23B* relative gene expression in K562 sh-CTR, sh-SEC23B-70 and sh-SEC23B-74 cells was assessed at all the time points of the erythroid differentiation, at days 0 (0D), 2 (2D) and 5 (5D) from the addition of hemin. An increase of *SEC23B* levels in K562 sh-CTR cells from day 0 was observed, whereas both K562 sh-SEC23B-70 and sh-SEC23B-74 cells exhibited a gradual decrease of *SEC23B* levels during the hemin-induced differentiation (Figure III.3B).

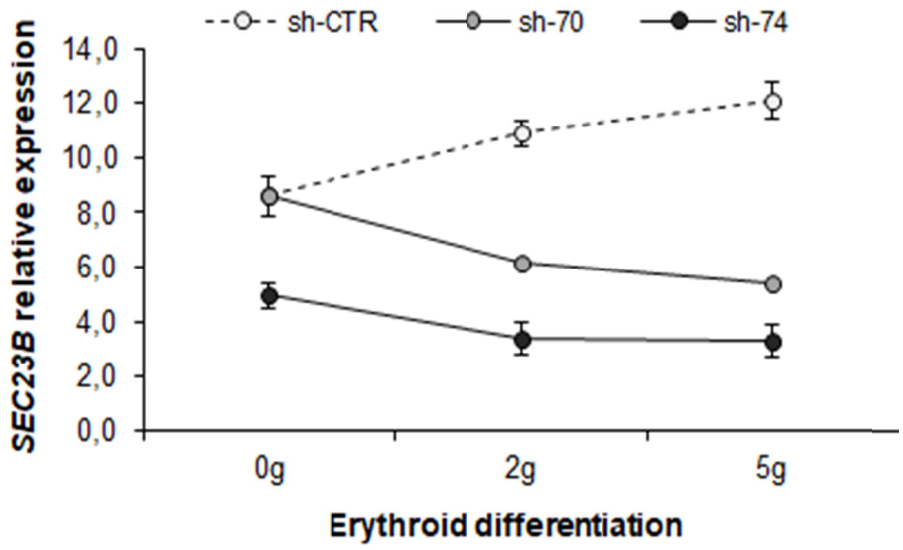

Figure III.3B. *SEC23B* relative gene expression (q-RT PCR) in K562 sh-CTR, sh-SEC23B-70 and sh-SEC23B-74 cells at 0 day (0D), 2 days (2D), and 5 days (5D) after hemin treatment. β-actin is the reference gene. Data are presented as mean ± SD.

The same analysis was conducted for the evaluation of the SEC23B protein expression in K562 sh-CTR, sh-SEC23B-70 and sh-SEC23B-74 cells at day 0, day 2 and day 5. In this case, K562 sh-CTR cells did not exhibit a marked increase of SEC23B protein during the hemin-induced erythroid differentiation, but a reduction of the protein levels in K562 sh-SEC23B-70 and sh-SEC23B-74 was still observed at days 2 and 5 (Figure III.3C).

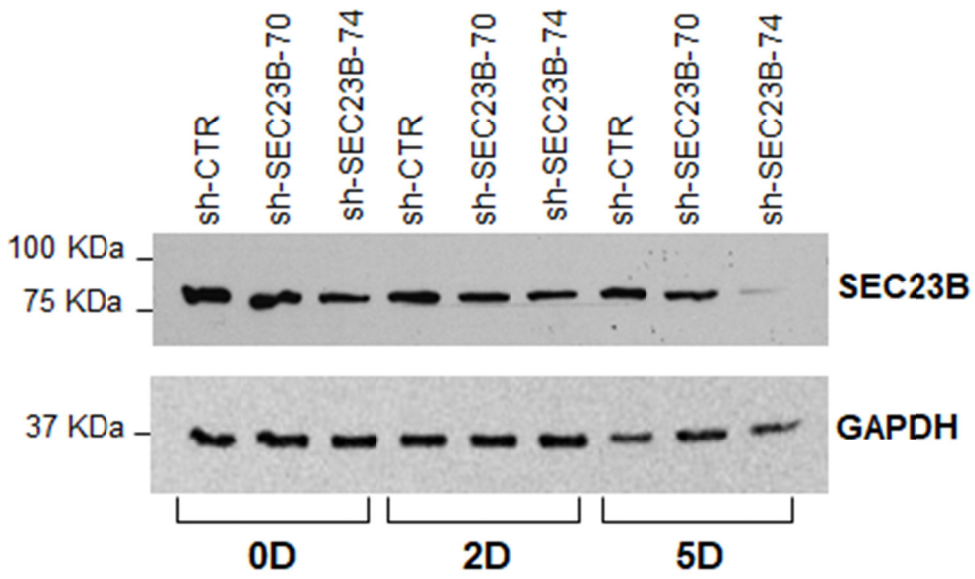

Figure III.3C. Western Blot assay showing SEC23B protein levels of K562 sh-CTR, sh-SEC23B-70 and sh-SEC23B-74 during the erythroid differentiation, from day 0 to days 2 and 5. Both the sh-SEC23B70 and sh-SEC23B-74 showed downregulation of SEC23B protein. GAPDH is the reference protein used as a loading control.

Finally, *SEC23A* gene expression of K562 sh-CTR, sh-SEC23B-70 and sh-SEC23B-74 was also measured during the hemin-based treatment on 0, 2 and 5 days. K562 sh-SEC23B-70 cells confirmed the silencing of this gene also after the induction of the erythroid differentiation while, interestingly, K562 sh-SEC23B-74 showed higher levels of *SEC23A* at day 0 (as already observed) but, moreover, a strong upregulation of SEC23A during the hemin treatment still was observed, with its highest levels at day 2. Instead, K562 sh-CTR cells did not show significant changes in *SEC23A* gene expression following the addition of hemin (Figure III.3D).

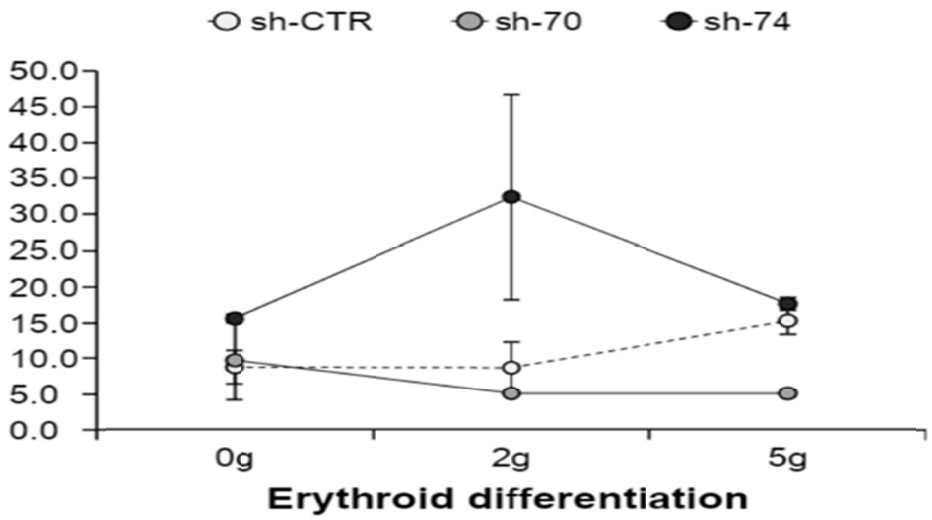

Figure III.3D. *SEC23A* gene expression levels of K562 sh-CTR, sh-SEC23B-70, and sh-SEC23B-74 during the time points of the erythroid differentiation are shown (days 0-2-5). While K562 sh-CTR cells did not show significant differences during the treatment, sh-SEC23B-70 cells showed a gradual decrease from day 0, while sh-SEC23B.74 cells exhibited an increase of *SEC23A* levels at day 0, but also a marked upregulation at 2 and 5 days. Relative gene expression of *SEC23A* in K562 sh-CTR, sh-SEC23B-70 and sh-SEC23B-74 cells was obtained through the comparison with β-actin as a reference gene.

4. Investigation of GDF11 role in CDAII pathogenesis

Given a large number of studies proposing GDF11 as a marker of β-thalassemia, we decided to investigate its expression in CDAII patients compared to the healthy controls (HCs). We selected 22 SEC23B-related CDA II patients and 17 HCs in order to measure GDF11 levels in the peripheral blood mononucleate cells (PBMC). CDAII patients were diagnosed on the basis of typical CDAII clinical features and molecular diagnosis (Table III.1).

Table S1. Clinical features of CDA II patients included in the study

Origin	Age* (years)	RBC (10^6/µL)	Hb (g/dL)	Ht (%)	MCV (fL)	MCH (pg)	MCHC (g/dL)	RDW (%)	PLT (10^3/µL)	Retics abs count (/µL)	Tb (mg/dL)	Ub (mg/dL)	Ferritin (ng/mL)	TSAT (%)	Reference PMID
Italy	29	3.70	10.3	31.7	85.7	27.7	32.3	22.0	574	110.3	1.1	0.9	469	-	21850656
Italy	43	3.34	10.5	31.3	93.9	31.6	33.5	-	286	90.0	4.9	3.8	437	95	21850656
Italy	3	3.48	9.8	30.3	87.1	28.2	32.3	26.6	408	265.7	2.4	1.6	47	61	21850656
Italy	10	3.23	9.5	26.1	83.4	29.0	35.2	-	-	42.3	3.4	2.8	206	58	20941788
Italy	5	2.67	8.7	24.5	91.0	32.8	35.5	-	357	80.1	2.5	2.1	200	70	20941788
Italy	7	3.89	10.2	30.6	79.0	26.2	33.2	21.1	294	58.4	1.9	1.3	119	52	25044164
Italy	13	4.46	11.5	34.4	77.0	25.8	33.4	17.7	518	26.8	0.2	0.1	21	15	25044164
Italy	35	3.41	10.1	31.0	91.1	29.7	32.6	21.9	706	35.0	0.8	0.6	1883	112	25044164
USA	13	3.07	7.6	24.0	76.0	24.8	31.8	21.2	363	76.8	2.3	2.0	82	-	23453696
USA	18	2.96	11.6	34.0	114.0	39.2	34.3	18.6	1065	32.6	4.8	4.3	216	99	25044164
Turkey	2	2.62	7.7	21.8	82.7	29.5	35.6	13.5	235	31.4	2.9	2.4	977	-	25044164
Turkey	2	2.63	7.0	21.2	81.0	26.7	33.1	22.9	400	207.8	1.4	1.2	244	-	25044164
Turkey	10	2.40	6.7	20.3	84.7	27.9	32.9	24.3	415	19.2	-	-	100	-	25044164
Turkey	8	3.36	9.5	27.5	81.8	28.3	34.6	20.7	474	26.9	1.8	1.5	25	-	25044164
Turkey	7	2.09	6.1	18.3	87.0	29.4	33.7	13.7	232	150.5	2.5	1.9	1218	-	25044164
Greece	4	2.85	8.9	27.0	94.7	31.3	33.1	20.1	281	83.5	1.7	1.2	64	61	25044164
Turkey	13	3.57	11.7	33.5	94.0	31.5	33.5	14.0	266	164.2	4.6	3.8	-	-	27540014
Turkey	4	3.37	9.2	27.8	82.5	27.3	33.1	22.9	271	47.2	2.2	1.8	461	96	27540014
Turkey	15	3.59	11.0	30.8	93.2	33.3	35.1	15.2	256	82.6	3.1	2.9	46	-	27540014
Turkey	1.5	3.34	10.4	30.5	91.3	31.0	34.0	14.7	390	66.8	0.3	0.2	80.5	-	27540014
Turkey	12	3.17	9.4	28.1	88.7	29.6	33.4	17.0	746	126.8	2.4	2.1	1763	-	-
Greece	27	3.00	9.9	29.9	92.0	33.0	-	-	187	105.0	4.2	3.9	117	-	27540014

RBC, red blood cells; Hb, hemoglobin; Ht, hematocrit; MCV, mean corpuscular value; MCH, mean corpuscular hemoglobin; MCHC, mean corpuscular hemoglobin concentration; RDW, RBC distribution width; PLT, platelet count; Tb, total bilirubin; Ub, unconjugated bilirubin; TSAT, transferrin saturation; PMID, PubMed ID.

*Age at diagnosis.

Table III.1. This is the list of CDAII selected patients, with their country of origin, their age at diagnosis and all the relevant clinical parameters: hematological features such as RBC, Hb, Ht, MCV, MCH, MCHC, RDW, Reticulocyte count, PLT but also bilirubin and iron markers, necessary for the evaluation of CDAII symptoms (jaundice and iron overload, respectively).

The *ex vivo* gene expression analysis showed higher *GDF11* levels in PBMC of CDA II patients compared to those measured in the PBMC of HCs. Particularly, a 3.8-fold increased expression was observed in CDAII patients *vs* healthy controls (Figure III.4A).

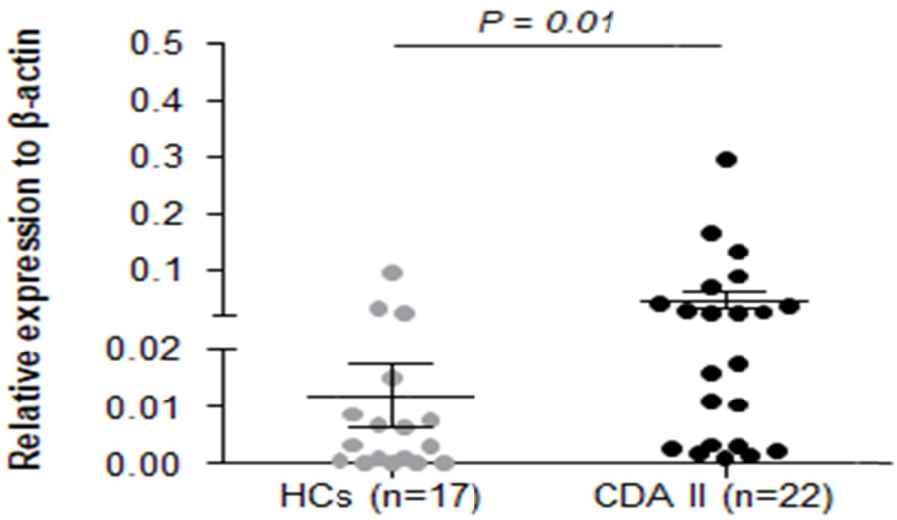

Figure III.4A. Gene expression analysis of GDF11 by qRT-PCR on peripheral blood mononuclear cells from healthy controls (n=17) and CDAII SEC23B-related patients (n=22) is shown. Higher levels of GDF11 gene expression in patients compared to the HCs were observed. β-actin is the reference gene. P-value <0.05 by Mann Whitney test.

Then, in order to confirm this trend, a protein expression analysis by Western Blot was performed. In this case, considering that GDF11 acts as a cytokine, so it is secreted to bind cell surface receptors, we measured the amount of secreted GDF11. For this purpose, this analysis was performed on plasma samples from 12 CDAII patients and 15 healthy controls (HCs). Higher levels of GDF11 in CDAII patients were observed compared to the healthy controls. These results are highlighted by the densitometric quantification of all the samples analyzed by Western Blot (Figure III.4B).

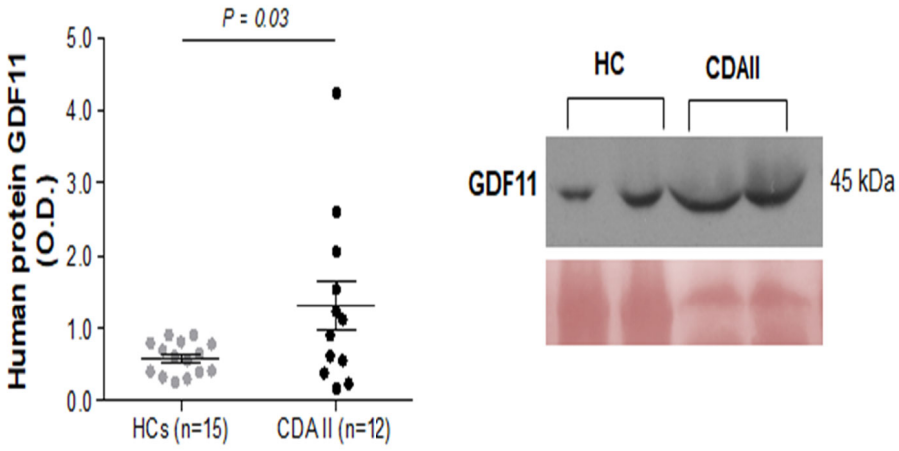

Figure III.4B. On the left panel, quantification of GDF11 by Western Blot in plasma samples from HCs (n=15) and CDAII patients (n=12) is shown. Values were obtained by optical density using Ponceau stain bands as a reference. P-value <0.05 by Mann Whitney test. On the right panel, a Western Blot image shows the trend represented by the total quantification of GDF11 performed on the selected plasma samples.

Moreover, GDF11 expression was also assessed on our CDAII *in vitro* model. Indeed, gene expression analysis through qRT-PCR was performed on K562 sh-SEC23B-70 and sh-SEC23B-74 cells compared to K562 sh-CTR cells after 5 days of erythroid differentiation induced by addition of hemin. K562 sh-SEC23B-70 cells showed a marked increase of GDF11 levels compared to K562 sh-CTR cells, as well as K562 sh-SEC23B-74, although in this case a slight upregulation was observed when compared with the GDF11 levels of K562 sh-CTR cells (Figure III.4C).

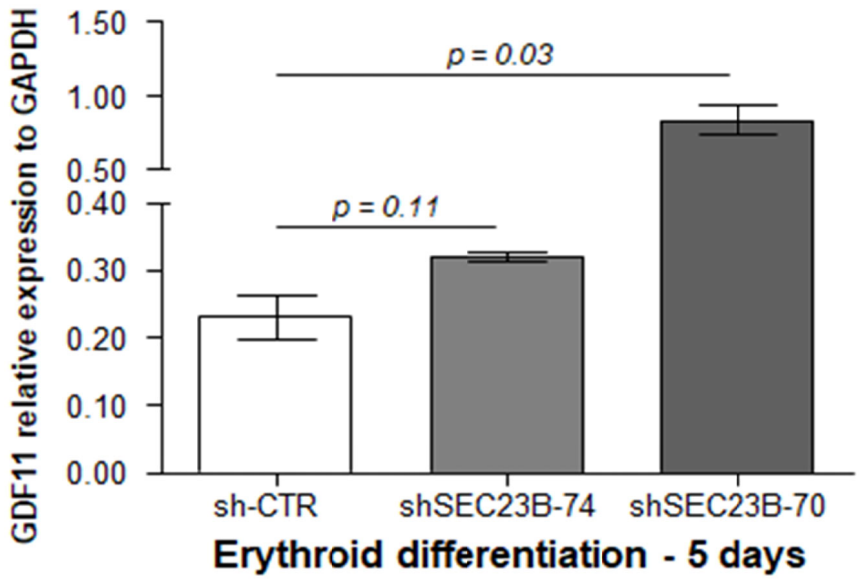

Figure III.4C. mRNA levels of GDF11 in K562 sh-SEC23B-70 and sh-SEC23B-74 cells compared with the levels detected in K562 sh-CTR cells, following 5 days of hemin-based treatment, are shown. GAPDH is the reference gene. Data are presented as mean ± SD. P-value by Student t-test; ** $p < 0.01$; * $p < 0.05$.

Finally, the amount of GDF11 secreted by K562 sh-SEC23B-70 and sh-SEC23B-74 cells was also measured in comparison with K562 sh-CTR cells. Supernatants of these clones, following 5 days of differentiation, were analyzed by Western Blot, similarly to CDAII patients and healthy controls plasma samples. However, the quantitative differences between K562 sh-SEC23B cells (both sh-SEC23B-70 and sh-SEC23B-74) and K562 sh-CTR cells were not significant (Figure III.4D).

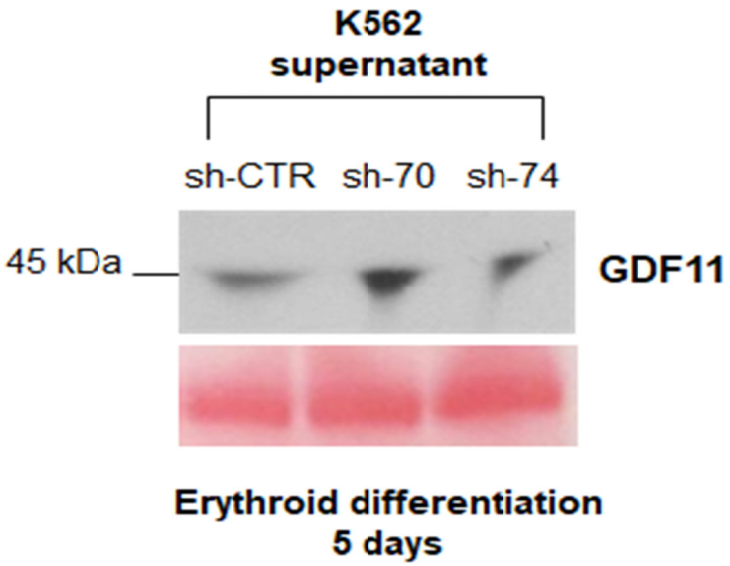

Figure III.4D. Quantification of GDF11 by Western Blot in supernatants collected from K562 sh-CTR, sh-SEC23B-70 and sh-SEC23B-74 cells is shown. Ponceau stain bands were used as a reference.

5. Cell viability assay on K562 sh-SEC23B cells following RAP-011 treatment

After the characterization of this CDAII *in vitro* model, we decided to rely on it to assess the effects of the recombinant protein RAP-011 (murine ortholog of ACE-011) on ineffective erythropoiesis. However, prior to initiating this treatment, we needed to establish the suitable concentrations of drug for our cells and if this drug had any cytotoxic effect. These analyses were performed only on K562 sh-SEC23B-74 and sh-CTR cells since K562 sh-SEC23B-70 does not reproduce all the expected features of CDAII disease, such as the lacking of upregulation of paralog gene *SEC23A*.

K562 sh-CTR and sh-SEC23B-74 cells were treated with two different concentrations of RAP-011, 50 µm and 100 µm, in order to establish the correct concentration to use for the *in vitro* treatments. Cell viability was assessed through MTT assay, that allows us the detection of the cells with normal metabolic activity, for 3 days from the administration of the drugs. K562 sh-CTR cells administered with RAP-011 50 µm showed an increase of

viability from day 0 to day 3 with a peak during the day 2, while K562 sh-SEC23B-74 cells showed constant viability during all the time points. Instead, treatment with RAP-011 100 µm produced a decrease of viability after day 1 in K562 sh-CTR cells and after day 2 in sh-SEC23B-74 cells (Figure III.5A).

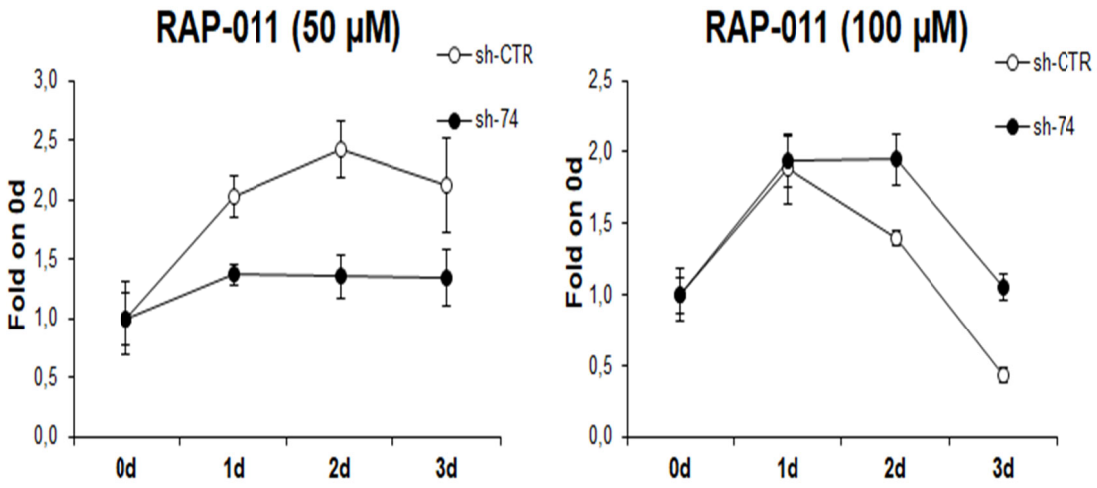

Figure III.5A. Cell viability **(**MTT) assay after RAP-011 50 µm and RAP-011 100 µm addition. Values are obtained through the fold on the viability of day 0. RAP-011 50 µm addition produced a gradual increase in viability for K562 sh-CTR cells, whereas sh-SEC23B-74 cells exhibited a constant trend from day 1. For both K562 sh-CTR and sh-SEC23B-74 cells treated with RAP-011 100 µm, a reduction in viability from day 2 was observed.

Then, we compared the viability of K562 sh-CTR and sh-SEC23B-74 cells treated with RAP-011 50 µm and with the vehicle to exclude any cytotoxic effect due to the drug administration. For both the K562 sh-CTR and sh-SEC23B-74 cells, there was an overlap between the viability curves of RAP-011-treated cells and vehicle-treated cells until the day 2, while an increased survival of K562 sh-SEC23B-74 cells following RAP-011 administration was observed from day 3 (Figure III.5B).

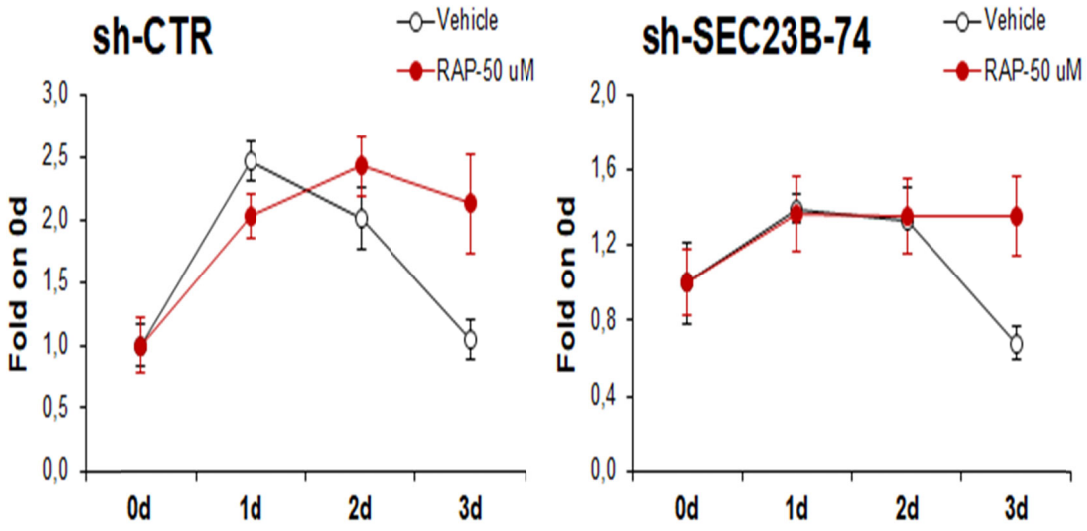

Figure III.5B. MTT assay comparing cell viability between vehicle and RAP-011 administration for 3 days from the start of the treatment. K562 sh-CTR cells treated with RAP-011 50 µm showed an increase until day 2, while vehicle-based treatment exhibited an earlier decrease in viability (day 1). Conversely, K562 sh-SEC23B-74 cells treated with vehicle and RAP-011 µm showed the same trend of viability, except for day 3 when the advantage of RAP-011 treated cells compared to the vehicle-treated cells was observed.

6. GDF11 administration actives the SMAD2 protein phosphorylation

In order to reproduce the microenvironment of CDA II marrow, we administered human recombinant GDF11 cytokine to K562 cellular medium. GDF11 has known to bind Activin Receptor IIA (and IIB), leading to the activation of the intracellular SMAD2 pathway, through the augmented phosphorylation of this protein (Rochette L et al. Pharmacol Ther. 2015; Nomura T et al. Biochem Biophys Res Commun. 2008). To establish the correct timing of GDF11 activity on our cellular model, K562 sh-CTR cells were first induced to differentiation by hemin addition and were treated with GDF11 at days 2 and 5, the same time points used for the other experiments. The administration of GDF11 (50 ng/ml) to K562 sh-CTR cells for 3 hours increased the phosphorylation of SMAD2 protein

at day 2 and day 5 of differentiation, compared to the non treated K562 sh-CTR cells (Figure III.6A).

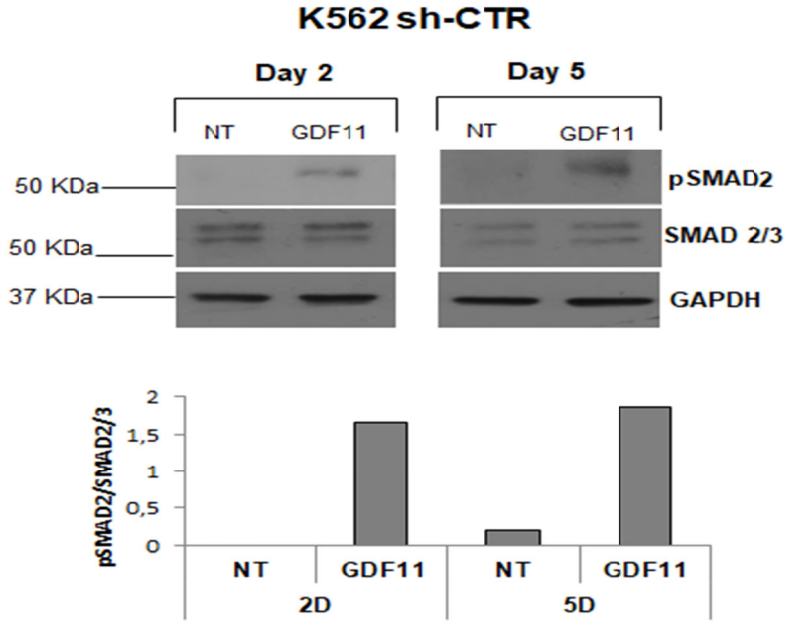

Figure III.6A. Protein expression by Western blot of total and phosphorylated SMAD2 protein in K562 sh-CTR cells hemin-treated and sh-CTR cells hemin + GDF11-treated at day 2 and day 5. In both cases, the activity of GDF11 was evaluated after 3 hours from the administration. SMAD2/3 represents total intracellular SMAD2 and SMAD3 proteins and it is used to normalize the phosphorylation levels. GAPDH is used as a loading control. Phosphorylation levels following GDF11 addition are highlighted by the densitometric quantification.

Since no significant differences between these two treatments (at day 2 and day 5) were observed, another treatment for K562 sh-CTR and sh-SEC23B-74 cells was performed following 2 days of differentiation. In this case, a time-course analysis was realized, assessing the phosphorylation of SMAD2 in shorter time frames. Particularly, we focused our analysis on 0.5 hours, 1 hour and 2 hours of treatment with the cytokine. In this case, both K562 sh-CTR and sh-SEC23B-74 cells exhibited an increased amount of

phosphorylated SMAD2 protein at 0 and 2 hours, with the highest amount at 0.5 hours time (Figure III.6B)

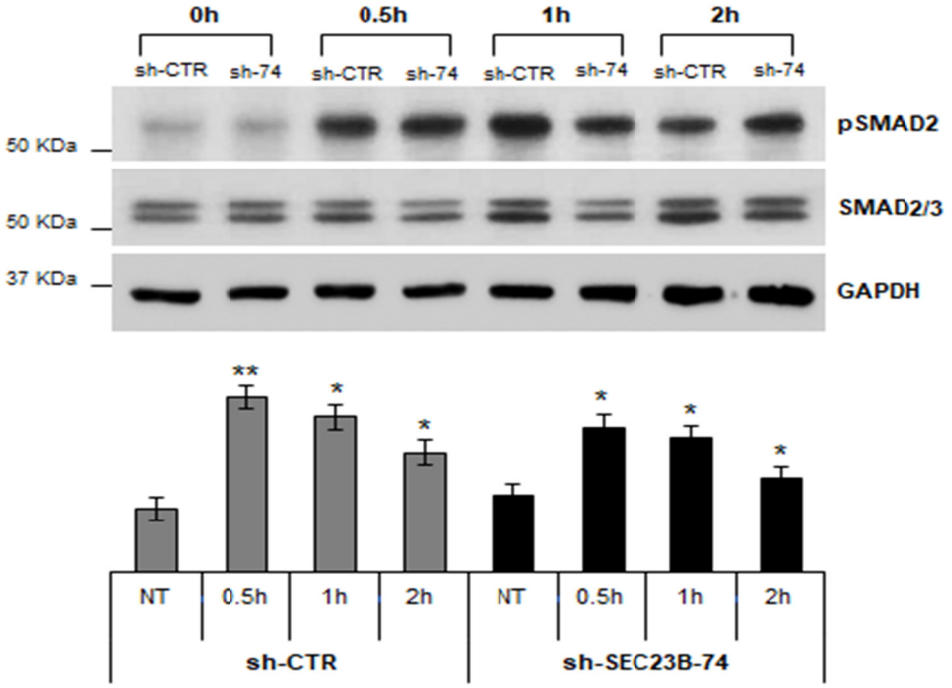

Figure III.6B. Western blot showing the time-course of SMAD2 phosphorylation following GDF11 provision to K562 sh-CTR and sh-SEC23B-74 cells. These effects were observed at 0.5, 1 and 2 hours. SMAD 2/3 is the control used to normalize the phosphorylation of SMAD2 protein. GAPDH is used as a loading control. Densitometric quantification of phosphorylated SMAD2 protein at 0 and 2 hours is shown. Data are presented as mean ± SD. P-value by Student t-test; ** $p < 0.01$; * $p < 0.05$.

7. RAP-011 decreases SMAD2 phosphorylation GDF11-mediated

Following the evaluation of SMAD2 phosphorylation time-course in K562 sh-CTR and sh-SEC23B-74 cells, we focused on studying the potential of RAP-011 to antagonize GDF11 activity. Indeed, we compared the levels of pSMAD2 in K562 sh-CTR and sh-SEC23B-74 cells treated with GDF11 and with both GDF11 and RAP-011. The highest decrease in the

amount of phosphorylated SMAD2, equal to 0.5 fold, between GD11-treated cells and GDF11+RAP-011-treated cells was observed after 1 hour of combined treatment (Figure III.7A).

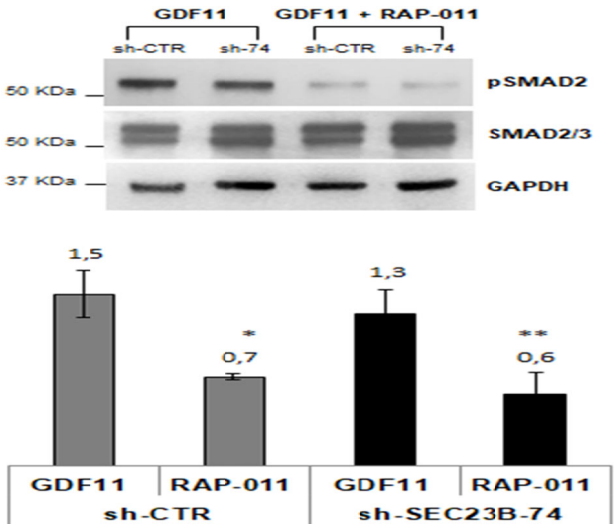

Figure III.7A. Western Blot panel showing phosphorylated SMAD2 in K562 sh-CTR and sh-SEC23B-74 cells treated with GDF11 and treated with GDF11+RAP-011. GDF11+RAP-011 treated cells show low levels of phosphorylated SMAD2 protein compared to the GDF11-treated cells, following 1 hour of treatment. Quantification was performed through densitometries, showing 0.5 fold less of phosphorylated SMAD2 protein in GDF11+RAP-011-treated cells compared to GDF11-treated cells. SMAD2/3 protein is used as a control to normalize phosphorylated SMAD2. GAPDH is used as a loading control. Data are presented as mean ± SD. P-value by Student t-test; ** $p < 0.01$; * $p < 0.05$.

However, also in the other points of our time-course, 0.5 and 2 hours, we observed significant differences in the concentration of pSMAD2 in K562 sh-CTR and sh-SEC23B-74 cells following the administration of GDF11 with RAP-011 (Figure III.7B).

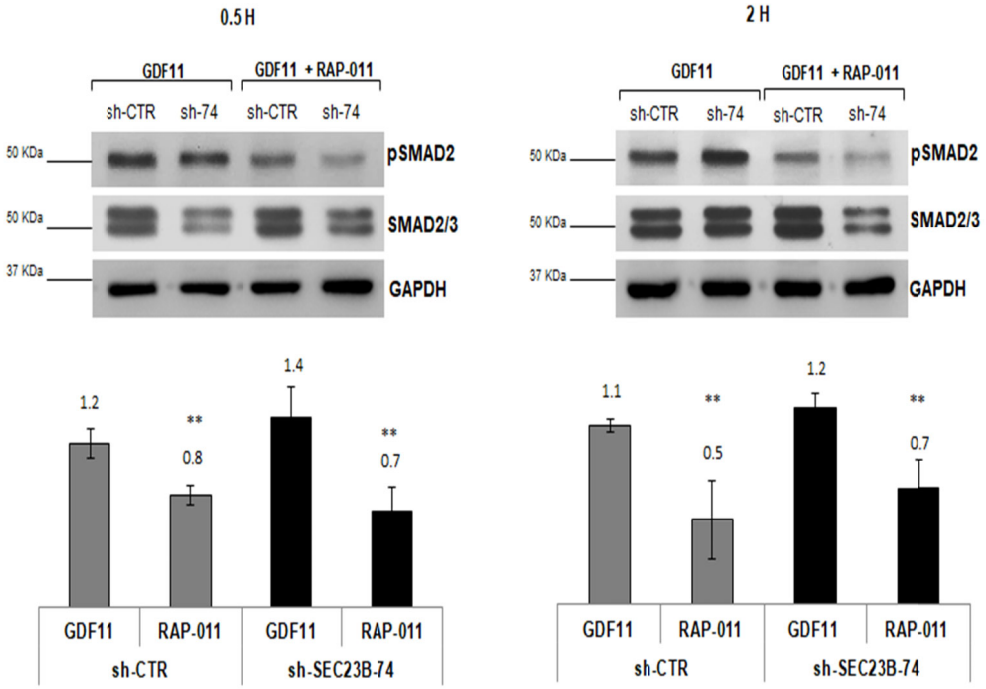

Figure III.7B. Western Blot panel showing phosphorylated SMAD2 in K562 sh-CTR and sh-SEC23B-74 cells treated with GDF11 and treated with GDF11+RAP-011 at 0.5 hours (left panel) and 2 hours (right panel). GDF11+RAP-011 treated cells show low levels of phosphorylated SMAD2 protein compared to the GDF1-treated cells. Densitometric quantification of phosphorylated SMAD2 protein in GDF11+RAP-011-treated cells compared to GDF11-treated cells is shown. GDF11-RAP-011 K562 sh-CTR cells show 34% and 55% (respectively at 0.5 and 2 hours treatment) in less of pSMAD2 compared to the GDF11-treated cells while sh-SEC23B-74 exhibit 50% and 42% less. SMAD2/3 protein is used as a control to normalize phosphorylated SMAD2. GAPDH is used as a loading control. Data are presented as mean ± SD. P-value by Student t-test; ** $p < 0.01$; * $p < 0.05$.

8. RAP-011 treatment induces the nuclear translocation of GATA1 transcription factor

To investigate the consequences of the administration of RAP-011, we decided to investigate the role of GATA1, a major transcription factor of the erythroid lineage. To this aim, the isolation of nuclear proteins from K562 sh-CTR and sh-SEC23B-74 clones treated with GDF11 and treated with GDF11+RAP-011 was performed. For these evaluations, we

chose 1 hour of exposure for both GDF11 and GDF11+RAP-011, given the highest levels of RAP-011 efficiency. By Western Blot, we compared the expression levels of nuclear GATA1 in GDF11+RAP-011-treated cells compared to those detected in GDF11-treated cells. Increased expression of GATA1 in the nuclear compartment after RAP-011 treatment for both the clones was observed, especially for K562 Sh-SEC23B-74, where a 3.8-fold increase was detected (Figure III.8A). Then, augmented expression of the molecular chaperone HSP-70 in nuclear fractions of K562 sh-CTR and sh-SEC23B-74 RAP-011-treated cells was also observed compared to the same clones treated with GDF11 (Figure III.8A).

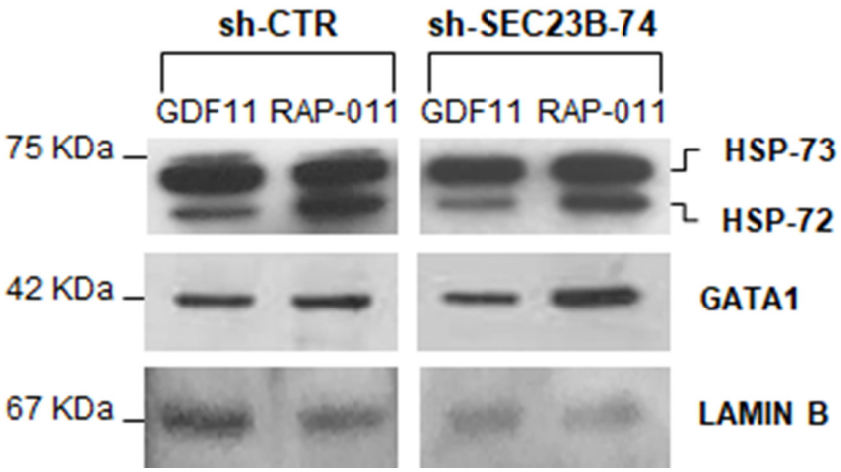

Figure III.8A. Expression levels of GATA1 and its molecular chaperone HSP-70 in the nuclear compartment of K562 sh-CTR and sh-SEC23B-74 clones treated with GDF11 and GDF11+RAP-011. HSP-70 shows two different isoforms, HSP-72, that is inducible while the other isoform, HSP-73 has a constitutive expression. Both GATA1 and HSP70 (HSP-72) shows upregulation in sh-CTR and sh-SEC23B-74 cells after RAP-011 administration compared to the levels observed in the same clones following GDF11 provision. This difference is particularly marked in sh-SEC23B-74 cells treated with RAP-011. LAMIN B is used as a nuclear loading control.

Since this increased nuclear translocation could be due to the RAP-011 effects on GDF11 pathway, we decided to assess the expression of the SMAD2/SMAD3 pathway nuclear mediator, that is SMAD4. We compared the protein expression levels of SMAD4 in the nuclear compartment of K562 sh-CTR and sh-SEC23B-74 cells following the addition of GDF11 or GDF11 plus RAP-011. A decreased amount of SMAD4 in RAP-011-treated cells was observed when compared to the GDF11-treated cells (Figure III.8B).

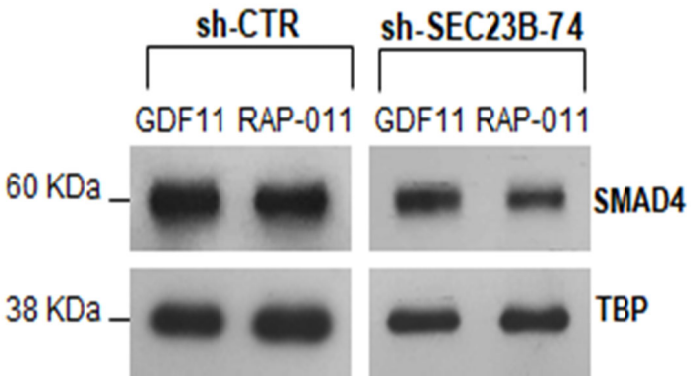

Figure III.8B. Western Blot showing protein levels of SMAD4 in the nuclear compartment of K562 sh-CTR and sh-SEC23B-74 cells treated with GDF11 or GDF11+RAP-011. A decrease in SMAD4 is observed following RAP-011 administration in both the clones, especially for sh-SEC23B-74 cells. TBP (TATA Binding Protein) is used as a nuclear loading control.

Densitometric quantification of the protein levels of GATA1, HSP-70 and SMAD4 in K562 sh-CTR and sh-SEC23B-74 cells after addition of GDF11 or GDF11+RAP-011 was performed (Figure III.8C).

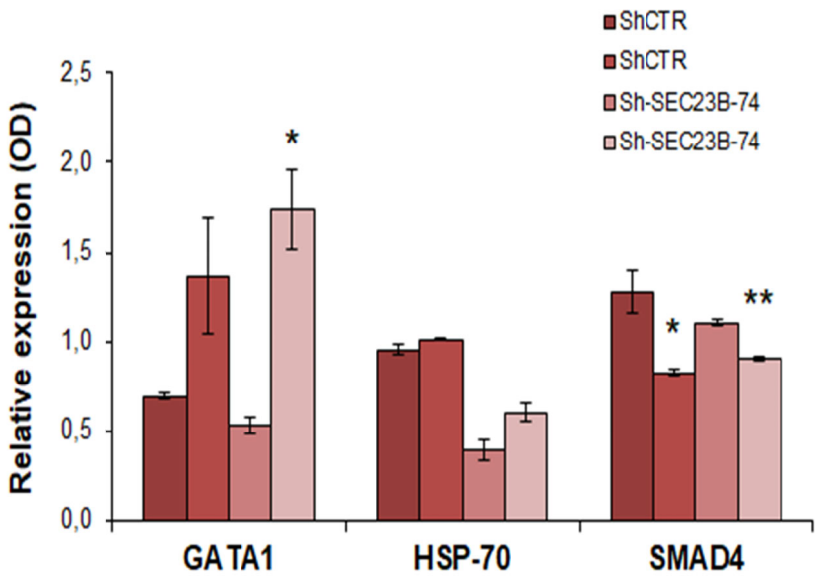

Figure III.8C. Densitometric quantification of GATA1, HSP-70, and SMAD4 in nuclear compartments of K562 sh-CTR and sh-SEC23B-74 cells treated with GDF11 or with GDF11+RAP-011 is shown. The values are obtained through the normalization with loading controls, LAMIN B and TBP. The trend observed is an increase of GATA1 and HSP-70 and a decrease of SMAD4 in RAP-011-treated cells compared to the GDF11-treated cells. Data are presented as mean ± SD. P-value by Student t-test; ** $p < 0.01$; * $p < 0.05$.

Finally, immunofluorescence analysis was carried out in order to establish if RAP-011 could affect the localization of erythroid transcription factor GATA1, as we observed by Western Blot. Particularly, increased localization of the protein GATA1 in the nuclear compartment was observed in K562 sh-CTR and sh-SEC23B-74 cells treated with the combination GDF11+RAP-011, (Figure III.8D).

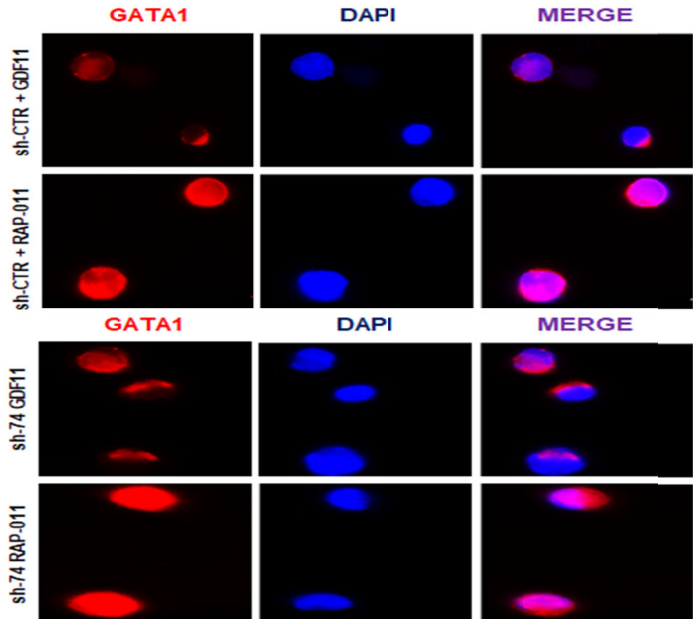

Figure III.8D. Immunofluorescence analysis of K562 sh-CTR and sh-SEC23B-74 cells after 1 hour of GDF11 administration compared to the same cells treated for 1 hour with GDF11+RAP-011. Localization of GATA1 is shown in red, due to the emission at 567 nm, while DAPI is seen in blue and it represents the nuclear structures. The merge between these two colors, at different emissions, is helpful to detect the degree of the nuclear localization of a specific protein. In this case, for both K562 sh-CTR and sh-SEC23B-74 RAP-011-treated cells an increased localization in the nuclear compartment was observed, in comparison with the detection of the same protein in GDF11-treated cells.

9. RAP-011 affects erythroid markers gene expression

The increased nuclear translocation of the transcription factor GATA1 suggested us that the drug could work by favoring the expression of some erythroid markers. For this reason, we investigated the gene expression of some genes involved in the erythroid development and functions. First, we assessed the gene expression levels of *GATA1* itself and *KLF1*, the other peculiar transcription factor of red blood cells development, in K562 sh-CTR and sh-SEC23B-74 cells treated with GDF11 and treated with GDF11+RAP-011. This analysis was performed after 1 hour of treatment (in accordance with the other evaluations). K562

sh-CTR and sh-SEC23B-74 cells treated with GDF11+RAP-011 showed an increase in gene expression of *GATA1* and *KLF1* (Figure III.9A).

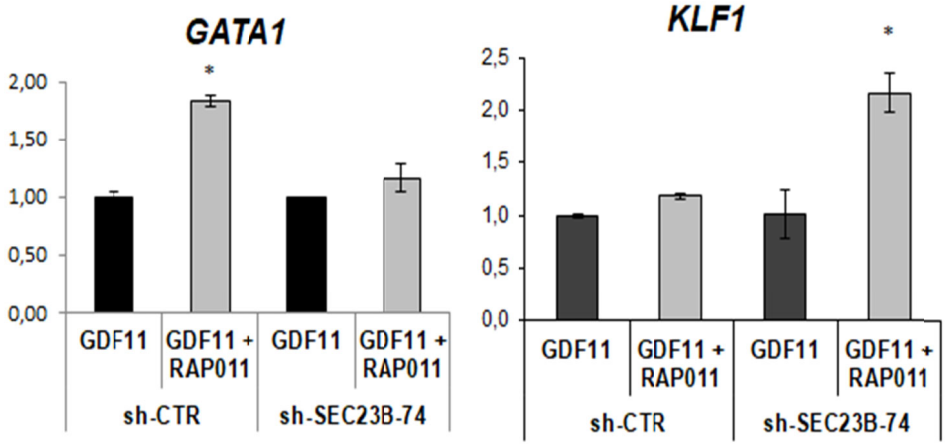

Figure III.9A. Gene expression analyses of K562 sh-CTR and sh-SEC23B-74 cells treated with GDF11 and treated with GDF11+RAP-011 for *GATA1* and *KLF1* genes. An upregulation of *GATA1* for sh-CTR and sh-SEC23B-74 cells is shown following the addition of RAP-011 (even if a slight increase concerning sh-SEC23B-74 clone), as well as *KLF1* is upregulated in both the clones, especially for sh-SEC23B-74 clone. GAPDH is the reference gene. Data are presented as mean ± SD. P-value by Student t-test; ** $p < 0.01$; * $p < 0.05$.

Then, the gene expression of other typical red cells differentiation markers was assessed, such as *HBG* and *ALAS2*. As regards the first gene, encoding the fetal hemoglobin, K562 sh-CTR cells did not show any significant changes in expression following the RAP-011 provision, while a marked upregulation is shown by K562 sh-SEC23B-74 RAP-011 treated cells. Otherwise, *ALAS2* gene expression underwent an augmented expression in K562 sh-CTR RAP-011-treated cells compared with the GDF11-treated cells, but the ligand trap did not seem to produce relevant increases in K562 sh-SEC23B-74 cells (Figure III.9B).

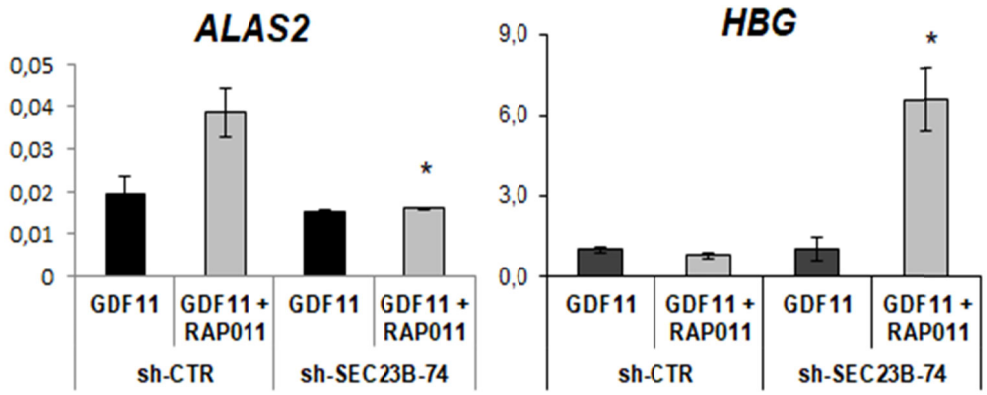

Figure III.9B. Gene expression analyses of K562 sh-CTR and sh-SEC23B-74 cells treated with GDF11 and treated with GDF11+RAP-011 for *ALAS2* and *HBG* genes. Marked upregulation of *ALAS2* for sh-CTR cells and a slight one for sh-SEC23B-74 cells were shown following the addition of RAP-011. Instead, *HBG* expression did not show changes in K562 sh-CTR cells treated with GDF11 and GDF11+RAP-011, while a strong increase in its gene levels was observed for sh-SEC23B-74 cells treated with RAP-011. GAPDH is the reference gene. Data are presented as mean ± SD. P-value by Student t-test; ** $p < 0.01$; * $p < 0.05$.

10. RAP-011 affects the apoptotic pathway

After the assessment of the drug effects on erythrocytes differentiation markers, we decided to investigate the beneficial effects of RAP-011 on our CDAII model. Gene expression analyses of Bcl-2 members were performed on K562 sh-CTR and sh-SEC23B-74 following the addition of RAP-011, to establish if there could be effects on cell death pathway. *Bcl-2* gene encodes the anti-apoptotic member of the family, as well as *Bcl-xL*, while *Bax* and *Bad* encode the pro-apoptotic members. K562 sh-CTR cells did not show differences in *Bcl-2* levels between GDF11-treatment and GDF11+RAP-011-treatment, but K562 sh-SEC23B-74 cells showed a strong increase of *Bcl-2* expression following the GDF11+RAP-011 addition, compared to the single GDF11 treatment. However, the trend showed by *Bcl-xL* is not compatible with what observed with Bcl-2. Indeed, while K562

sh-CTR cells exhibited an augmentation of *Bcl-xL* gene levels, sh-SEC23B-74 cells showed a downregulation of the same gene. In order to investigate further on the apoptotic pathway, we also measured gene levels of two pro-apoptotic members, *Bax* and *Bad*. In this case, a decrease in the gene levels of *Bax* and *Bad*, responsible for apoptotic cell death, was observed in both K562 sh-CTR and sh-SEC23B-74 following the GDF11+RAP-011-based treatment (Figure III.10)

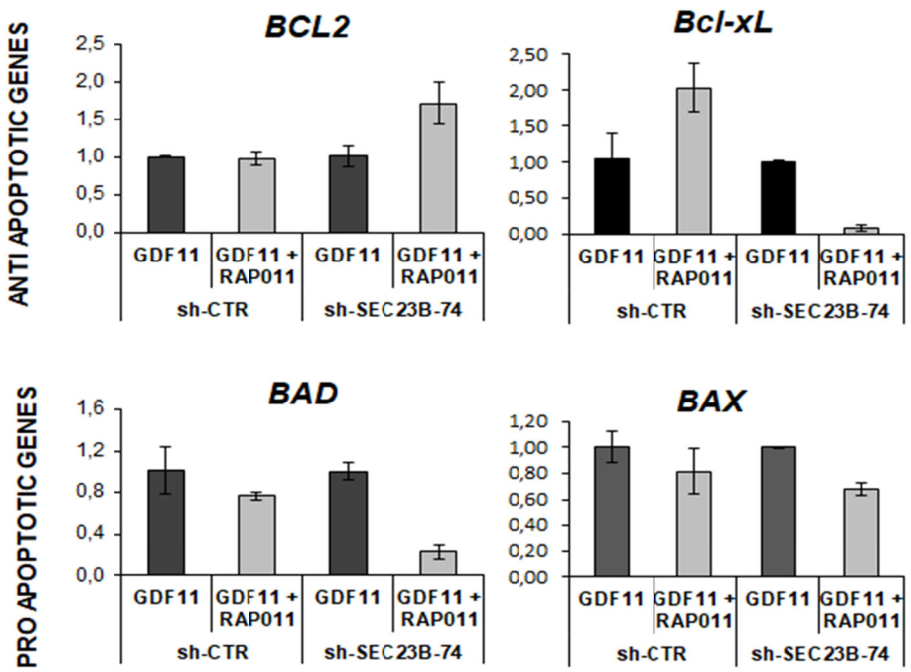

Figure III.10. In the panel at the top, relative gene expression of *Bcl-2* and *Bcl-xL* in K562 sh-CTR and sh-SEC23B-74 cells following GDF11+RAP-011 treatment was shown, in comparison with the same clones treated only with GDF11. Both the genes play antiapoptotic functions, but the levels detected are opposite since *Bcl-2* was upregulated in sh-SEC23B-74 cells treated with RAP-011 but in the same cells, a strong downregulation of *Bcl-xL* was observed. Instead, K562 sh-CTR cells showed nonrelevant changes in *Bcl-2* gene expression following RAP-011 addition, but upregulation of *Bcl-xL* was shown.

In the lower panel, relative gene expression of *Bax* and *Bad*, pro-apoptotic members of Bcl-2 family, in K562 sh-CTR and sh-SEC23B-74 treated or not treated cells with RAP-011, was shown. Both the genes showed, in K562 sh-CTR cells as well as sh-SEC23B-74 cells, a decrease of gene levels after the administration of RAP-011, in comparison with the levels detected in GDF11-treated cells. Data are presented as mean ± SD. P-value by Student t-test; ** $p < 0.01$; * $p < 0.05$.

11. RAP-011 induces feedback mechanisms on activin receptors genes

Given the structure of RAP-011, composed of the extracellular part of the Activin receptor IIA, we decided to measure gene expression levels of this receptor in K562 sh-CTR and

sh-SEC23B-74 cells treated with GDF11 and GDF11+RAP-011. Given the role of the Activin Receptor IIB in the activation of GDF11 pathway (as well as other ligands), we also performed a gene expression analysis for Activin Receptor IIB in K562 sh-CTR and sh-SEC23B-74 cells GDF11-treated compared with the same cells RAP-011-treated. For both the genes, *Acvr2a* and *Acvr2b,* we observed a similar trend in K562 sh-CTR and sh-SEC23B-74 cells following RAP-011 delivery. Indeed, in K562 sh-CTR cells no significant changes were observed after RAP-011-based treatment, compared to the GDF11-treated cells, but only a slight increase. Instead, sh-SEC23B-74 cells treated with RAP-011 exhibited a marked downregulation of *Acvr2a* and *Acvr2b* genes, maybe due to a feedback mechanism induced by the drug administration (Figure III.11A).

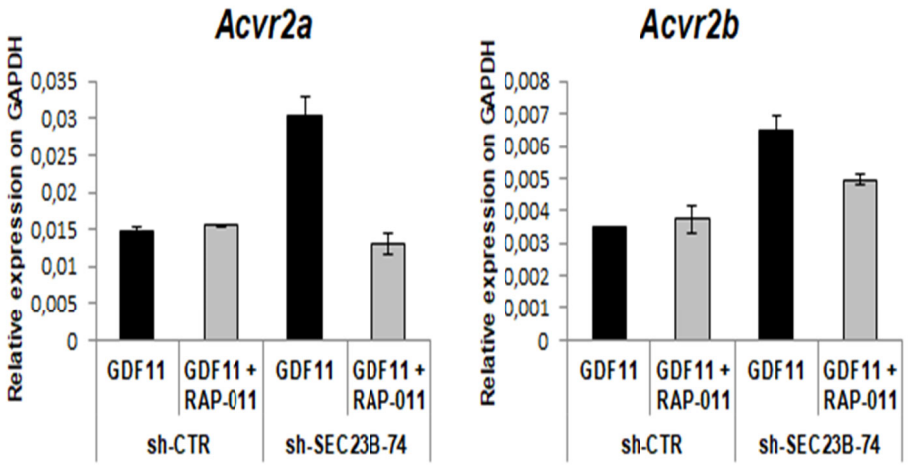

Figure III.11A. Gene expression analysis of *Acvr2a* and *Acvr2b* in K562 sh-CTR and sh-SEC23B-74 cells treated with GDF11 and with GDF11+RAP-011 was shown. K562 sh-SEC23B-74 cells exhibited a marked decrease in gene expression while for K562 sh-CTR cells no variations were observed with and without the drug. GAPDH is the reference gene. Data are presented as mean ± SD. P-value by Student t-test; ** $p < 0.01$; * $p < 0.05$.

Moreover, the role of the other two activin receptors, AcvrI and AcvrIB, was investigated too. Gene expression analysis of *Acvr1* and *Acvr1b* was performed on K562 sh-CTR and sh-SEC23B-74 cells, both treated with GDF11 and with GDF11+RAP-011. A decrease of both *Acvr1* and *Acvr1b* levels following GDF11+RAP-011 administration to K562 sh-CTR and sh-SEC23B-74 cells was observed (Figure III.11B).

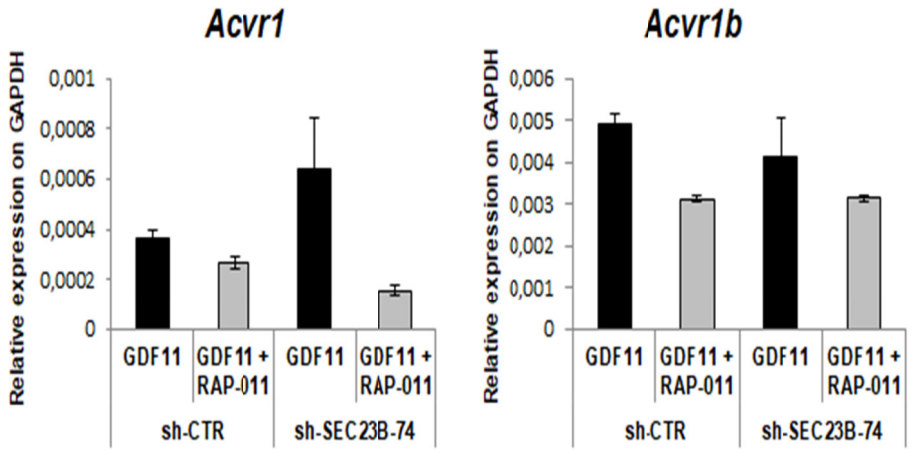

Figure III.11B. Gene expression analysis of *Acvr1* and *Acvr1b* in K562 sh-CTR and sh-SEC23B-74 cells treated with GDF11 and with GDF11+RAP-011. Downregulation of these genes was observed for both K562 sh-CTR and sh-SEC23B-74 cells. GAPDH is the reference gene. Data are presented as mean ± SD. P-value by Student t-test; ** $p < 0.01$; * $p < 0.05$.

In order to correlate the results of gene expression of the erythroid markers of the apoptotic pathway members with the activin receptors genes, a heatmap was created. In this graph, decreases and increases in the expression of certain genes in K562 sh-CTR and sh-SEC23B-74 cells are shown. These results were obtained as a fold change between the values of gene expression of K562 sh-CTR and sh-SEC23B-74 cells treated with RAP-011 and the same cells treated with GDF11 (Figure III.10C).

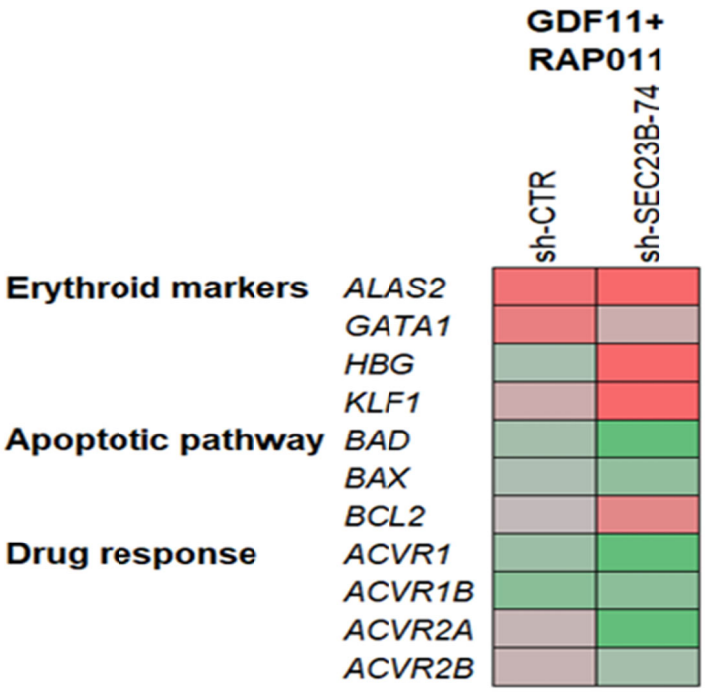

Figure III.11C. This Heatmap shows decreases and increases of certain genes in K562 sh-CTR and sh.SEC23B-74 cells treated with GDF11+RAP-011 when compared to the levels detected in the same cells treated with only GDF11. The analyzed genes are divided into three categories: the erythroid markers, such as *GATA1* and *KLF1*, the members of the apoptotic pathway and the activin receptors genes. Increases in gene expression are indicated by red, decreases in green. As regards the erythroid makers, all the genes underwent an upregulation following RAP-011 addition for both sh-CTR and sh-SEC23B-74 cells, except the *HBG* in K562 sh-CTR cells. For the apoptotic pathway, *Bcl-2* levels showed an increase while *Bax* and *Bad* exhibited a downregulation following the treatment. Finally, all the activin receptors genes showed a downregulation after the RAP-011 provision, except the *Acvr2a* and *Acvr2b* in K562 sh-CTR cells.

12. RAP-011 treatment acts on the cell cycle by overcoming the maturation block

We analyzed the cell cycle phases of K562 sh-CTR and sh-SEC23B-74 clones treated with GDF11 and with GDF11+RAP-011 by flow cytometry analysis (FACS). The analysis highlighted an increase of sh-CTR and sh-SEC23B-74 cells in G1 and G2 phases after

RAP-011 addition while a reduced proportion of the cells in S phase, following RAP-011 treatment, was observed. (Figure III.12A).

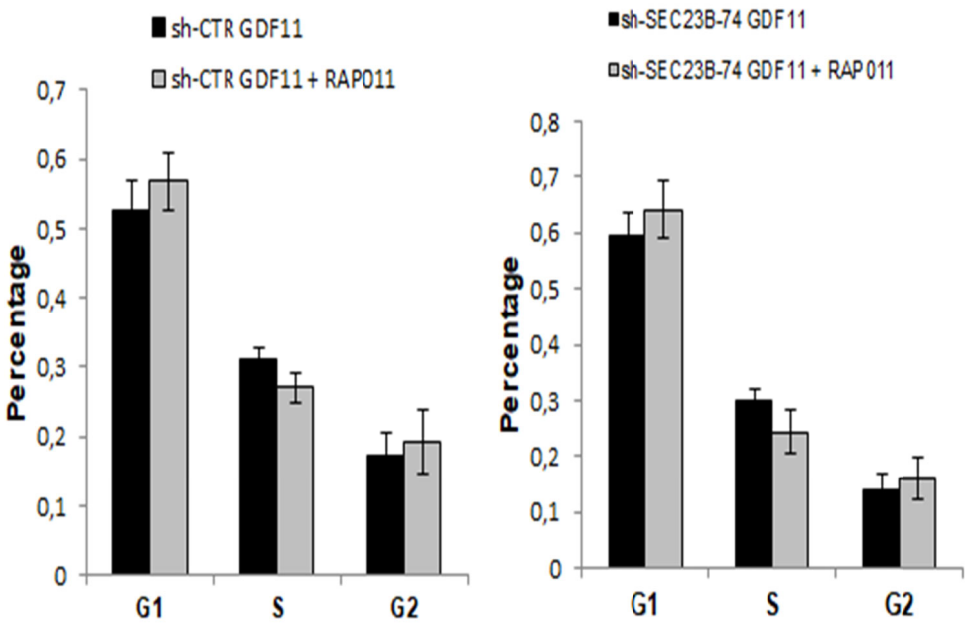

Figure III.12A. The results of cell cycle analysis of K562 sh-CTR and sh-SEC23B-74 cells treated with GDF11 and with GDF11 + RAP-011 are shown. This analysis was based on the percentages of cells in each phase of the cell cycle. In this case, a tendency to the increase was observed for G1 and G2 phases of sh-CTR and sh-SEC23B-74 cells treated with GDF11+RAP-011 compared to the same cells treated with only GDF11. Conversely, a decrease of the S phase following the RAP-011 addition in both sh-CTR and sh-SEC23B-74 cells was shown.

In order to confirm these results, we investigated the *CCNA2* gene, encoding cyclin A2 whose levels reach the highest peak during the synthesis phase. Thus, by gene expression analysis, a strong decrease of CCNA2 levels for sh-CTR and sh-SEC23B-74 cells after RAP-011 administration was observed, in accordance to what observed by cell cycle analysis of the S phase (Figure III.12B).

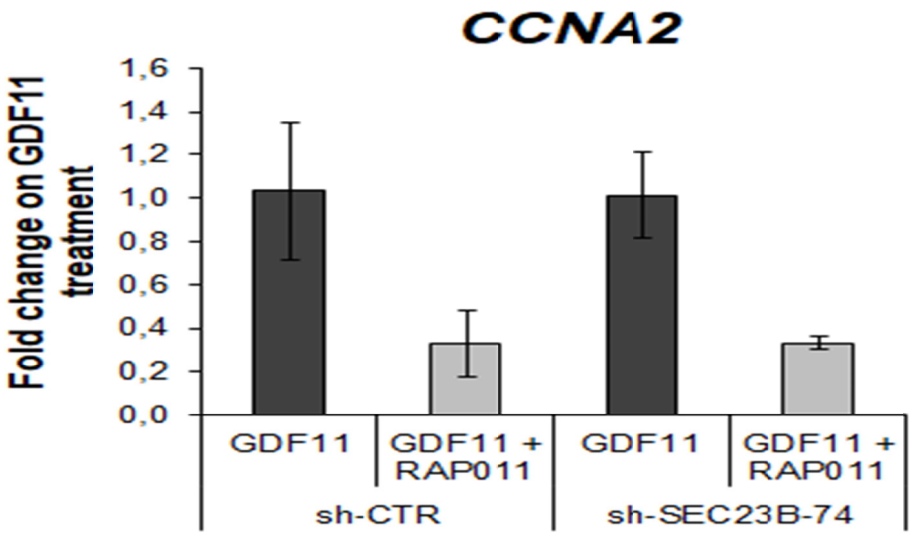

Figure III.12B. Gene expression analysis of *CCNA2* in K562 sh-CTR and sh-SEC23B-74 cells treated with GDF11 and GDF11+RAP-011. For both the clones, the combined treatment, GDF11+RAP-011, produced downregulation of *CCNA2* gene. GAPDH is the reference gene.

13. ERFE expression is affected by RAP-011 treatment

We next investigated the effects of RAP-011 on *ERFE*, the erythroid regulator of hepcidin, that has been recently indicated as a marker of dyserythropoiesis, especially for its involvement in the iron overload establishment, one of the main complications linked to this disorder. Gene expression of *ERFE* in K562 sh-CTR and sh-SEC23B-74 cells was assessed in order to evaluate any changes due to RAP-011 activity. While sh-CTR cells did not show significant differences between GDF11 and RAP-011 administration, a marked downregulation was observed as regards sh-SEC23B-74 cells following RAP-011-based treatment (Figure III.13A).

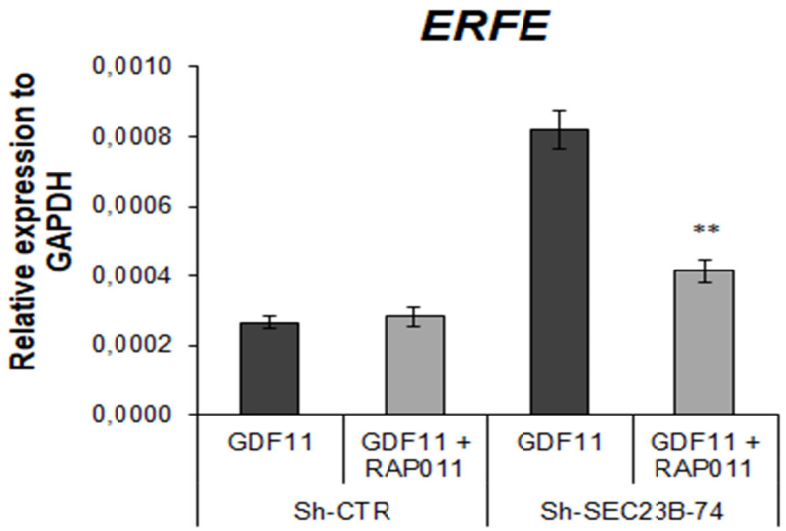

Figure III.13A. Gene expression analysis of *ERFE* on K562 sh-CTR and sh-SEC23B-74 cells treated with GDF11 and with RAP-011 was shown. While K562 sh-CTR cells treated with RAP-011 did not seem to show any differences following RAP-011 addition, a marked decrease in ERFE expression was observed for sh-SEC23B-74 cells treated with RAP-011. GAPDH is the reference gene. Data are presented as mean ± SD. P-value by Student t-test; ** $p < 0.01$; * $p < 0.05$.

By Western Blot, ERFE protein expression in GDF11 and GDF11+RAP-011 treated cells was investigated. This analysis showed that, following RAP-011 addition, sh-CTR cells exhibited no significant changes of ERFE expression, compared to GDF11-treated cells, but sh-SEC23B-74 cells exhibited a marked downregulation of ERFE protein following RAP-011 addition (Figure III.13B).

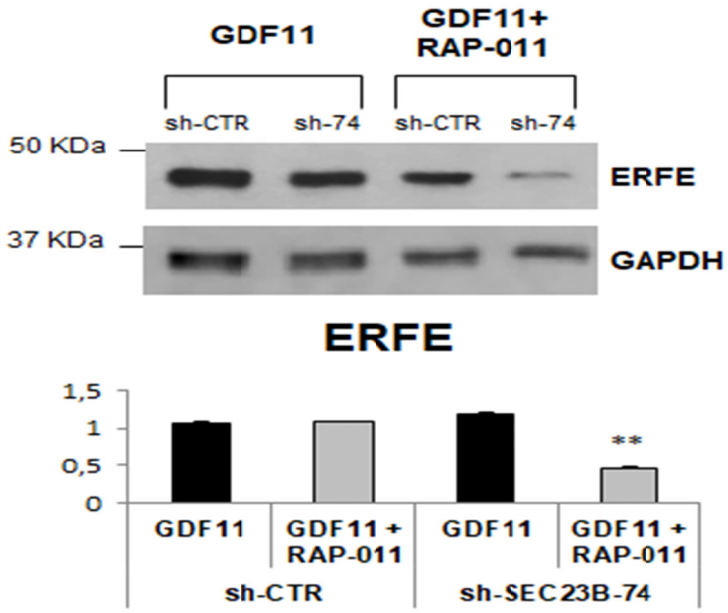

Figure III.13B. Protein expression analysis of ERFE on K562 sh-CTR and sh-SEC23B-74 cells treated with GDF11 and GDF11+RAP-011. While no significant differences in ERFE levels were observed for sh-CTR cells after the RAP-011 administration, a strong decrease in protein levels was shown by sh-SEC23B-74 RAP-011-treated cells. GAPDH is the reference protein. Quantification of protein levels was possible thanks to optical densitometries. Data are presented as mean ± SD. P-value by Student t-test; ** $p < 0.01$; * $p < 0.05$.

IV. DISCUSSION

Congenital Dyserythropoietic Anemias are red blood cells disorders hallmarked by defective erythroid maturation. Consequences of this maturation block are the establishment of ineffective erythropoiesis condition and related morphological abnormalities charged to the erythroblasts (Renella R et al. Hematol Oncol Clin North Am. 2009; Iolascon et al. Haematologica, 2012). Due to these features, CDAs can be considered subtypes of bone marrow failure syndromes (Iolascon et al. Blood, 2013). Among these, CDA type II is the most common form with more than 400 described cases so far (Russo et al. Am J Hematol. 2014; Bianchi et al. Br J Haematol. 2016). Typical clinical features of CDA II are anemia, relative reticulocytopenia, jaundice, splenomegaly, gallstones, and iron overload. Due to the phenotypic manifestations, this disorder has been misdiagnosed with the hereditary spherocytosis (HS) (King MJ et al. Int J Lab Hematol. 2015), until the causative gene, *SEC23B*, was identified in 2009 (Schwarz et al. Nat Genet. 2009). Molecular diagnosis, based on *SEC23B* sequencing, helped to improve the management of CDA II patients. Indeed, a correct diagnosis between these two diseases should avoid the worsening of the iron overload condition (Danise P et al. Clin Lab Haematol. 2001). CDA II is inherited with an autosomal recessive pattern, indeed patients are homozygous or compound heterozygous (Schwarz et al. Nat Genet. 2009;

Bianchi P et al. Hum Mutat. 2009). Sequencing led to the identification of more than 100 different mutations in the *SEC23B* gene, with some of these occurring more frequently in specific geographic areas. The elevated frequency of some mutations has been demonstrated to be due to the founder effect in those areas (Russo R et al. Am J Hematol. 2013, Russo R et al. Am J Hematol. 2014; Amir A et al. Acta Haematol. 2011). While great advances have been reached in the diagnostic process of CDA II, an evaluation of the functional effects of *SEC23B* gene loss-of-function still lacks. Difficulties in reaching this aim can be explained by the ubiquitous role of SEC23B, that is not involved in a specific erythroid function. Indeed, SEC23B encoded protein is part of the COPII complex, involved in the vesicle trafficking of newly synthesized proteins from endoplasmic reticulum towards the Golgi apparatus. This function is played by this gene ubiquitously, and for this reason, it has not been explained why the loss of function of this gene is the basis of only a red blood cell disorder (Russo R et al. Am J Hematol. 2013). Maybe, the erythrocytes maturation requires the transport of a specific product in the vesicle trafficking that is lacking with the downregulation of SEC23B. Recently, some *SEC23B* variants were associated with Cowden syndrome, that is an autosomal-dominant disorder characterized by the onset of epithelial cancers (Yehia L et al. Am J Hum Genet. 2015; Yehia L et al. Hum Mol Genet. 2018). However, concerning the CDA II, a SEC23B-deficient mouse model was generated but it does not reproduce the anemic phenotype observed in CDAII patients, but only degeneration of secretory tissues, such as the pancreas and salivary glands (Tao J et al. Proc Natl Acad Sci USA, 2012). The explanation of this lacking phenotype can be found in the compensatory role played by the paralogous gene of *SEC23B: SEC23A*. The proteins encoded by SEC23A and SEC23B have the same functions in the COPII complex but, probably, their expression varies between humans and mice, and among the different tissues (Iolascon A et al. Blood, 2013). In this case, the deficiency of *SEC23B* is not sufficient because of the massive presence of *SEC23A*. The

compensatory role of this gene in CDA II was demonstrated since patients, expressing lower levels of *SEC23B*, showed an upregulation of *SEC23A*, aimed at ameliorating the anemic phenotype (Russo R et al. Am J Hemat. 2014). Moreover, CDA II mouse models failed to exhibit human features probably because of an overlap between the functions of these two paralog genes. Indeed, SEC23B-deficiency in mice resulted in lethality, given the constitutive role of this gene, so chimeric mice with a deficiency restricted to the erythroid compartment were obtained. Still, these mice did not show the anemic phenotype as well as red cells abnormalities, hypoglycosylation of band 3 and erythroid hyperplasia were not observed (Khoriaty et al. Mol Cell Biol. 2014). However, *SEC23B* deficiency involved pancreatic dysfunctions responsible for the lethality, while a normal pancreatic development was shown by *SEC23A* deficient mice (Khoriaty et al. Sci Rep. 2016). The functions of these genes are interchangeable with different levels of expression in the organs between human and mice. The overlap of their functions was clear since the insertion of S*EC23A* coding sequence in *SEC23B*-deficient mice rescued their lethal pancreatic phenotype (Khoriaty et al. Proc Natl Acad Sci U S A 2018).

Given the absence of a reliable mouse model of CDAII, we decided to study the traits of this disorder through the establishment of an "*in vitro*" model. We selected the K562 cell line that shares some features with the erythroid lineage since these cells derive from the myeloid lineage, as well as the erythrocytes. These cells were demonstrated to reproduce some typical traits of red blood cells, when treated with some drugs, such as hemin (Benz EJ Jr et al. Nature, 1979) or sodium butyrate (Lozzio CB et al. Nature, 1979). We decided to induce K562 cells in erythroid differentiation by administering both these drugs, in order to select the most effective method to reproduce erythroid characteristics. The outcome of these experiments was evaluated by the increase of the transferrin receptor (CD71) on the cells surface by flow cytometry analysis. Indeed, the expression of this surface marker is significantly higher in red blood cells compared to the other cell types (Liu Q et al. Leuk

Lymphoma, 2014). K562 cells treated with hemin showed a greater increase of CD71 receptors on their surfaces than the cells treated with sodium butyrate. Our CDA II *in vitro* model was established through the stable silencing of *SEC23B* expression in K562 cells. Particularly, we generated two K562 clones stably silenced for *SEC23B*, i.e. sh-SEC23B-70 and sh-SEC23B-74. The assessment of SEC23B expression confirmed the silencing for both the clones compared with the clone K562 sh-CTR at the gene and protein level. The main difference between the two clones lies in the different expression of the paralog gene *SEC23A*. Indeed, K562 sh-SEC23B-74 clone showed an up-regulation of *SEC23A*, while sh-SEC23B-70 clone showed similar levels of silencing of the paralogs, maybe due to a non-specific activity of the short hairpin. This observation is in line with previous studies on low *SEC23B* expression alleles that are not associated with CDA II severe clinical presentation because of a compensatory expression of the paralog *SEC23A*, as previously mentioned (Russo R et al. Am J Hematol. 2014). Moreover, when we tested the ability of these clones to reproduce erythroid features following the stimulation induced by hemin, K562 sh-SEC23B-70 and sh-SEC23B-74 underwent a depletion of CD71 positive cells during the days 2 and 5 considered for the experiment, while the clone sh-CTR showed an increase in the percentage of cells expressing the transferrin receptor, as expected for a positive control. Following this experiment, we also measured the levels of SEC23B for the entire duration of the experiment in our SEC23B-silenced models as well as SEC23A. The results confirm the silencing of SEC23B at the gene and protein level, as well as the upregulation of SEC23A in sh-SEC23B-74 clone. These results suggest the use of these clones as a CDA II cell model capable to reproduce the defects in the differentiation at the basis of this disorder.

The establishment of this model gave us the opportunity to explore the therapeutic options aimed at the overcoming of the defect causative of CDA II. Indeed, nowadays, blood transfusion therapy or treatments with erythropoiesis-stimulating agents (ESA), such as

recombinant erythropoietin, are the front line therapies for anemia associated with ineffective erythropoiesis (Gambale et al. Expert Rev Hematol. 2016; Motta I et al. Expert Opin Investig Drugs, 2017). However, both treatments are not without risks, and in some cases, they are not effective (Aapro et al. Ann Oncol. 2018). Therefore, there is a clinical need for novel agents supporting ineffective erythropoiesis with a different mechanism of action from existing ESA. Although the recent progress in our knowledge of molecular and functional pathways during normal and pathological erythropoiesis, limited therapeutic options are available to treat ineffective erythropoiesis.

ACE-011, as well as its murine counterpart RAP-011, is a chimeric protein in which the extracellular domain of the ActRIIA receptor is fused to the Fc portion of the human IgG1 antibody. ACE-011 antagonizes activin and several other members of the TGF-β superfamily that signal through the ActRIIA. Clinical trials based on Sotatercept (ACE-011) in healthy post-menopausal women led to the enhanced bone formation and decreased bone resorption, as expected, but surprisingly this treatment also produced an amelioration of hematologic parameters, such as increased hemoglobin (Hb) and hematocrit levels (Ruckle J et al. J Bone Miner Res 2009; Raje N et al. Curr Opin Mol Ther, 2010; Sherman ML et al. J Clin Pharmacol. 2013). These effects on erythroid parameters encouraged to assess the functionality of this drug on ineffective erythropoiesis. Recently, a phase II clinical trial for β-thalassemic patients was performed in order to evaluate the tolerability and the efficacy of the chimeric protein. This study involved both transfusion-dependent and non-transfusion-dependent patients who were treated with different doses of Sotatercept for 22 months. An increase in hemoglobin values of >1 g/dl was observed in non-transfusion-dependent patients for 12 weeks, while for transfusion-dependent patients a >20% reduction in transfusion burden was obtained for 24 weeks. Furthermore, this study demonstrated the tolerability of the drug on patients enrolled in the trial (Cappellini MD et al. Haematologica, 2019).

These findings led researchers to assess the effects of the chimeric protein on ineffective erythropoiesis through different *in vitro* and *in vivo* studies that produced encouraging results (Iancu-Rubin et al. Exp Hematol. 2013; Carrancio S et al. Br J Haematol. 2014; Dussiot et al. Nat Med. 2014; Langdon et al. Am J Hematol. 2015). ACE-011 and its murine analog RAP-011 neutralizes GDF11 functions by inhibiting its binding to the ActRIIA or ActRIIB and the consequent downstream pathway.

Due to the shared pathomechanisms between β-thalassemia and CDA II, we firstly evaluated the role of GDF11 in the pathogenesis of CDA II through the measurement of GDF11 expression in patients compared to HCs. Our analyses highlighted the overexpression of GDF11 in CDA II patients compared to HCs at the gene and protein level, and these findings suggested a similar role for GDF11 in both CDA II and β-thalassemia.

A slight increase of GDF11 cytokine production in K562 *SEC23B*-silenced cells compared to non-silenced ones was observed. However, the extent of this increase was not as significant as the one observed in *ex vivo* evaluation on CDA II patients. This difference between *ex vivo* and *in vitro* analyses may lie in the absence of systemic production of GDF11 as regards K562 cell line.

Because sh-SEC23B-70 clone did not reproduce one of the traits of CDA II, showing downregulation of the paralogous gene *SEC23A*, we decided to perform a treatment based on RAP-011 on sh-SEC23B-74 clone, in parallel with the sh-CTR clone, as a positive control. Before treating cells, we tested if the drug could have any cytotoxic effect on our cells, so we used different concentrations of RAP-011 on sh-CTR and sh-SEC23B-74 clones. After selecting the right concentration of the drug, we evaluated the viability of treated cells compared to the cells treated with the vehicle. Still, cells exhibited an increased survival following the administration of RAP-011.

However, given the proposed role for GDF11 in the ineffective erythropoiesis, we administered the cytokine to cells in order to simulate the pathologic context and to analyze the effects of the interaction between GDF11 and RAP-011. GDF11 activity is exerted through the binding of an activin receptor (IIA or IIB) and the consequent activation of a downstream pathway whose first step is the increased phosphorylation of an intracellular mediator, the protein SMAD2. In our model, the administration of GDF11 to both sh-CTR and sh-SEC23B-silenced cells produced increased phosphorylation of SMAD2 at different times, as expected, while the combined treatment of GDF11 and RAP-011 produced an inhibition of GDF11-receptor binding that led to reduced phosphorylation of SMAD2. These data show the effectiveness of this treatment in the inhibition of GDF11-activated pathway. However, in order to understand how the inhibition of this pathway could improve erythroid survival, we investigated the role of the transcription factor GATA1 during the drug treatment. Some studies (Arlet JB et al. Curr Opin Hematol. 2016) demonstrated that ineffective erythropoiesis in β-thalassemia leads to a major involvement of chaperone heat-shock protein 70 (HSP70) in order to facilitate the refolding of the denatured proteins; therefore, HSP70 cannot exert its chaperone function towards cytoplasmic GATA1 that is more prone to caspase 3-mediated cleavage. Main consequences of this condition are a reduced GATA1 nuclear translocation and an altered erythroid gene expression that is consistent with bone marrow syndromes. We focused on GATA1 protein expression in the nuclear compartment in order to check if GDF11 and/or RAP-011 could affect its localization. Both sh-CTR and sh-SEC23B nuclear extracts showed a greater amount of GATA1 after RAP-011 administration compared to the amount of GATA1 observed in samples treated with GDF11. Interestingly, HSP70 showed the same trend, i.e. a higher nuclear concentration in RAP-011-treated samples compared to those treated with GDF11. Moreover, we investigated the role of SMAD4, another mediator of TGF-β signaling, that exerts its functions by forming a heterotrimeric complex

in the nucleus with SMAD2 and SMAD3 proteins (Shi Y et al. Nature, 1997; Chacko et al. Nat Struct Biol. 2001; Chacko et al. Mol Cell. 2004). Thus, it should be necessary for the nuclear transmission of GDF11 signaling, maybe through alteration of target genes transcription. In our case, RAP-011-treatment led to a decrease in SMAD4 protein expression at the nuclear level in both sh-CTR and sh-SEC23B-74 clones. A decreased amount of nuclear SMAD4, following RAP-011 administration, should be linked to the increased GATA1 nuclear translocation and transcriptional activity. The increased nuclear localization of GATA1 was confirmed by immunofluorescence assay.

Hence, we analyzed gene expression of some of the most representative erythroid markers besides *GATA1*, like *KLF1* that encodes the homonymous erythroid transcriptional factor, *HBG* that encodes the γ-globin, *ALAS2* gene that codifies an enzyme involved in the heme biosynthetic pathway. In agreement with the enhanced nuclear translocation of GATA1 transcription factor-mediated by RAP-011, we observed an increased expression of specific genes of erythroid lineage in SEC23B-silenced cells. Afterward, we evaluated the effects of this treatment on the cell death pathway through the gene expression analysis of Bcl-2 family members. These genes regulate different aspects of cell death since some play an anti-apoptotic role while others show pro-apoptotic functions. In the case, we assessed *Bcl-2* that is involved in the inhibition of the apoptosis and we found increased levels of gene expression in sh-CTR and sh-SEC23B-74 RAP-011-treated cells, and *Bcl-xL* where a different trend is observed. Instead, gene levels of two apoptosis activators, *Bax* and *Bad*, were lower in sh-CTR and sh-SEC23B-74 cells following RAP-011 administration. In order to find any correlations between these effects on protein and gene expression after the administration of RAP-011, we assessed the expression of the activin receptors (type I, IB, IIA, and IIB) that are responsible for the GDF11 signaling. Analysis of gene expression showed that RAP-011 leads to reduced gene expression of all these receptors, mostly concerning sh-SEC23B-74 cells. These results are explained by the ligand trap function

played by RAP-011. Indeed, removal of GDF11 from circulation prevents the cytokine from binding to the activin receptor II and this may cause a decreased synthesis of receptors. Moreover, FACS cell cycle analysis showed a similar trend for sh-CTR and sh-SEC23B-74 RAP-011-treated cells as regards the percentage of cells in each phase of the cell cycle. Indeed, we observed an increased percentage of G1 and G2 phase with a decreased number of cells in S-phase. Thus, gene expression analysis of cyclin A2 gene, *CCNA2*, whose levels are at peak in S phase, confirms the FACS cell cycle analysis since it showed a decrease in *CCNA2* gene expression for RAP-011-treated cells. These results highlight the role of RAP-011 in promoting the overcome of the maturation block that is characterized by a higher amount of cells arrested in S-phase (Libani IV et al. Blood, 2008).

Interestingly, we investigated also the ERFE gene and protein expression after RAP-011 treatment. ERFE encodes erythroferrone, a protein involved in iron overload condition establishment that is one of the main complications arising from dyserythropoiesis, and for its role, it was recently proposed as a marker of iron-loading anemias as CDA II and β-thalassemia (Kautz L et al. Blood, 2015; Latour C et al. Haematologica, 2017; Russo R et al. Blood, 2016). Interestingly, while sh-CTR-treated cells did not show significant differences in gene and protein expression compared to that observed in GDF11-treated cells, sh-SEC23B-74 cells exhibited a marked decrease of ERFE at mRNA and protein level, in response to RAP-011 administration. These data seem to show effects on the iron overload by restoring physiological levels of the erythroferrone hormone.

Conclusions

Herein, we firstly established an *in vitro* model reproducing CDA II features, such as the defect in the erythroid differentiation, due to the lack of the SEC23B functions. Then, we proposed the role of GDF11 as a trigger of the ineffective erythropoiesis of CDA II and

supported the hypothesis that RAP-011 administration produces beneficial effects in a cellular model of CDA II. The inhibition of GDF11-signaling pathway seems to translate in a more intense transcriptional activity of erythroid markers that may allow undifferentiated erythroblasts to overcome the maturation arrest. The comparison between the GDF11-pathway, with and without the administration of RAP-011, is described in Figure IV.

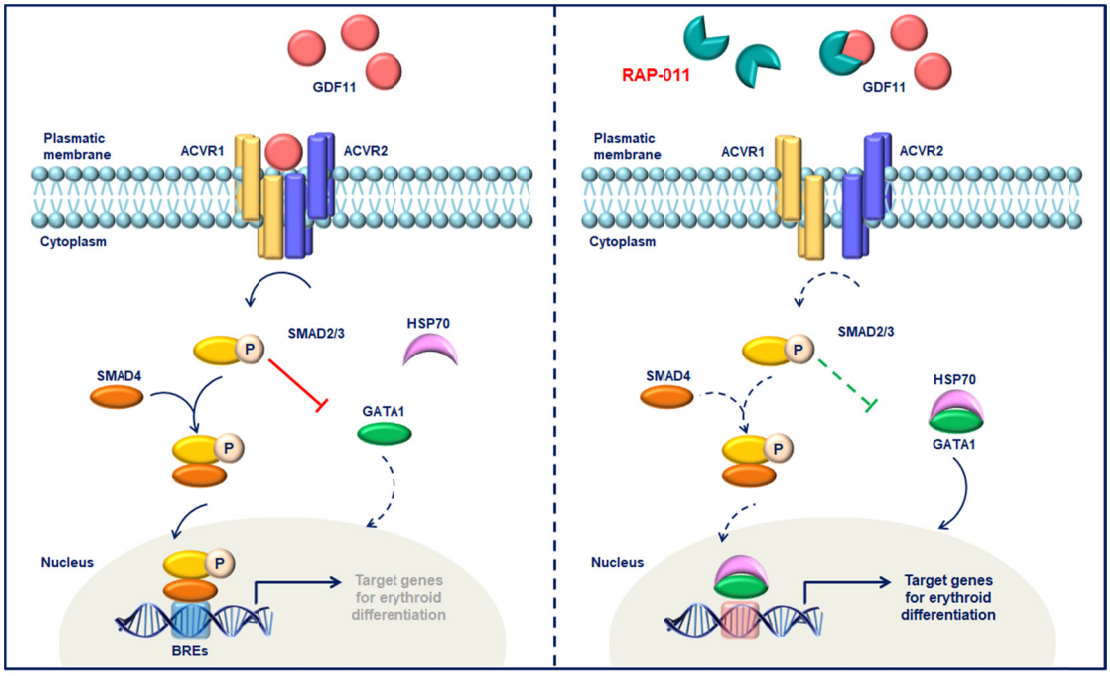

Figure IV. In the first panel, on the left, GDF11 has shown to bind the Activin Receptor II, with the consequent formation of the heterotetramer with the Activin Receptor I. The assembly of these receptors result in the increased phosphorylation of SMAD2 and SMAD3 proteins, leading to the formation of a complex with SMAD4 protein. This complex migrates towards the nucleus, by inhibiting GATA1 nuclear translocation and transcriptional functions. In the second panel, RAP-011 "traps" GDF11 avoiding its binding to the Activin Receptors. Phosphorylation of SMAD2 protein is not stimulated, so GATA1 is free to migrate towards the nuclear compartment with its molecular chaperone HSP-70 and to exert its erythroid functions.

These results may encourage the use of Sotatercept (ACE-011) as a therapeutic drug for CDA II patients. This is in agreement with the recent results obtained by a phase II clinical trial based on Sotatercept on β-thalassemic patients (Cappellini et al. Haematologica, 2019). Indeed, both transfusion-dependent and non-transfusion-dependent patients exhibited a good response in terms of increase of Hb values, reduction of RBC transfusions (for the first class of patients) and, finally, a reduction of systemic iron overload (Cappellini et al. Haematologica, 2019).

Future perspectives

Given the creation of this *in vitro* model of CDAII, based on *SEC23B* silencing performed on K562 cells, there are different aspects of the disease that can be studied or assessed through different assays. However, the next step of our study will lead us to explore new ways to engineer cells in order to obtain a more accurate picture of the disease that is the object of our study. Nowadays, genome editing strategies are based on CRISPR-Cas9 system, that can be used to "delete" a certain gene from the genome or to "insert" a specific mutation, responsible for a certain phenotype (Ran Fa et al. Nat Protoc. 2013). In our case, we aimed at obtaining a *SEC23B* gene knockout from HUDEP-2 cells. This cell line represents the first described source of immortalized erythroid progenitors so far. Given the abilities of these cells to give rise to enucleated RBCs and to produce human hemoglobin and other specific erythroid markers (Kurita R et al. PLoS One, 2013), these cells can represent a deep breakthrough in the knowledge of pathogenetic mechanisms of red blood cells disorders, among which there is the CDA II.

Moreover, a more detailed description of the mechanisms of ineffective erythropoiesis underlying the CDAII, and the related systemic consequences, such as the iron overload,

can be possible thanks to the establishment of an animal model. Difficulties in obtaining a reliable mouse model of CDAII are due to the role played by *SEC23B* paralog gene, *SEC23A*, whose increased expression tends to compensate the downregulation of the causative gene, hiding the effects of *SEC23B* knockdown and making impossible to observe a typical anemic phenotype. A reliable mouse model could be obtained through an inducible and tissue-specific downregulation of both the genes confined to the erythroid compartment. This could represent a way to reproduce in a mouse model the clinical situation of the disease in the humans.

Both these CDAII models, HUDEP-2 knockout for *SEC23B* and the mouse knockdown for *SEC23B* and *SEC23A*, could be useful to assess the efficiency of an approach based on gene therapy. By introducing a lentiviral vector expressing the SEC23B coding sequence, it should be possible to overcome the defects in the erythroid differentiation due to the lack of SEC23B itself. This could represent a turning point for CDAII patients because it could lead to a complete restore of the phenotype from the disease. Indeed, the most interesting aspect of the strategies based on the gene therapy can be found in the power of the vectors to integrate stably in a genome host, replacing a gene that resulted non-functional because of low levels of expression or a structural defect.

References

Aapro M, Beguin Y, Bokemeyer C, Dicato M, Gascón P, Glaspy J, Hofmann A, Link H, Littlewood T, Ludwig H, Österborg A, Pronzato P, Santini V, Schrijvers D, Stauder R, Jordan K, Herrstedt J; ESMO Guidelines Committee. *Management of anaemia and iron deficiency in patients with cancer: ESMO Clinical Practice Guidelines*. Ann Oncol. 2018 Oct 1;29(Suppl 4):iv271.

Ahmed MR, Chehal A, Zahed L, Taher A, Haidar J, Shamseddine A, O'Hea AM, Bienz N, Dgany O, Avidan N, Beckmann JS, Tamary H, Higgs D, Vyas P, Wood WG, Wickramasinghe SN. *Linkage and mutational analysis of the CDAN1 gene reveals genetic heterogeneity in congenital dyserythropoietic anemia type I*. Blood. 2006 Jun 15;107(12):4968-9.

Akhurst RJ, Hata A. *Targeting the TGFβ signalling pathway in disease*. Nat Rev Drug Discov. 2012 Oct;11(10):790-811.

Amir A, Dgany O, Krasnov T, Resnitzky P, Mor-Cohen R, Bennett M, Berrebi A, Tamary H. *E109K is a SEC23B founder mutation among Israeli Moroccan Jewish patients with congenital dyserythropoietic anemia type II.* Acta Haematol. 2011;125(4):202-7.

Andolfo I, De Falco L, Asci R, Russo R, Colucci S, Gorrese M, Zollo M, Iolascon A. *Regulation of divalent metal transporter 1 (DMT1) non-IRE isoform by the microRNA Let-7d in erythroid cells*. Haematologica. 2010 Aug;95(8):1244-52.

Angelucci E, Barosi G, Camaschella C, Cappellini MD, Cazzola M, Galanello R, Marchetti M, Piga A, Tura S. *Italian Society of Hematology practice guidelines for the management of iron overload in thalassemia major and related disorders.* Haematologica. 2008 May;93(5):741-52.

Arlet JB, Dussiot M, Moura IC, Hermine O, Courtois G. *Novel players in β-thalassemia dyserythropoiesis and new therapeutic strategies.* Curr Opin Hematol. 2016 May;23(3):181-8.

Arnaud L, Saison C, Helias V, Lucien N, Steschenko D, Giarratana MC, Prehu C, Foliguet B, Montout L, de Brevern AG, Francina A, Ripoche P, Fenneteau O, Da Costa L, Peyrard T, Coghlan G, Illum N, Birgens H, Tamary H, Iolascon A, Delaunay J, Tchernia G, Cartron JP. *A dominant mutation in the gene encoding the erythroid transcription factor KLF1 causes a congenital dyserythropoietic anemia.* Am J Hum Genet. 2010 Nov 12;87(5):721-7.

Ask K, Jasencakova Z, Menard P, Feng Y, Almouzni G, Groth A. *Codanin-1, mutated in the anaemic disease CDAI, regulates Asf1 function in S-phase histone supply.* EMBO J. 2012 Apr 18;31(8):2013-23.

Babbs C, Roberts NA, Sanchez-Pulido L, McGowan SJ, Ahmed MR, Brown JM, Sabry MA; WGS500 Consortium, Bentley DR, McVean GA, Donnelly P, Gileadi O, Ponting CP, Higgs DR, Buckle VJ. *Homozygous mutations in a predicted endonuclease are a novel cause of congenital dyserythropoietic anemia type I.* Haematologica. 2013 Sep;98(9):1383-7.

Bennett GD and Kay MM. *Homeostatic removal of senescent murine erythrocytes by splenic macrophages.* Exp Hematol, 1981 Mar;9(3):297-307.

Benz EJ Jr, Murnane MJ, Tonkonow BL, Berman BW, Mazur EM, Cavallesco C, Jenko T, Snyder EL, Forget BG, Hoffman R. *Embryonic-fetal erythroid characteristics of a human leukemic cell line.* Proc Natl Acad Sci U S A. 1980 Jun;77(6):3509-13.

Bewersdorf JP, Zeidan AM. *Transforming growth factor (TGF)-β pathway as a therapeutic target in lower risk myelodysplastic syndromes*. Leukemia. 2019 Jun;33(6):1303-1312.

Bianchi P, Fermo E, Vercellati C, Boschetti C, Barcellini W, Iurlo A, Marcello AP, Righetti PG, Zanella A. *Congenital dyserythropoietic anemia type II (CDAII) is caused by mutations in the SEC23B gene*. Hum Mutat. 2009 Sep;30(9):1292-8.

Bianchi P, Schwarz K, Högel J, Fermo E, Vercellati C, Grosse R, van Wijk R, van Zwieten R, Barcellini W, Zanella A, Heimpel H. *Analysis of a cohort of 101 CDAII patients: description of 24 new molecular variants and genotype-phenotype correlations*. Br J Haematol. 2016 Nov;175(4):696-704.

Blood Reviews, 2014 Mar;28(2):49-66.

Breda L, Rivella S. *Modulators of erythropoiesis: emerging therapies for hemoglobinopathies and disorders of red cell production*. Hematol Oncol Clin North Am. 2014 Apr;28(2):375-86.

Cappellini MD, Porter J, Origa R, Forni GL, Voskaridou E, Galactéros F, Taher AT, Arlet JB, Ribeil JA, Garbowski M, Graziadei G, Brouzes C, Semeraro M, Laadem A, Miteva D, Zou J, Sung V, Zinger T, Attie KM, Hermine O. *Sotatercept, a novel transforming growth factor β ligand trap, improves anemia in β-thalassemia: a phase II, open-label, dose-finding study.* Haematologica. 2019 Mar;104(3):477-484.

Carolien M. Woolthuis and Christopher Y. Park. *Hematopoietic stem/progenitor cell commitment to the megakaryocyte lineage.* Blood, 2016 Mar 10;127(10):1242-8.

Carrancio S, Markovics J, Wong P, Leisten J, Castiglioni P, Groza MC, Raymon HK, Heise C, Daniel T, Chopra R, Sung V. *An activin receptor IIA ligand trap promotes erythropoiesis resulting in a rapid induction of red blood cells and haemoglobin*. Br J Haematol. 2014 Jun;165(6):870-82.

Casanovas G, Swinkels DW, Altamura S, Schwarz K, Laarakkers CM, Gross HJ, Wiesneth M, Heimpel H, Muckenthaler MU. *Growth differentiation factor 15 in patients with congenital dyserythropoietic anaemia (CDA) type II*. J Mol Med (Berl). 2011 Aug;89(8):811-6.

Chacko BM, Qin B, Correia JJ, Lam SS, de Caestecker MP, Lin K. *The L3 loop and C-terminal phosphorylation jointly define Smad protein trimerization*. Nat Struct Biol. 2001 Mar;8(3):248-53.

Chacko BM, Qin BY, Tiwari A, Shi G, Lam S, Hayward LJ, De Caestecker M, Lin K. *Structural basis of heteromeric smad protein assembly in TGF-beta signaling*. Mol Cell. 2004 Sep 10;15(5):813-23.

Chirnomas SD and Kupfer GM. *The inherited bone marrow failure syndromes.* Pediatr Clin North Am. 2013 Dec;60(6):1291-310.

Ciovacco WA, Raskind WH, Kacena MA. *Human phenotypes associated with GATA-1 mutations.* Gene. 2008 Dec 31;427(1-2):1-6.

Danise P, Amendola G, Nobili B, Perrotta S, Miraglia Del Giudice E, Matarese SM, Iolascon A, Brugnara C. *Flow-cytometric analysis of erythrocytes and reticulocytes in*

congenital dyserythropoietic anaemia type II (CDA II): value in differential diagnosis with hereditary spherocytosis. Clin Lab Haematol. 2001 Feb;23(1):7-13.

De Franceschi L, Turrini F, del Giudice EM, Perrotta S, Olivieri O, Corrocher R, Mannu F, Iolascon A. *Decreased band 3 anion transport activity and band 3 clusterization in congenital dyserythropoietic anemia type II.* Exp Hematol. 1998 Aug;26(9):869-73.

Dgany O, Avidan N, Delaunay J, Krasnov T, Shalmon L, Shalev H, Eidelitz-Markus T, Kapelushnik J, Cattan D, Pariente A, Tulliez M, Crétien A, Schischmanoff PO, Iolascon A, Fibach E, Koren A, Rössler J, Le Merrer M, Yaniv I, Zaizov R, Ben-Asher E, Olender T, Lancet D, Beckmann JS, Tamary H. *Congenital dyserythropoietic anemia type I is caused by mutations in codanin-1.* Am J Hum Genet. 2002 Dec;71(6):1467-74

Di Pierro E, Russo R, Karakas Z, Brancaleoni V, Gambale A, Kurt I, Winter SS, Granata F, Czuchlewski DR, Langella C, Iolascon A, Cappellini MD. *Congenital erythropoietic porphyria linked to GATA1-R216W mutation: challenges for diagnosis*. Eur J Haematol. 2015 Jun;94(6):491-7.

Dussiot M, Maciel TT, Fricot A, Chartier C, Negre O, Veiga J, Grapton D, Paubelle E, Payen E, Beuzard Y, Leboulch P, Ribeil JA, Arlet JB, Coté F, Courtois G, Ginzburg YZ, Daniel TO, Chopra R, Sung V, Hermine O, Moura IC. *An activin receptor IIA ligand trap corrects ineffective erythropoiesis in β-thalassemia*. Nat Med. 2014 Apr;20(4):398-407.

Ear J, Huang H, Wilson T, Tehrani Z, Lindgren A, Sung V, Laadem A, Daniel TO, Chopra R, Lin S. *RAP-011 improves erythropoiesis in zebrafish model of Diamond-Blackfan anemia through antagonizing lefty1*. Blood. 2015 Aug 13;126(7):880-90.

Fargo JH, Kratz CP, Giri N, Savage SA, Wong C, Backer K, Alter BP, Glader B. *Erythrocyte adenosine deaminase: diagnostic value for Diamond-Blackfan anaemia*. Br J Haematol. 2013 Feb;160(4):547-54.

Gambale A, Iolascon A, Andolfo I, Russo R. *Diagnosis and management of congenital dyserythropoietic anemias*. Expert Rev Hematol. 2016 Mar;9(3):283-96.

Gao J, Chen YH, Peterson LC. *GATA family transcriptional factors: emerging suspects in hematologic disorders*. Exp Hematol Oncol. 2015 Oct 6;4:28.

Geiduschek JB, Singer SJ. *Molecular changes in the membranes of mouse erythroid cells accompanying differentiation.* Cell, 1979 Jan;16(1):149-63.

Gregory CJ and Eaves AC. *Human marrow cells capable of erythropoietic differentiation in vitro: definition of three erythroid colony responses*. Blood, 1977 Jun;49(6):855-64.

Harrison CA, Al-Musawi SL, Walton KL. *Prodomains regulate the synthesis, extracellular localisation and activity of TGF-β superfamily ligands*. Growth Factors. 2011 Oct;29(5):174-86.

Hattangadi SM, Wong P, Zhang L, Flygare J, Lodish HF. *From stem cell to red cell: regulation of erythropoiesis at multiple levels by multiple proteins, RNAs, and chromatin modifications*. Blood, 2011 Dec 8;118(24):6258-68.

Heimpel H, Matuschek A, Ahmed M, Bader-Meunier B, Colita A, Delaunay J, Garcon L, Gilsanz F, Goede J, Högel J, Kohne E, Leichtle R, Munoz J, Perrotta S, Piscopo C, Renella R, Schwarz K, Smolenska-Sym G, Wickramasinghe S, Zanella A, Iolascon A. *Frequency of congenital dyserythropoietic anemias in Europe.* Eur J Haematol. 2010 Jul;85(1):20-5.

Iancu-Rubin C, Mosoyan G, Wang J, Kraus T, Sung V, Hoffman R. *Stromal cell-mediated inhibition of erythropoiesis can be attenuated by Sotatercept (ACE-011), an activin receptor type II ligand trap.* Exp Hematol. 2013 Feb;41(2):155-166.e17.

Iolascon A, Andolfo I, Barcellini W, Corcione F, Garçon L, De Franceschi L, Pignata C, Graziadei G, Pospisilova D, Rees DC, de Montalembert M, Rivella S, Gambale A, Russo R, Ribeiro L, Vives-Corrons J, Martinez PA, Kattamis A, Gulbis B, Cappellini MD, Roberts I, Tamary H; Working Study Group on Red Cells and Iron of the EHA. *Recommendations regarding splenectomy in hereditary hemolytic anemias.* Haematologica. 2017 Aug;102(8):1304-1313.

Iolascon A, Esposito MR, Russo R. *Clinical aspects and pathogenesis of congenital dyserythropoietic anemias: from morphology to molecular approach.* Haematologica. 2012 Dec;97(12):1786-94.

Iolascon A, Heimpel H, Wahlin A, Tamary H. *Congenital dyserythropoietic anemias: molecular insights and diagnostic approach.* Blood. 2013 Sep 26;122(13):2162-6.

Iolascon A, Russo R, Delaunay J. *Congenital dyserythropoietic anemias*. Curr Opin Hematol. 2011 May;18(3):146-51.

Iolascon A, Russo R, Esposito MR, Asci R, Piscopo C, Perrotta S, Fénéant-Thibault M, Garçon L, Delaunay J. *Molecular analysis of 42 patients with congenital dyserythropoietic anemia type II: new mutations in the SEC23B gene and a search for a genotype-phenotype relationship*. Haematologica. 2010 May;95(5):708-15.

Jaffray JA, Mitchell WB, Gnanapragasam MN, Seshan SV, Guo X, Westhoff CM, Bieker JJ, Manwani D. *Erythroid transcription factor EKLF/KLF1 mutation causing congenital dyserythropoietic anemiatype IV in a patient of Taiwanese origin: review of all reported cases and development of a clinical diagnostic paradigm*. Blood Cells Mol Dis. 2013 Aug;51(2):71-5.

Julianne N. P. Smith and Laura M. Calvi. *Current concepts in bone marrow microenvironmental regulation of hematopoietic stem and progenitor cells.* Stem Cells, 2013 Jun;31(6):1044-50.

Kautz L, Jung G, Du X, Gabayan V, Chapman J, Nasoff M, Nemeth E, Ganz T. *Erythroferrone contributes to hepcidin suppression and iron overload in a mouse model of β-thalassemia*. Blood. 2015 Oct 22;126(17):2031-7.

Kautz L, Jung G, Valore EV, Rivella S, Nemeth E, Ganz T. *Identification of erythroferrone as an erythroid regulator of iron metabolism.* Nat Genet. 2014 Jul;46(7):678-84.

Kautz L, Nemeth E. *Molecular liaisons between erythropoiesis and iron metabolism.* Blood. 2014 Jul 24;124(4):479-82.32.

Khoriaty R, Everett L, Chase J, Zhu G, Hoenerhoff M, McKnight B, Vasievich MP, Zhang B, Tomberg K, Williams J, Maillard I, Ginsburg D. *Pancreatic SEC23B deficiency is sufficient to explain the perinatal lethality of germline SEC23B deficiency in mice*. Sci Rep. 2016 Jun 14;6:27802.

Khoriaty R, Hesketh GG, Bernard A, Weyand AC, Mellacheruvu D, Zhu G, Hoenerhoff MJ, McGee B, Everett L, Adams EJ, Zhang B, Saunders TL, Nesvizhskii AI, Klionsky DJ, Shavit JA, Gingras AC, Ginsburg D. *Functions of the COPII gene paralogs SEC23A and SEC23B are interchangeable in vivo.* Proc Natl Acad Sci U S A. 2018 Aug 14;115(33):E7748-E7757.

Khoriaty R, Vasievich MP, Jones M, Everett L, Chase J, Tao J, Siemieniak D, Zhang B, Maillard I, Ginsburg D. *Absence of a red blood cell phenotype in mice with hematopoietic deficiency of SEC23B.* Mol Cell Biol. 2014 Oct 1;34(19):3721-34.

King MJ, Garçon L, Hoyer JD, Iolascon A, Picard V, Stewart G, Bianchi P, Lee SH, Zanella A; International Council for Standardization in Haematology. *ICSH guidelines for*

the laboratory diagnosis of nonimmune hereditary red cell membrane disorders. Int J Lab Hematol. 2015 Jun;37(3):304-25.

Komrokji R, Garcia-Manero G, Ades L, Prebet T, Steensma DP, Jurcic JG, Sekeres MA, Berdeja J, Savona MR, Beyne-Rauzy O, Stamatoullas A, DeZern AE, Delaunay J, Borthakur G, Rifkin R, Boyd TE, Laadem A, Vo B, Zhang J, Puccio-Pick M, Attie KM, Fenaux P, List AF. *Sotatercept with long-term extension for the treatment of anaemia in patients with lower-risk myelodysplastic syndromes: a phase 2, dose-ranging trial.* Lancet Haematol. 2018 Feb;5(2):e63-e72.

Koury MJ. *Abnormal erythropoiesis and the pathophysiology of chronic anemia.*

Koury MJ and Bondurant MC. *Erythropoietin retards DNA breakdown and prevents programmed death in erythroid progenitor cells.* Science, 1990. Apr 20;248(4953):378-81.

Koury ST, Koury MJ, Bondurant MC. *Cytoskeletal distribution and function during the maturation and enucleation of mammalian erythroblasts*. J Cell Biol, 1989 Dec 1; 109(6): 3005–3013.

Kurita R, Suda N, Sudo K, Miharada K, Hiroyama T, Miyoshi H, Tani K, Nakamura Y. *Establishment of immortalized human erythroid progenitor cell lines able to produce enucleated red blood cells*. PLoS One. 2013;8(3):e59890.

Langdon JM, Barkataki S, Berger AE, Cheadle C, Xue QL, Sung V, Roy CN. *RAP-011, an activin receptor ligand trap, increases hemoglobin concentration in hepcidin transgenic mice.* Am J Hematol. 2015 Jan;90(1):8-14

Latour C, Wlodarczyk MF, Jung G, Gineste A, Blanchard N, Ganz T, Roth MP, Coppin H, Kautz L. *Erythroferrone contributes to hepcidin repression in a mouse model of malarial anemia.* Haematologica. 2017 Jan;102(1):60-68.

Lee JC, Gimm JA, Lo AJ, Koury MJ, Krauss SW, Mohandas N, Chasis JA. *Mechanism of protein sorting during erythroblast enucleation: role of cytoskeletal connectivity.* Blood, 2004 Mar 1;103(5):1912-9.

Libani IV, Guy EC, Melchiori L, Schiro R, Ramos P, Breda L, Scholzen T, Chadburn A, Liu Y, Kernbach M, Baron-Lühr B, Porotto M, de Sousa M, Rachmilewitz EA, Hood JD, Cappellini MD, Giardina PJ, Grady RW, Gerdes J, Rivella S. *Decreased differentiation of erythroid cells exacerbates ineffective erythropoiesis in beta-thalassemia*. Blood. 2008 Aug 1;112(3):875-85.

Liljeholm M, Irvine AF, Vikberg AL, Norberg A, Month S, Sandström H, Wahlin A, Mishima M, Golovleva I. *Congenital dyserythropoietic anemia type III (CDA III) is caused by a mutation in kinesin family member, KIF23*. Blood. 2013 Jun 6;121(23):4791-9.

Liu Q, Wang M, Hu Y, Xing H, Chen X, Zhang Y, Chen Y, Bu D and Zhu P. *The Usefulness of CD71 Expression by Flow Cytometry in the Diagnosis of Acute Leukemia*. Leuk Lymphoma. 2014 Apr;55(4):892-8.

Lotinun S, Pearsall RS, Davies MV, Marvell TH, Monnell TE, Ucran J, Fajardo RJ, Kumar R, Underwood KW, Seehra J, Bouxsein ML, Baron R. *A soluble activin receptor Type IIA fusion protein (ACE-011) increases bone mass via a dual anabolic-antiresorptive effect in Cynomolgus monkeys.* Bone. 2010 Apr;46(4):1082-8.

Lozzio CB, Lozzio BB. *Human chronic myelogenous leukemia cell-line with positive Philadelphia chromosome*. Blood. 1975 Mar;45(3):321-34.

Méndez-Ferrer S, Michurina TV, Ferraro F, Mazloom AR, Macarthur BD, Lira SA, Scadden DT, Ma'ayan A, Enikolopov GN, Frenette PS. *Mesenchymal and haematopoietic stem cells form a unique bone marrow niche.* Nature, 2010 Aug 12;466(7308):829-34.

Merika M and Orkin SH. *Functional synergy and physical interactions of the erythroid transcription factor GATA-1 with the Krüppel family proteins Sp1 and EKLF.* Mol Cell Biol, 1995 May;15(5):2437-47.

Mies A, Hermine O, Platzbecker U. *Activin Receptor II Ligand Traps and Their Therapeutic Potential in Myelodysplastic Syndromes with Ring Sideroblasts*. Curr Hematol Malig Rep. 2016 Dec;11(6):416-424.

Mies A, Platzbecker U. *Increasing the effectiveness of hematopoiesis in myelodysplastic syndromes: erythropoiesis-stimulating agents and transforming growth factor-β superfamily inhibitors.* Semin Hematol. 2017 Jul;54(3):141-146.

Modi G, Shah S, Madabhavi I, Panchal H, Patel A, Uparkar U, Anand A, Parikh S, Patel K, Shah K, Revannasiddaiah S. *Successful Allogeneic Hematopoietic Stem Cell Transplantation of a Patient Suffering from Type II Congenital Dyserythropoietic Anemia A Rare Case Report from Western India*. Case Rep Hematol. 2015;2015:792485.

Motta I, Scaramellini N, Cappellini MD. *Investigational drugs in phase I and phase II clinical trials for thalassemia.* Expert Opin Investig Drugs. 2017 Jul;26(7):793-802.

Nomura T, Ueyama T, Ashihara E, Tateishi K, Asada S, Nakajima N, Isodono K, Takahashi T, Matsubara H, Oh H. *Skeletal muscle-derived progenitors capable of differentiating into cardiomyocytes proliferate through myostatin-independent TGF-beta family signaling.* Biochem Biophys Res Commun. 2008 Jan 25;365(4):863-9.

Odartchenko N, Cottier H, Bond VP. *A study on ineffective erythropoiesis in the dog.* Cell Tissue Kinet. 1971 Jan;4(1):107-12.

Paddison PJ, Caudy AA, Bernstein E, Hannon GJ, Conklin DS. *Short hairpin RNAs (shRNAs) induce sequence-specific silencing in mammalian cells.* Genes Dev. 2002 Apr 15;16(8):948-58.

Pellegrin S, Haydn-Smith KL, Hampton-O'Neil LA, Hawley BR, Heesom KJ, Fermo E, Bianchi P, Toye AM. *Transduction with BBF2H7/CREB3L2 upregulates SEC23A protein in erythroblasts and partially corrects the hypo-glycosylation phenotype associated with CDAII.* Br J Haematol. 2019 Mar;184(5):876-881.

Piga A, Perrotta S, Gamberini MR, Voskaridou E, Melpignano A, Filosa A, Caruso V, Pietrangelo A, Longo F, Tartaglione I, Borgna-Pignatti C, Zhang X, Laadem A, Sherman ML, Attie KM. *Luspatercept improves hemoglobin levels and blood transfusion requirements in a study of patients with β-thalassemia.* Blood. 2019 Mar 21;133(12):1279-1289.

Platzbecker U, Germing U, Götze KS, Kiewe P, Mayer K, Chromik J, Radsak M, Wolff T, Zhang X, Laadem A, Sherman ML, Attie KM, Giagounidis A. *Luspatercept for the treatment of anaemia in patients with lower-risk myelodysplastic syndromes (PACE-MDS): a multicentre, open-label phase 2 dose-finding study with long-term extension study.* Lancet Oncol. 2017 Oct;18(10):1338-1347.

Raje N, Vallet S. *Sotatercept, a soluble activin receptor type 2A IgG-Fc fusion protein for the treatment of anemia and bone loss.* Curr Opin Mol Ther. 2010 Oct;12(5):586-97.

Ran FA, Hsu PD, Wright J, Agarwala V, Scott DA, Zhang F. *Genome engineering using the CRISPR-Cas9 system.* Nat Protoc. 2013 Nov;8(11):2281-2308.

RC Gregory, Taxman DJ, Seshasayee D, Kensinger MH, Bieker JJ, Wojchowski DM. *Functional interaction of GATA1 with erythroid Krüppel-like factor and Sp1 at defined erythroid promoters.* Blood, 1996 Mar 1;87(5):1793-801.

Renella R, Wood WG. *The congenital dyserythropoietic anemias*. Hematol Oncol Clin North Am. 2009 Apr;23(2):283-306.

Renella R, Roberts NA, Brown JM, De Gobbi M, Bird LE, Hassanali T, Sharpe JA, Sloane-Stanley J, Ferguson DJ, Cordell J, Buckle VJ, Higgs DR, Wood WG. *Codanin-1 mutations in congenital dyserythropoietic anemia type 1 affect HP1{alpha} localization in erythroblasts.* Blood. 2011 Jun 23;117(25):6928-38.

Rochette L, Zeller M, Cottin Y, Vergely C. *Growth and differentiation factor 11 (GDF11): Functions in the regulation of erythropoiesis and cardiac regeneration*. Pharmacol Ther. 2015 Dec;156:26-33.

Roy NBA, Babbs C. *The pathogenesis, diagnosis and management of congenital dyserythropoietic anaemia type I*. Br J Haematol. 2019 May;185(3):436-449.

Ruckle J, Jacobs M, Kramer W, Pearsall AE, Kumar R, Underwood KW, Seehra J, Yang Y, Condon CH, Sherman ML. *Single-dose, randomized, double-blind, placebo-controlled study of ACE-011 (ActRIIA-IgG1) in postmenopausal women*. J Bone Miner Res. 2009 Apr;24(4):744-52.

Russo R, Andolfo I, Manna F, De Rosa G, De Falco L, Gambale A, Bruno M, Mattè A, Ricchi P, Girelli D, De Franceschi L, Iolascon A. *Increased levels of ERFE-encoding FAM132B in patients with congenital dyserythropoietic anemia type II*. Blood. 2016 Oct 6;128(14):1899-1902.

Russo R, Andolfo I, Manna F, Gambale A, Marra R, Rosato BE, Caforio P, Pinto V, Pignataro P, Radhakrishnan K, Unal S, Tomaiuolo G, Forni GL, Iolascon A. *Multi-gene panel testing improves diagnosis and management of patients with hereditary anemias*. Am J Hematol. 2018 May;93(5):672-682.

Russo R, Esposito MR, Iolascon A. *Inherited hematological disorders due to defects in coat protein (COP)II complex*. Am J Hematol. 2013 Feb;88(2):135-40.

Russo R, Marra R, Andolfo I, De Rosa G, Rosato BE, Manna F, Gambale A, Raia M, Unal S, Barella S, Iolascon A. *Characterization of Two Cases of Congenital Dyserythropoietic Anemia Type I Shed Light on the Uncharacterized C15orf41 Protein.* Front Physiol. 2019 May 22;10:621.

Russo R, Gambale A, Esposito MR, Serra ML, Troiano A, De Maggio I, Capasso M, Luzzatto L, Delaunay J, Tamary H, Iolascon A. *Two founder mutations in the SEC23B gene account for the relatively high frequency of CDA II in the Italian population*. Am J Hematol. 2011 Sep;86(9):727-32.

Russo R, Gambale A, Langella C, Andolfo I, Unal S, Iolascon A. *Retrospective cohort study of 205 cases with congenital dyserythropoietic anemia type II: definition of clinical and molecular spectrum and identification of new diagnostic scores*. Am J Hematol. 2014 Oct;89(10):E169-75.

Russo R, Langella C, Esposito MR, Gambale A, Vitiello F, Vallefuoco F, Ek T, Yang E, Iolascon A. *Hypomorphic mutations of SEC23B gene account for mild phenotypes of congenital dyserythropoietic anemia type II*. Blood Cells Mol Dis. 2013 Jun;51(1):17-21.

Satchwell TJ, Pellegrin S, Bianchi P, Hawley BR, Gampel A, Mordue KE, Budnik A, Fermo E, Barcellini W, Stephens DJ, van den Akker E, Toye AM. *Characteristic phenotypes associated with congenital dyserythropoietic anemia (type II) manifest at different stages of erythropoiesis.* Haematologica. 2013 Nov;98(11):1788-96.

Sato K and Nakano A. *Mechanisms of COPII vesicle formation and protein sorting.* FEBS Lett. 2007 May 22;581(11):2076-82.

Schwarz K, Iolascon A, Verissimo F, Trede NS, Horsley W, Chen W, Paw BH, Hopfner KP, Holzmann K, Russo R, Esposito MR, Spano D, De Falco L, Heinrich K, Joggerst B, Rojewski MT, Perrotta S, Denecke J, Pannicke U, Delaunay J, Pepperkok R, Heimpel H. *Mutations affecting the secretory COPII coat component SEC23B cause congenital dyserythropoietic anemia type II*. Nat Genet. 2009 Aug;41(8):936-40.

Shalev H, Perez-Avraham G, Kapelushnik J, Levi I, Rabinovich A, Swinkels DW, Brasse-Lagnel C, Tamary H. *High levels of soluble serum hemojuvelin in patients with congenital dyserythropoietic anemia type I*. Eur J Haematol. 2013 Jan;90(1):31-6.

Sherman ML, Borgstein NG, Mook L, Wilson D, Yang Y, Chen N, Kumar R, Kim K, Laadem A. *Multiple-dose, safety, pharmacokinetic, and pharmacodynamic study of sotatercept (ActRIIA-IgG1), a novel erythropoietic agent, in healthy postmenopausal women.* J Clin Pharmacol. 2013 Nov;53(11):1121-30.

Shi Y, Hata A, Lo RS, Massagué J, Pavletich NP. *A structural basis for mutational inactivation of the tumour suppressor Smad4*. Nature. 1997 Jul 3;388(6637):87-93.

Siatecka M, Xue L, Bieker JJ. *Sumoylation of EKLF promotes transcriptional repression and is involved in inhibition of megakaryopoiesis*. Mol Cell Biol. 2007 Dec;27(24):8547-60.

Tamary H, Shalev H, Perez-Avraham G, Zoldan M, Levi I, Swinkels DW, Tanno T, Miller JL. *Elevated growth differentiation factor 15 expression in patients with congenital dyserythropoietic anemia type I.* Blood. 2008 Dec 15;112(13):5241-4.

Tao J, Zhu M, Wang H, Afelik S, Vasievich MP, Chen XW, Zhu G, Jensen J, Ginsburg D, Zhang B. *SEC23B is required for the maintenance of murine professional secretory tissues.* Proc Natl Acad Sci U S A. 2012 Jul 17;109(29):E2001-9.

Tsuchida K, Nakatani M, Hitachi K, Uezumi A, Sunada Y, Ageta H, Inokuchi K. *Activin signaling as an emerging target for therapeutic interventions.* Cell Commun Signal. 2009 Jun 18;7:15.

Unal S, Russo R, Gumruk F, Kuskonmaz B, Cetin M, Sayli T, Tavil B, Langella C, Iolascon A, Uckan Cetinkaya D. *Successful hematopoietic stem cell transplantation in a patient with congenital dyserythropoietic anemia type II*. Pediatr Transplant. 2014 Jun;18(4):E130-3.

Wickramasinghe SN and Wood WG. *Advances in the understanding of the congenital dyserythropoietic anaemias.* Br J Haematol. 2005 Nov;131(4):431-46.

Worthington JJ, Klementowicz JE, Travis MA. *TGFβ: a sleeping giant awoken by integrins*. Trends Biochem Sci. 2011 Jan;36(1):47-54.

Xiuli An and Narla Mohandas. *Erythroblastic islands, terminal erythroid differentiation and reticulocyte maturation.* Int J Hematol, 2011 Feb;93(2):139-143.

Yehia L, Jindal S, Komar AA, Eng C. *Non-canonical role of cancer-associated mutant SEC23B in the ribosome biogenesis pathway*. Hum Mol Genet. 2018 Sep 15;27(18):3154-3164.

Yehia L, Niazi F, Ni Y, Ngeow J, Sankunny M, Liu Z, Wei W, Mester JL, Keri RA, Zhang B, Eng C. *Germline Heterozygous Variants in SEC23B Are Associated with Cowden Syndrome and Enriched in Apparently Sporadic Thyroid Cancer*. Am J Hum Genet. 2015 Nov 5;97(5):661-76.

Zhang B, Metharom P, Jullie H, Ellem KA, Cleghorn G, West MJ, Wei MQ. *The significance of controlled conditions in lentiviral vector titration and in the use of multiplicity of infection (MOI) for predicting gene transfer events.* Genet Vaccines Ther. 2004 Aug 4;2(1):6.